FINAL REPORT

HOT HYDROGEN TESTING OF METALLIC TURBO PUMP MATERIALS

May 13, 1992 to May 12, 1993

Contract: NASA-39131 #11

Submitted to

NASA

Marshall Space Flight Center, AL 35812

by

Ralph Zee, Bryan Chin and Rohit Inamdar

Materials Engineering Program

Auburn University, AL 36849

HOT HYDROGEN TESTING OF METALLIC TURBO PUMP MATERIALS

Ralph Zee, Bryan Chin and Rohit Inamdar
Materials Engineering Program
Auburn University
Auburn, AL 36849

Table of Contents

I. Abstract of the Investigation 1

II. Introduction 2

III. Research 5

A. Materials Selection 5

B. Experimental System Development 5

B.1. Heating System 5

B.2. Experimental Chamber 6

B.3. Sample Preparation 11

B.4. Experimental Procedures 11

C. Results and Discussion 13

C.1. Isochronal Experiments 18

C.2. Isobaric Experiments 27

D. Conclusions 36

IV. Appendix 37

HOT HYDROGEN TESTING OF METALLIC TURBO PUMP MATERIALS

Ralph Zee, Bryan Chin and Rohit Inamdar
Materials Engineering Program
Auburn University, AL 36849

I. Abstract of the Investigation

The objectives of this investigation are to expose heat resistant alloys to hydrogen at elevated temperatures and to use various microstructural and analytical techniques to determine the chemical and rate process involved in degradation of these materials due to hydrogen environment. Inconel 718 and NASA-23 (wrought and cast) are candidate materials for this study. The degradation of these materials in the presence of 1 to 5 atmospheric pressure of hydrogen from 450°C to 1100°C was examined. The hydrogen facility at Auburn University was used for this purpose. Control experiments were also conducted wherein the samples were exposed to vacuum so that a direct comparison of the results would separate the thermal contribution from the hydrogen effects. The samples were analyzed prior to and after exposure. A residual gas collection system was used to determine the gaseous species produced by any chemical reaction that may have occurred during the exposure. Analysis of this gas sample shows only the presence of H_2 as expected. Analyses of the samples were conducted using optical microscopy, x-ray diffraction, scanning electron microscopy and weight change. There appears to be no change in weight of the samples as a result of hydrogen exposure. In addition no visible change on the surface structure was detected. This indicates that the materials of interest do not have strong interaction with hot hydrogen. This is consistent with the microstructure results.

II. Introduction

Inconel 718 and NASA-23, an Fe-Ni-Co-Cr heat resistant alloy, are two high temperature metallic alloys extensively used in the turbomachineries in the space shuttle main engine. These alloys are also proposed to be used in the thermal nuclear propulsion systems with hydrogen as a propellent. In this application, the turbomachinery components must b compatible with hot hydrogen at approximately 800°C. In th conducted to determine th

II. Introduction

Inconel 718 and NASA-23, an Fe-Ni-Co-Cr heat resistant alloy, are two high temperature metallic alloys extensively used in the turbomachineries in the space shuttle main engine. These alloys are also proposed to be used in the thermal nuclear propulsion systems with hydrogen as a propellent. In this application, the turbomachinery components must be compatible with hot hydrogen at approximately 800°C. In the past, studies have been conducted to determine the suitability of superalloys for medium-temperature gas turbine applications. However, most of the efforts have been concentrated on hydrogen embrittlement or hydrogen induced cracking, fatigue crack propagation in hydrogen environment, stress corrosion cracking etc. This makes it necessary to carry out a fundamental study involving diffusivity, hydride formation and weight loss after hydrogen exposure describing the degradation mechanism of these high temperature alloys in hydrogen environment.

Hydrogen degradation is a complex process and it strongly depends on temperature. Hydrogen can exist in solids in three forms namely hydride, solution and gas. At concentration levels below the solubility limit, hydrogen atoms occupy the interstitial sites of the matrix and solution strengthen the material, this is the trapped or immobile hydrogen. Hydrogen trapping can also be attributed to other microstructural features like voids, dislocations and grain boundaries. On the other hand, mobile hydrogen can lead to hydrogen embrittlement. At supersaturation levels, hydrides may be formed and most met\al hydrides are very brittle and hence contribute towards hydrogen embrittlement. Under irradiation environment, the presence of hydrogen in supersaturated levels, may also result in gas bubble

formation which has been observed experimentally under ion irradiation.

One particular feature of hydrogen is that it is extremely mobile. Activation energy of hydrogen in most metals is of the order of 10 kcal/mole with a pre-exponential coefficient of approximately 10^{-2} cm^2/s. This implies that diffusion is not the rate limiting step in the temperature range of interest in this study. It is therefore appropriate to assume that no concentration gradient exists in the bulk throughout the experiment making interpretation of the results much simplified.

The diatomic hydrogen gas (H_2) does not react directly with the materials due to its chemical stability. Even at ultra high temperatures like 4000°C, the fraction of atomic hydrogen in the hydrogen gas is negligible due to high binding energy of H_2 (104 Kcal/mole or 4.5eV/bond) which is much larger than the thermal energy available. This means that the first interactive process must be the dissociation of molecules into atomic hydrogen at the surface. This is followed by the rapid diffusion into the bulk as discussed in the preceding paragraph.

At high temperatures hydrogen solubility is very high, as a result hydride formation may not occur even at considerable hydrogen concentrations. Under this condition, the hydrogen atoms can occupy the interstitial sites of the material and alter the atomic bond strength which in turn affects the stability of the materials. When the material cools, the hydrogen may become trapped. Depending on the cooling rate and conditions, the system will either hydride or be supersaturated with hydrogen which is thermodynamically unstable. Both the conditions can lead to material degradation. However, at low and intermediate temperatures, hydrogen solubility being very low, hydrogen degradation of material can

mainly be due to hydride formation. The weight loss may result due to interaction of hydrogen with one or more alloying elements to form and evolve certain gaseous species.

This research addresses both physical and chemical aspects of interaction of hydrogen with one the said alloys. The study is designed to provide basic understanding of the forces that govern hydrogen degradation in materials at elevated temperatures. The main objectives are to develop a system which can expose metal to hydrogen at high temperatures and to determine the governing mechanisms for hydrogen degradation based on microstructural analyses using electron microscopy, x-ray diffraction and other techniques.

III. Research

A. Materials Selection

Materials used in this research was provided by the Metallurgy Research Branch of the National Aeronautics and Space Administration (NASA), George C. Marshall Space Flight Center. Several 0.250 inch specimen of cast as well as wrought NASA-23 (Fe 37.5%, Ni 31.8%, Co 14.9%, Cr 10.0% Nb 3.1%, Ti 2.5%, Al 0.14%, Mo 0.05%) and wrought Inconel 718 (Fe 18.0%, Ni 52.5%, cr 19.0%, Nb+ta 5.0%, Ti 0.9%, Al 0.5%) were obtained for analysis. Inconel 718 was precipitation heat treated as per AMS 5662F. The optical microscopy, x-ray diffraction (XRD) and energy dispersive x-ray spectroscopy (EDS) of as-received samples were used as references for the post reaction analyses of these materials.

B. Experimental System Development

The high temperatures needed combined with the potential for uncontrolled detonation of the hydrogen gas required careful design and operation of experiments in this investigation. A short description of the method used for heating, the experimental chamber, the sample preparation and the experimental procedure are described in the following sections.

B. 1. Heating System

The 50 kw induction generator at Auburn University was used for this purpose. The direct induction heating of the specimen was not feasible owing to the range of susceptibility in materials that were investigated in this study. A Nb-1Zr tube was used as the susceptor

which was heated by the induction field. The thickness of the tube was approximately 0.01". This was sufficient to absorb most of the RF power. The specimen were in form of small pieces and were placed inside the tube. In all experiments, effort was made to keep the shape and size of all the samples approximately the same. This is important to ensure that proper comparison can be made based on the volume and areal normalization. The specimen were then heated b radiation , convection and conduction of the heat generated in the susceptor. Heating of Nb-1Zr susceptor instead of direct induction heating of the specimen also provided a direct correlation between RF power and temperature which was independent of specimen properties. This direct correlation facilitates a simple means of temperature calibration. Temperature during the experiment was determined using infra-red optical pyrometer and tungsten-rhenium thermocouple. With the pyrometer, a correction was made for surface emissivity.

B. 2. Experimental Chamber

A double wall vacuum chamber was used to carry out the experiments. Figures 1 and 2 respectively show a photograph and a schematic drawing of the system. The inner chamber was 3/4 inch diameter Nb-1Zr tube and was also used as the susceptor for the induction field. The tube was typically seven to eight inches long and was tungsten inert gas (TIG) welded at one end. The tube was replaced periodically because of degradation due to thermal and hydrogen embrittlement and oxidation. The use of TIG weld eliminated the necessity to produce a vacuum tight swage-lock at one end. The other end was connected to a stainless steel gas/exit line using a swage-lock connection. The inner chamber was enclosed in a

stainless steel containment vessel (outer chamber) which was significantly larger. Since hydrogen was only introduced into the inner chamber, , this chamber this chamber was kept much small compared to the outer chamber due to safety considerations. The outer chamber was basically a large stainless steel "tee". On the outer chamber, three ports were designated back, front and top. Each port was 16 inches in diameter. The back port contained a vacuum line to the main pumping system. The front port contained the feedthrough for the induction coils, thermocouple, pressure sensor, hydrogen gas line and the venting to the chamber. The top port was removable and was used to place the samples inside the inner chamber. It also contained the viewport which was utilized by the pyrometer. The viewport also served as a safety device. The viewport was a flat circular piece of quartz that was slightly larger than the port hole in the top plate. The quartz was sealed against the face plate by vacuum inside the chamber and vacuum grease. This viewport served as a pressure relief device, if there was an undesirable pressure buildup in the outer chamber.

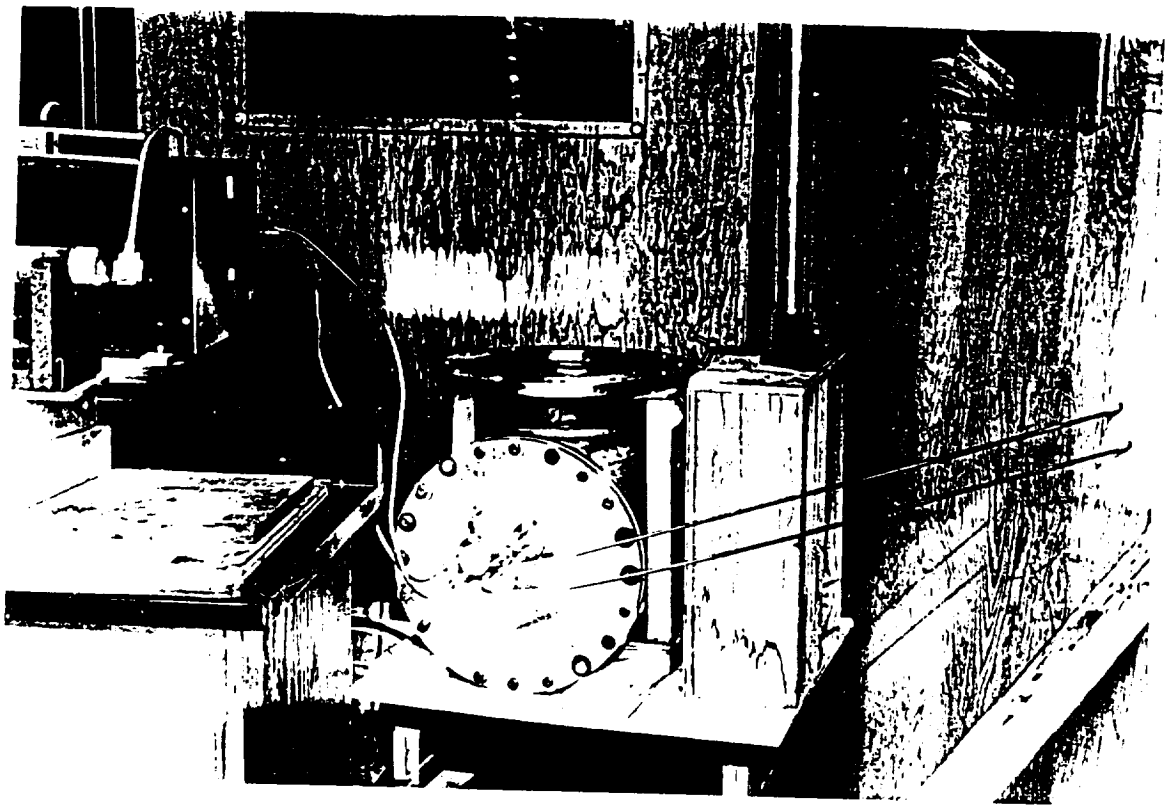

Figure 1.a. Experimental Setup.

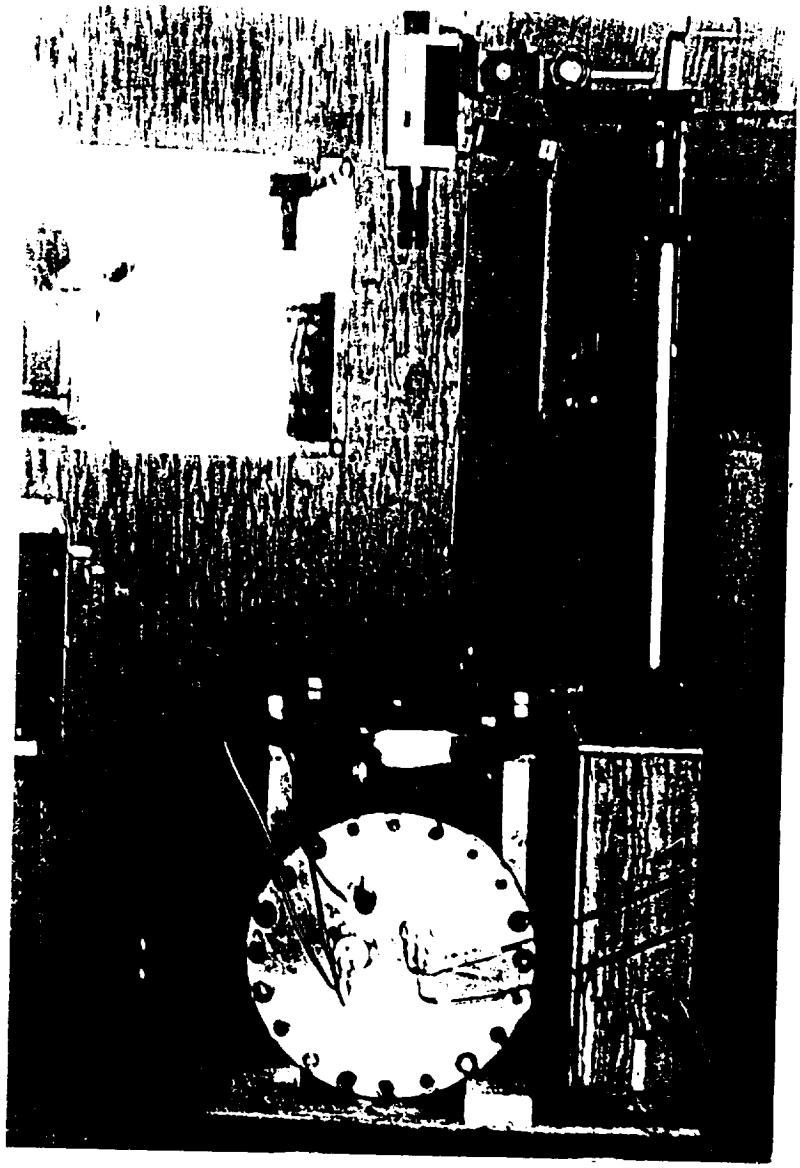

Figure 1.b. Experimental setup.

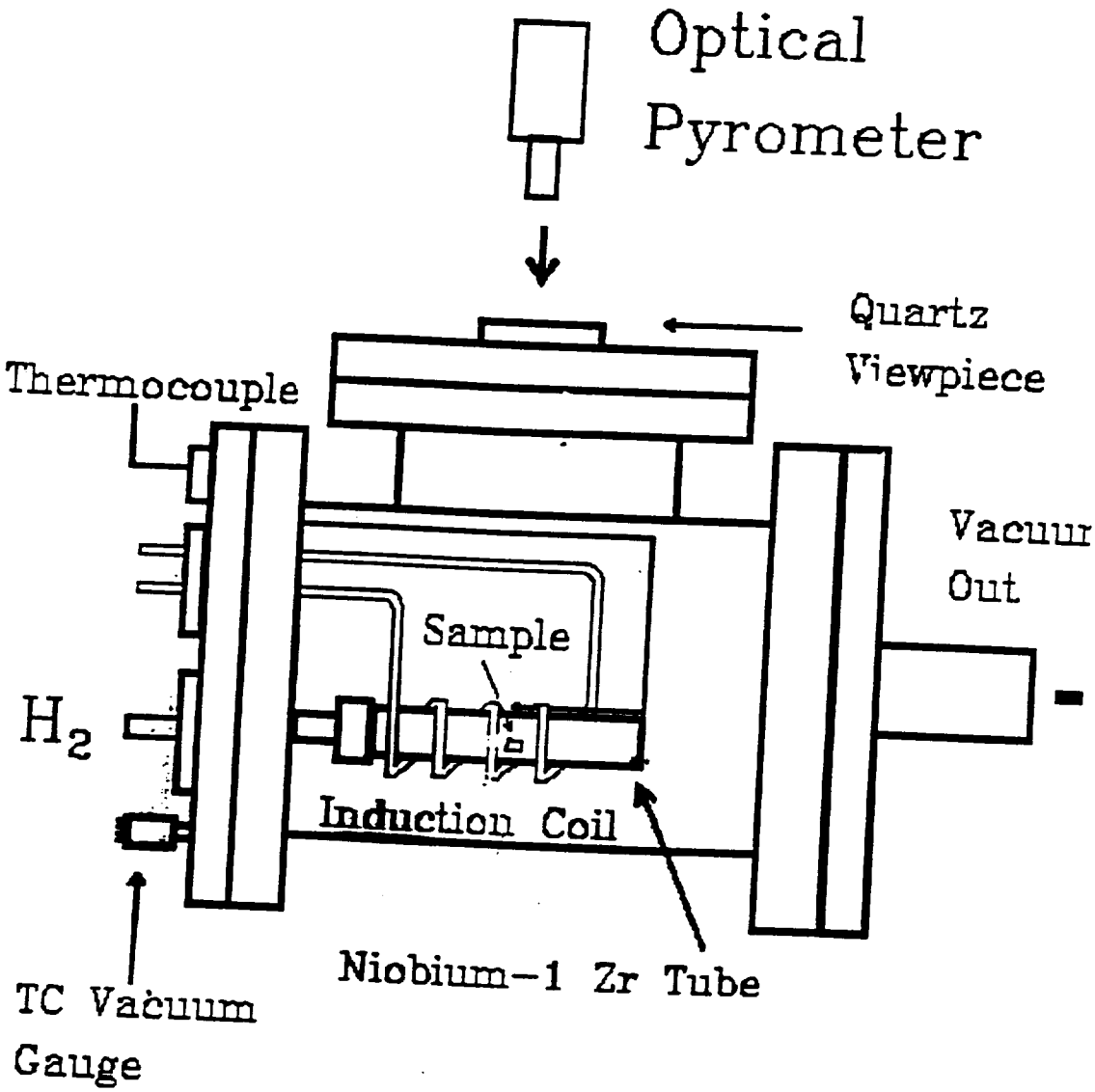

Figure 2. Schematic of Hydrogen Exposure Facility.

B. 3. Sample Preparation

The samples were cut into small pieces of desired shape using an electric discharge machine (EDM). These samples were then cleaned in acetone with the aid of ultrasonic cleaner, after which they were dried in a vacuum of one millitorr for an hour. This procedure ensures that there remains no trapped liquid which would outgass during the reaction. The outgassing would cause false readings on the weight change measurements. Once the sample was dry, its weight was precisely measured using an electrobalance. The color and overall physical appearance of the sample was also documented.

B. 4. Experimental Procedures

Once the samples were properly prepared, they were placed in the inner chamber. Care was taken to ensure that the samples were situated in the hot zone region. The hot zone is the region along Nb-1Zr tube. It lies inside the induction coil and is approximately 4" in length. The inner chamber was then secured to the hydrogen gas line via swage lock fittings inside the larger outer chamber. The temperature of hot zone was monitored throughout the experiment and was assumed to be the temperature of the specimen. Two devices were used to monitor the this temperature simultaneously. The first device was a C-type thermocouple (tungsten-rhenium). It was attached to the outside of Nb-1Zr tube and was in the hot zone section. The thermocouple leads passed through the front plate of the outer chamber and was connected to a digital readout externally. The second device used to monitor the temperature was an optical pyrometer. The infra-red pyrometer camera was focussed on to the same region as the thermocouple. The pyrometer was interfaced with a computer so that

computer so that continuous temperature readings could be permanently recorded. Two devices were used so that one could act as a standby if the other were to fail during the reaction. Also this enhanced the accuracy of the temperatures measured.

After the inner chamber was secured, it was tested for leaks using Varian helium leak detector. Once the inner chamber was checked for leaks and was found to be safe, the top plate was mounted and bolted shut. The outer chamber was also leak checked using the helium leak detector. Pressure values in both, the inner as well as the outer chamber were measured continuously throughout the experiment to enure that no leaks developed in the system during the experiment. After both the chambers were secured and found to be safe, the system was purged and then heated.

Prior to purging, both the chambers were evacuated until the best possible vacuum was obtained on these chambers. After this requirement was met with, the inner chamber was pressurized with hydrogen and re-evacuated. This was done to minimize the amount of oxygen (air) in the inner chamber. After purging the inner chamber, it was filled with hydrogen to desired pressure (ranging from 1atmosphere to 5 atmospheres). The inner chamber was then ready to be heated. Heating to desired temperature was carried out with care, raising the temperature gradually. This was necessary to avoid thermal shock to the system. Thermal shock to the system can cause rupture of the Nb-1Zr tube which in turn leads to premature termination of the experiment.

C. Results and Discussion

With an aim to compare as well as accurately interpret the effects of hydrogen and vacuum environments on the microstructure of the specimen, it was necessary to determine the structure of the as-received samples. X-ray diffraction, energy dispersive x-ray spectroscopy and optical microscopy were used in analyzing and verifying the initial condition of several virgin samples. Figures 3 through 5 on the following pages are the microstructure of these three samples obtained using optical microscope.

The experiments carried out in order to conduct this study can be divided into two basic groups, namely the isochronal and the isobaric. The temperature at which these experiments were conducted ranged from 400°C to 1100°C (one experiment was performed at 1350°C wherein the samples melted inside the crucible) Controlled experiments were also conducted in the environment without hydrogen. These experiments are referred to as dry runs. These dry runs were conducted with an idea of making direct comparison with hydrogen runs so as to comprehend the role played by hydrogen in degradation of these alloys at various temperature and pressure conditions. Table 1 lists all the important parameters involved during actual experimental process.

A detailed x-ray diffraction analysis was conducted on all the samples immediately following the test run. The x-ray spectra obtained from all these processed samples are included in appendix section of this report. Each spectrum is labelled with the sample name and the test number. For example, "Inconel 718 Test #1" is the XRD pattern for Inconel 718 sample processed at 810°C and 1atmospheric pressure of hydrogen for one hour.

Table 1. Important Experimental Parameters

Test #	Temperature (°C)	H_2 Pressure	Time (Hr)	Environment
1	810	1 atm.	1	Hydrogen
2	950	1 atm.	1	Hydrogen
3	1000	-	1	Vacuum
4	1100	1 atm.	1	Hydrogen
5	825	1 atm.	1	Hydrogen
6	400	5 atm.	1	Hydrogen
7	550	5 atm.	1	Hydrogen
8	970	-	2	Vacuum
9	900	2 atm.	3	Hydrogen
10	860	5 atm.	6	Hydrogen
11	865	5 atm.	6	Hydrogen
12	850	-	6	Vacuum
13	750	5 atm.	8	Hydrogen
14	800	-	8	Vacuum

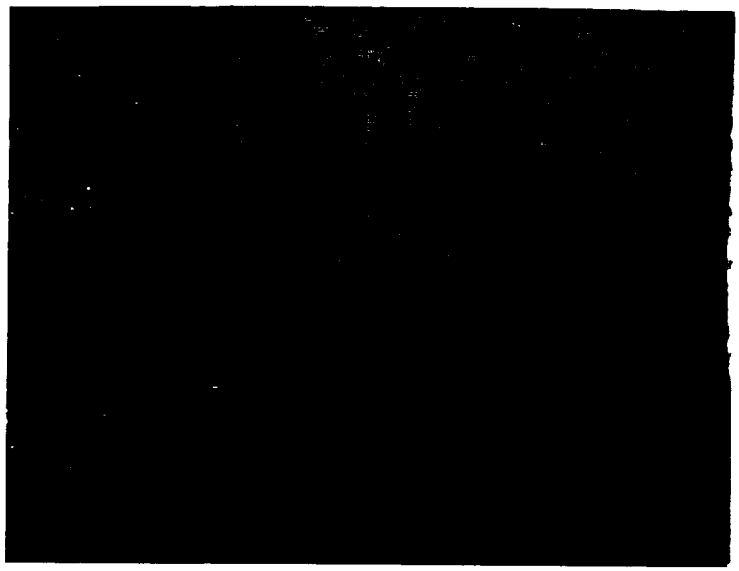

Inconel 718; 500X

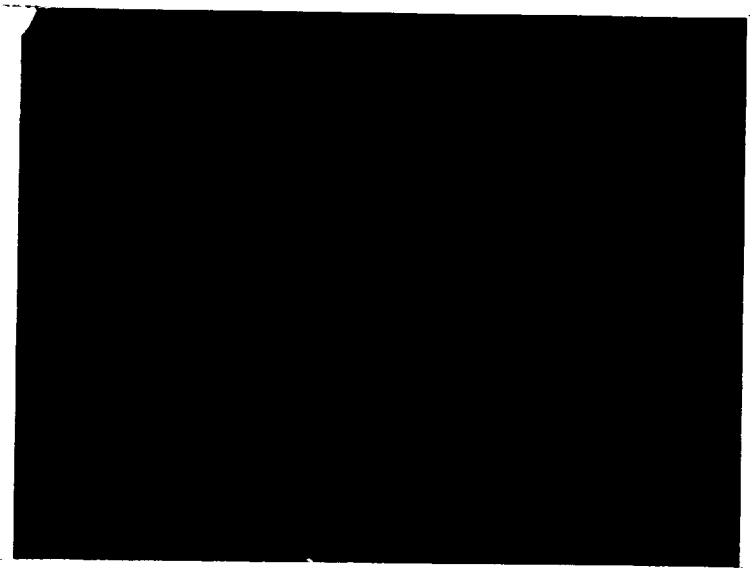

Inconel 718; 1000X

Figure 3. Microstructure of Inconel 718 in the as-received condition obtained using optical microscope.

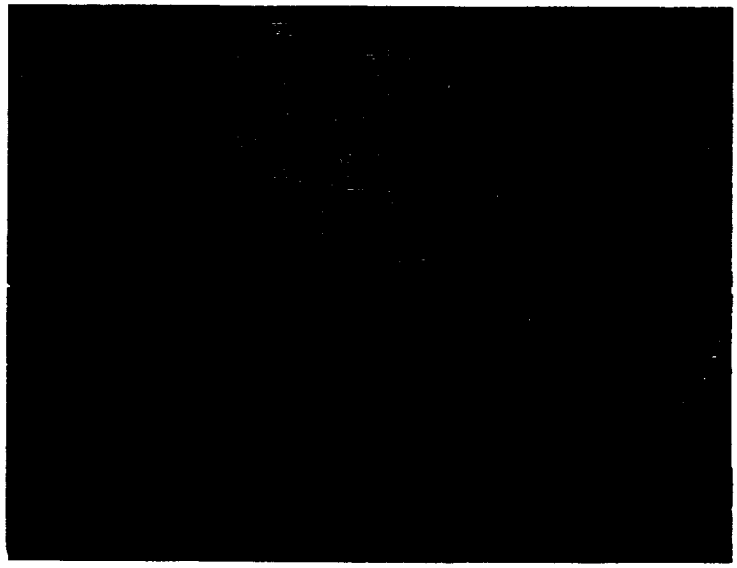

NASA-23 (C); 200X

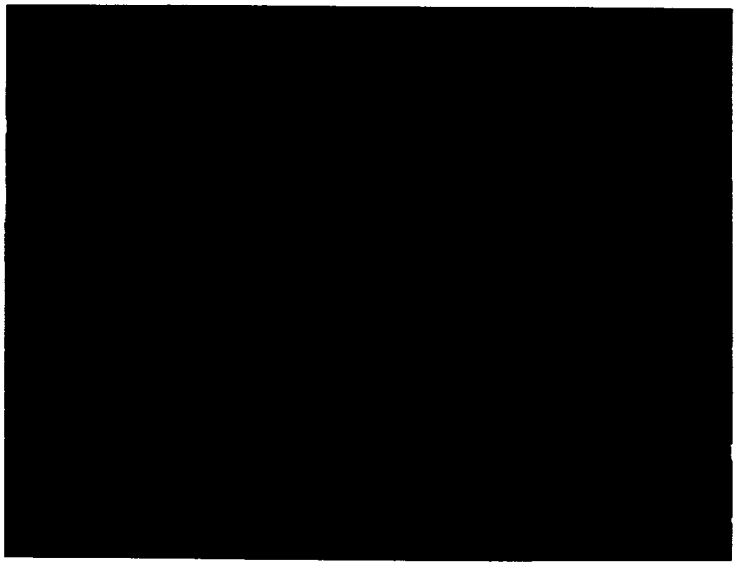

NASA-23 (C); 500X

Figure 4. Microstructure of NASA-23 (C) in the as-received condition obtained using optical microscope.

NASA-23 (W); 500X

Figure 5. Microstructure of NASA-23 (W) in the as-received condition obtained using optical microscope.

C. 1. Isochronal Experiments:

All the experiments conducted for a period of one hour fall under this category. The variable in these test runs was temperature, which ranged from 400°C to 1100°C as well as the pressure (ranging from 1atmosphere to 5atmospheres). NASA-23 (wrought) samples were received after first four experiments were completed and thus were not processed for the experiments #1 through #4. We can thus say that more detailed experiments were conducted for Inconel 718 and NASA-23 (cast) samples. All the specimens were analyzed in a similar way.

The first set of data collected after every test run was the weight of the sample, so as to observe any possible weight change during the process. There was no appreciable weight change for either of NASA-23 samples as well as the Inconel 718. All the samples did not show any deviation from the original weight even after hydrogen/vacuum exposure. Table 2 lists the weight of these samples before and after the exposure. A slight variation in weight for some samples could be because of the fact that samples might not have been properly dried (after they were cleaned in acetone) prior to starting the experiment.

Next step in the analysis was XRD. This analysis was performed immediately after the exposure so as to make a note of metastable phases, if any, were formed. These metastable phases can transform to a more stable phase as a function of time. The data were analyzed by using the Joint Community of Pattern Diffraction Standards (JCPDS) files for phase identification. Fink index was used to obtain information on d-spacing and the intensity in the XRD spectra. The XRD spectra obtained from NASA-23 (cast and wrought) and Inconel 718 virgin samples show same spectrum in each case. These correspond to

gamma prime phase which is the principal strengthening agent in most of Ni-Fe and Ni based superalloys. Gamma prime has an ordered Ll_2 crystal structure. This is mainly Ni_3Al or Ni_3AlTi. However, elemental substitution does occur wherein, cobalt and chromium replace some amount of Nickel, iron replaces some parts of Ni and Al. Titanium can replace some of aluminum. Gamma prime acts as a strengthening phase in these alloys since lattice parameter for the austenitic matrix (gamma) and gamma prime are similar giving rise to coherency.

After exposure to hydrogen and vacuum at different temperatures during these isochronal experiments, the only change that was identified in some of the x-ray spectra was that of sharpening of peaks accompanied by increase in intensity of these peaks. This indicated that recrystallization and grain growth occurred in the samples in the temperature range of 800 to 850°C. There was no shift in the peaks nor was there any appearance of new peaks or disappearance of the existing peaks. This indicated that no phase change occurred for these isochronal experiments even up to hydrogen pressures of 5 atmospheres and temperatures up to 1000°C. It was decided to conduct experiments for longer durations.

Detailed microstructural and EDS analyses were then conducted. Optical microscopy of these processed samples supports the results obtained by XRD analysis. Figures 6 through 12 are the optical micrographs of these specimens. Grain growth can be easily observed in the microstructure of samples for which peak sharpening effect is evident in the XRD. No change could be observed in the microstructure of the processed samples from that of virgin sample apart from a change in the grain size which was a consequence of a annealing and not from hydrogen exposure.

Table 2. Weight measurements For Isochronal Experiments

Test No.	Inconel 718 before	Inconel 718 after	NASA23C before	NASA23C after	NASA23W before	NASA23W after
1	1.2003	1.2003	0.9367	0.9368	-	-
2	1.1828	1.1828	2.1353	2.1352	-	-
3	0.9073	0.9073	1.1438	1.1438	-	-
4	1.2587	1.2587	1.0997	1.0997	-	-
5	0.9409	0.9409	1.1507	1.1506	2.0757	2.0756
6	1.1144	1.1144	1.0420	1.0420	1.1080	1.1080
7	0.9397	0.9397	1.0760	1.0760	1.0326	1.0326

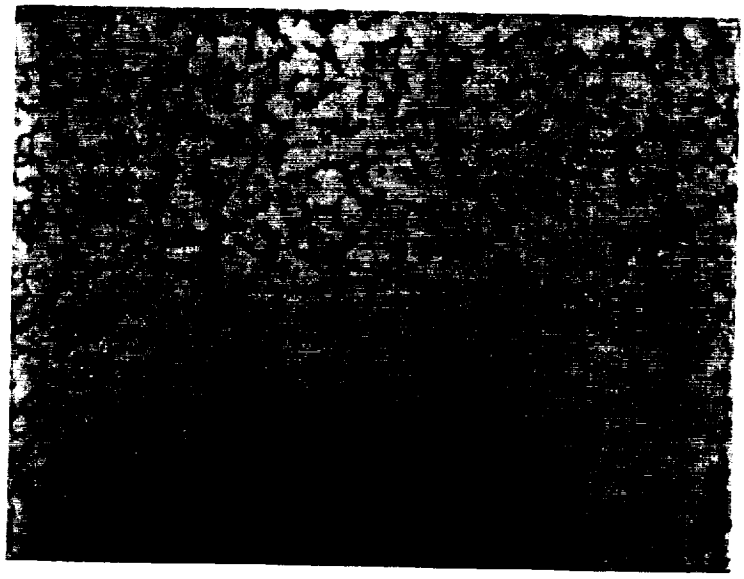

Inconel 718 Test #1; 500X

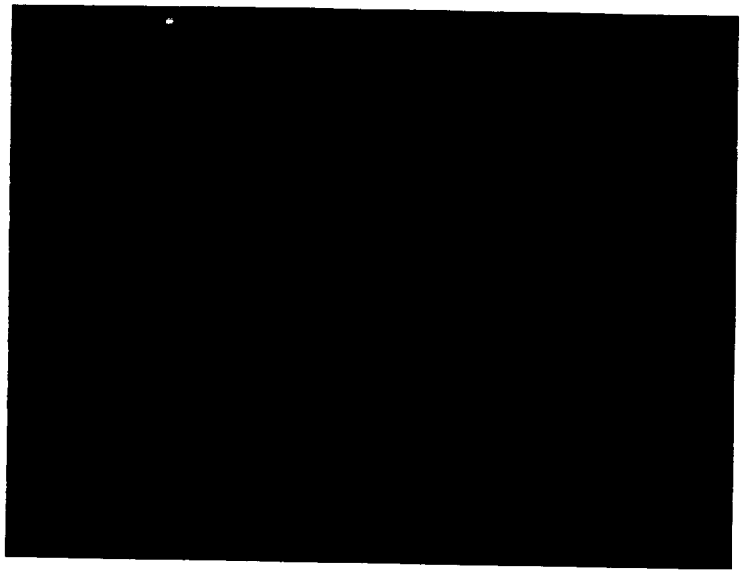

NASA-23 (C) Test #1; 200X

Figure 6. Optical Micrographs of Inconel 718 and NASA-23 (C) After Test #1.

Inconel 718 Test #2; 500X

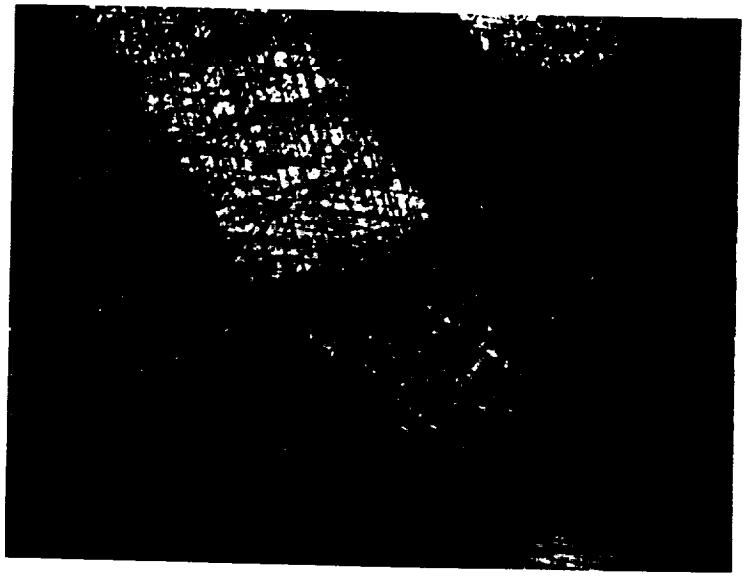

NASA-23 (C) Test #2; 200X

Figure 7. Optical Micrographs of Inconel 718 and NASA-23 (C) After Test #2.

Inconel 718 Test #3; 500X

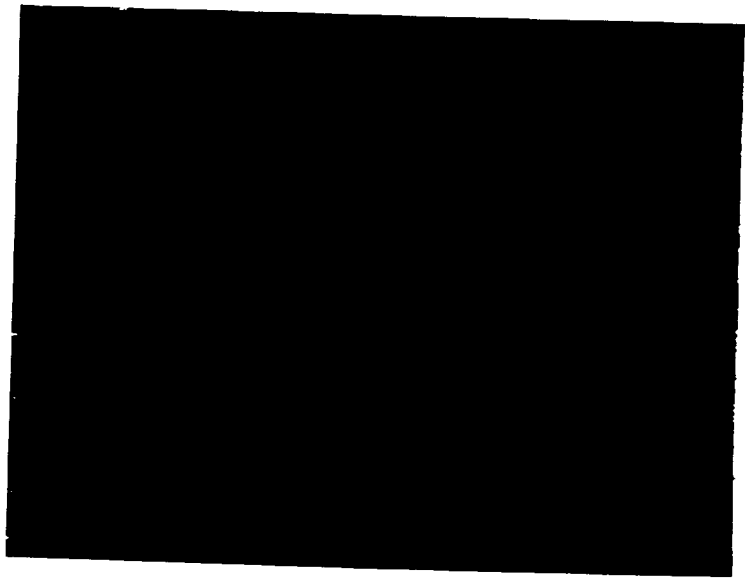

NASA-23 (C) Test #3; 200X

Figure 8. Optical Micrographs of Inconel 718 and NASA-23 (C) After Test #3.

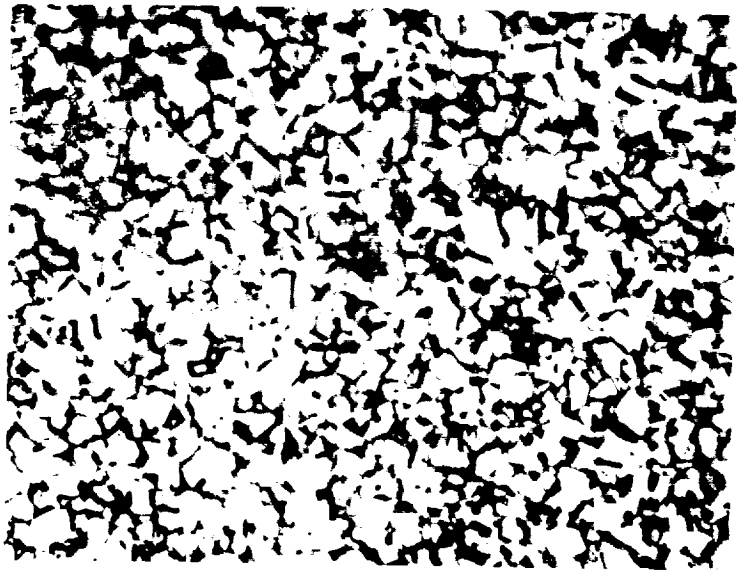

Inconel 718 Test #4; 500X

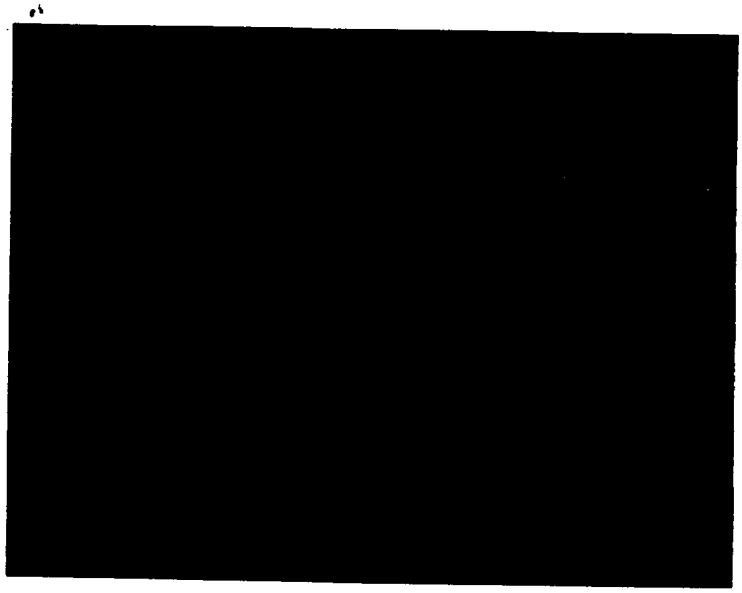

NASA-23 (C) Test #4; 200X

Figure 9. Optical Micrographs After Test #4.

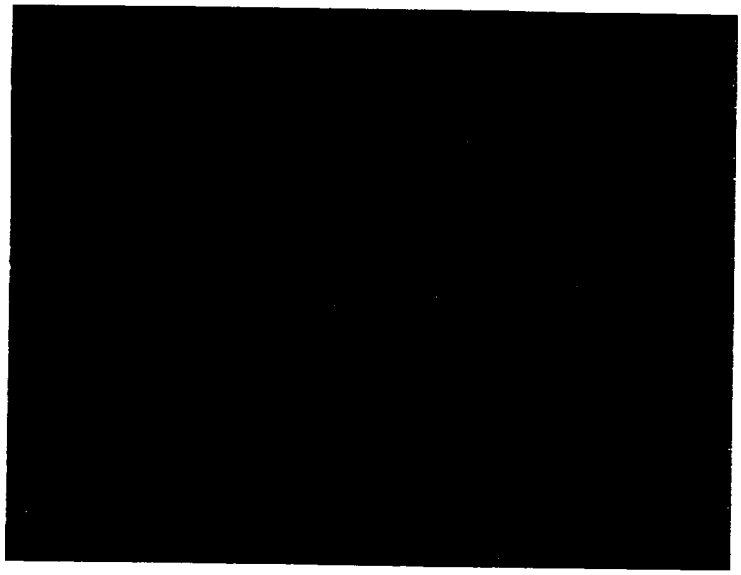

Inconel 718 Test #5; 500X

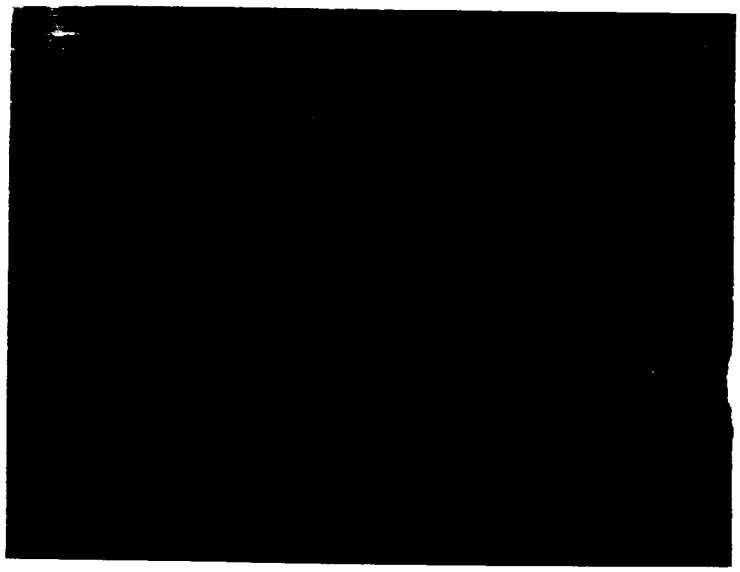

NASA-23 (C) Test #5; 200X

Figure 10. Optical Micrographs of Inconel 718 and NASA-23 (C) After Test #5.

NASA-23 (W) Test #5; 500X

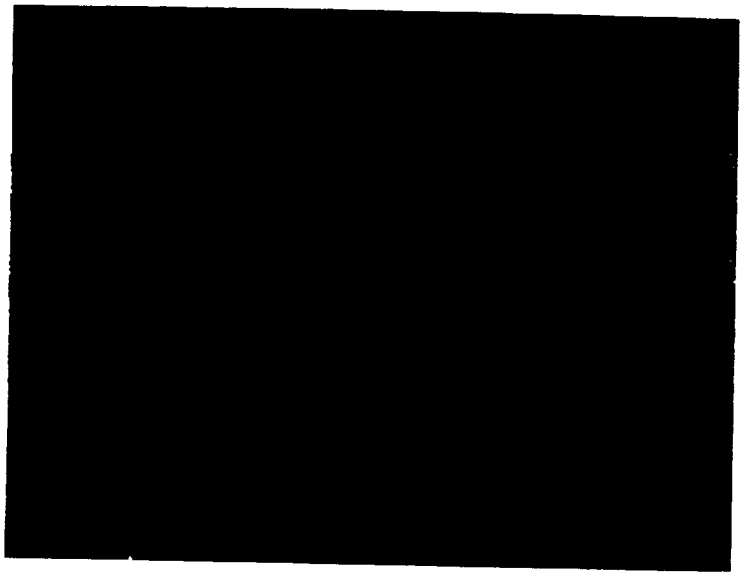

Inconel 718 Test #6; 500X

Figure 11. Optical Micrographs of NASA-23 (W) and Inconel 718.

C. 2. Isobaric Experiments

It was decide to conduct experiment for longer time durations (6 to 8 hours) while keeping hydrogen pressure in excess of atmosphere. Weight of the samples was documented prior to and after the test. This is listed in Table 3. on the following page. For all the isobaric experiments, like the previous set, no change in weight was observed in the processed samples. In addition no visible change on surface structure was noticeable. The analysis of residual gas species obtained after the experiment identified presence of only one gas namely hydrogen, as expected. Data obtained from one such gas analysis are listed in the appendix section.

X-ray diffraction pattern shows no additional peaks. Since no hydride peaks were obtained, in any of the x-ray spectra, it can be said that if at all any hydrides were formed during the hydrogen exposure, the amount was insignificant and below the detection limit of XRD. Similar to isochronal experiments, increase in the peak intensity was observed due to grain growth in some cases. The optical micrographs obtained from these experiments specimen are shown in figures 12 to 18.

Table 3. Weight Measurements For Isobaric Experiments

Test No.	Inconel 718 before	Inconel 718 after	NASA23C before	NASA23C after	NASA23W before	NASA23W after
8	0.9710	0.9710	1.0356	1.0356	0.9798	0.9798
9	1.1730	1.1729	0.9134	0.9134	1.1881	1.1881
10	0.8656	0.8656	0.8324	0.8324	0.7598	0.7598
11	1.1045	1.1045	1.1129	1.1129	0.9706	0.9707
12	1.0554	1.0554	0.9578	0.9578	0.9694	0.9693
13	0.8653	0.8653	1.1597	1.1597	0.8244	0.8244
14	0.9625	0.9625	1.1677	1.1677	1.1347	1.1347

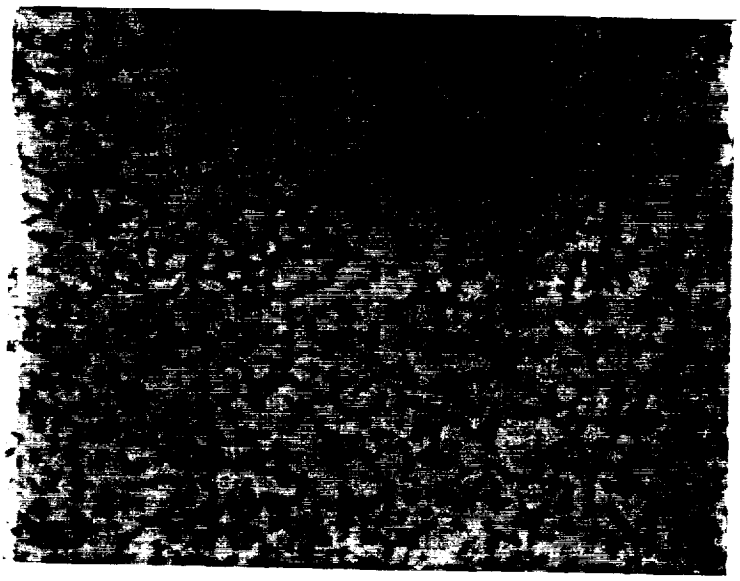

Inconel 718 Test #8; 500X

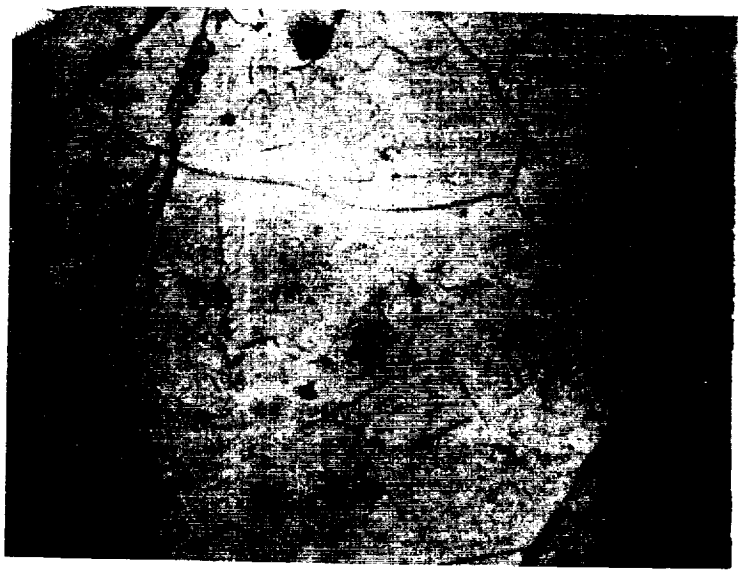

NASA-23 (C) Test #8; 200X

Figure 12. Optical Micrographs of Inconel 718 and NASA-23 After Test #8.

NASA-23 (W) Test #8; 500X

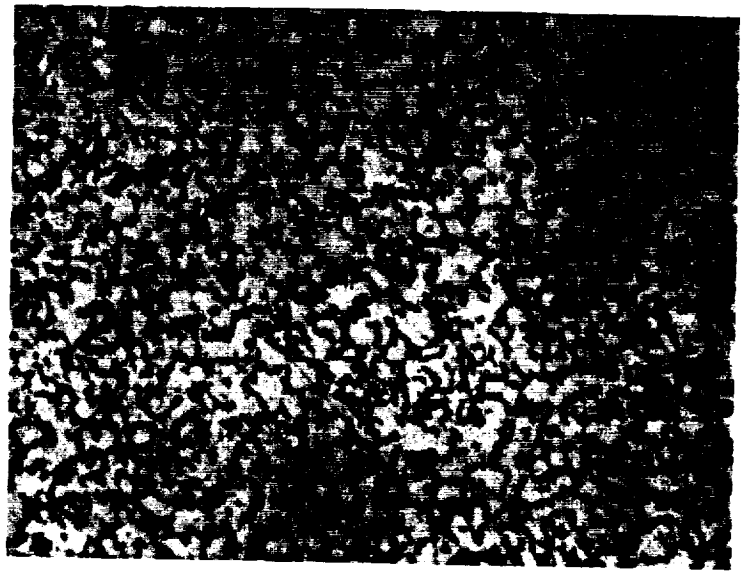

Inconel 718 Test #9; 500X

Figure 13. Optical Micrographs of NASA-23 (W) and Inconel 718.

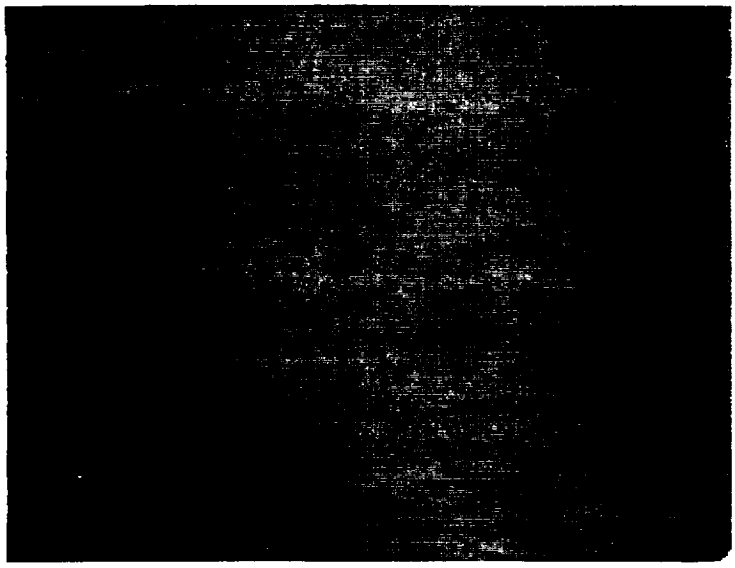

NASA-23 (C) Test #9; 200X

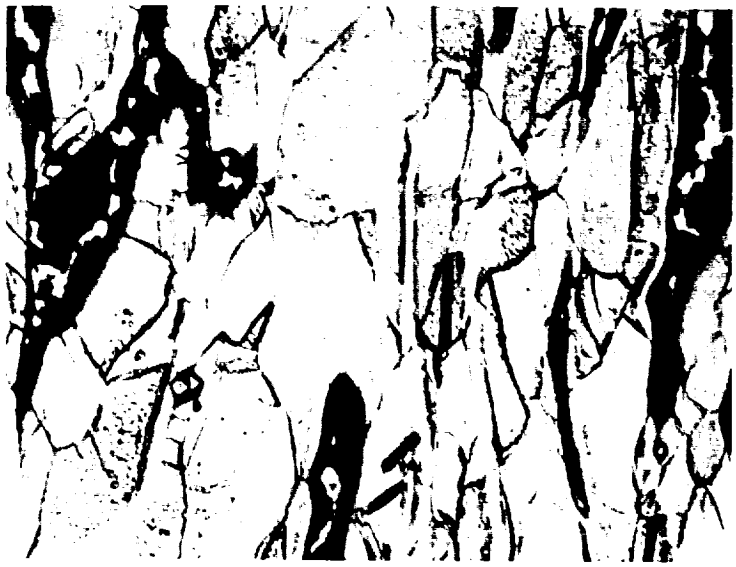

NASA-23 (W) Test #9; 500X

Figure 14. Optical Micrographs of Nasa-23 (Cast and Wrought) After Test #9.

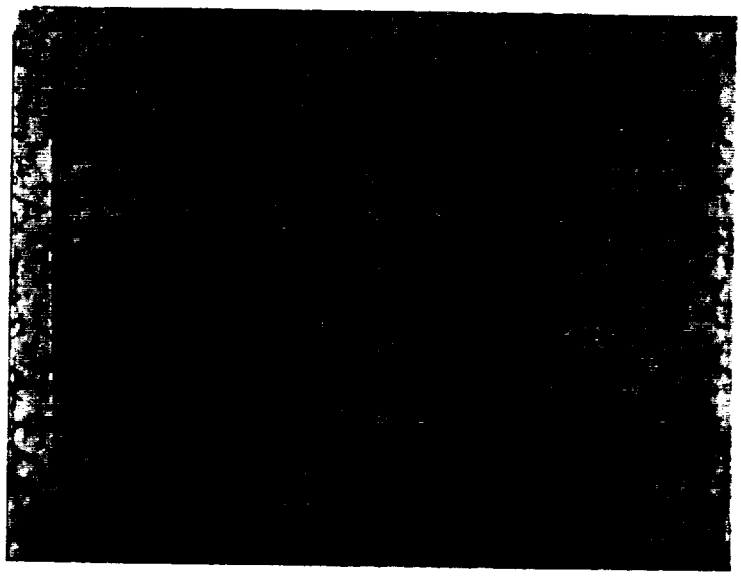

Inconel 718 Test #10; 500X

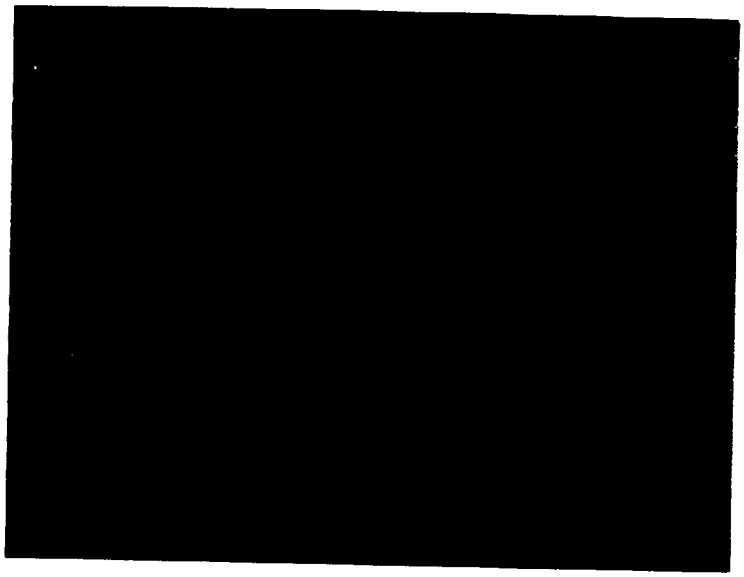

NASA-23 (C) Test #10; 200X

Figure 15. Optical Micrographs of Inconel 718 and NASA-23 (C) After Test #10.

NASA-23 (W) Test #10; 500X

Inconel 718 test #11; 500X

Figure 16. Optical Micrographs Of NASA-23 (W) and Inconel 718.

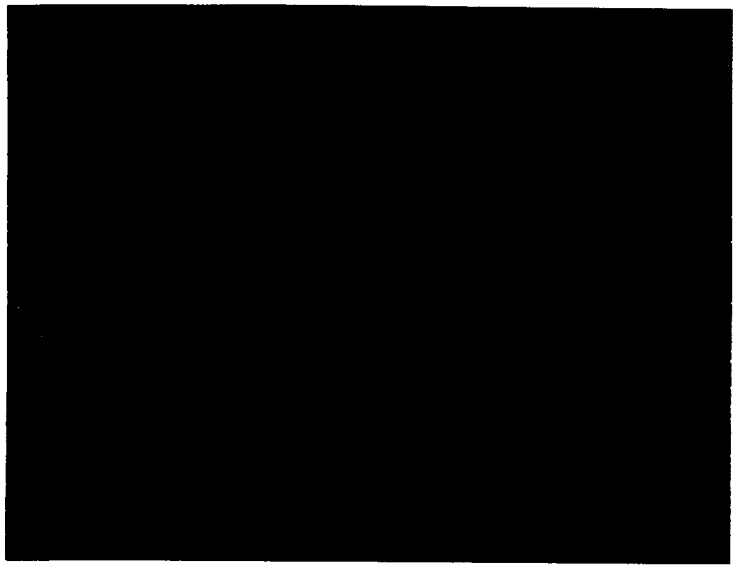

NASA-23 (C) Test #11; 200X

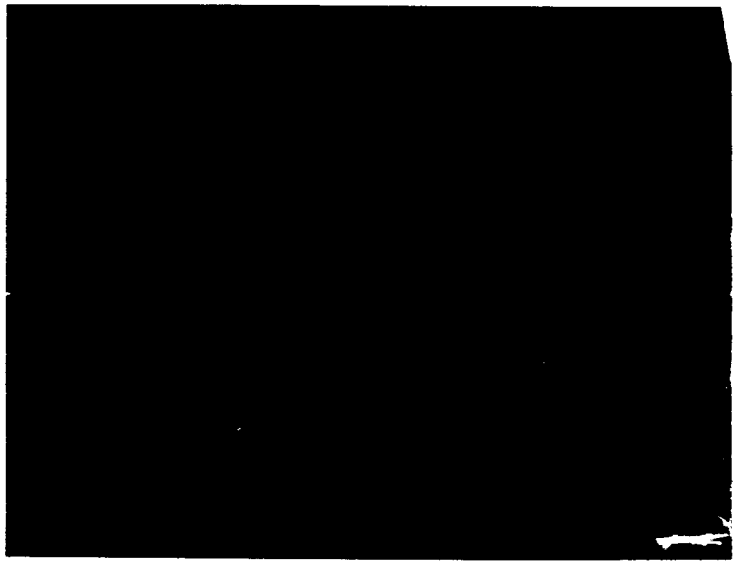

NASA-23 (W) Test #11; 500X

Figure 17. Optical MIcrographs of NASA-23 (Cast and Wrought) After Test #11.

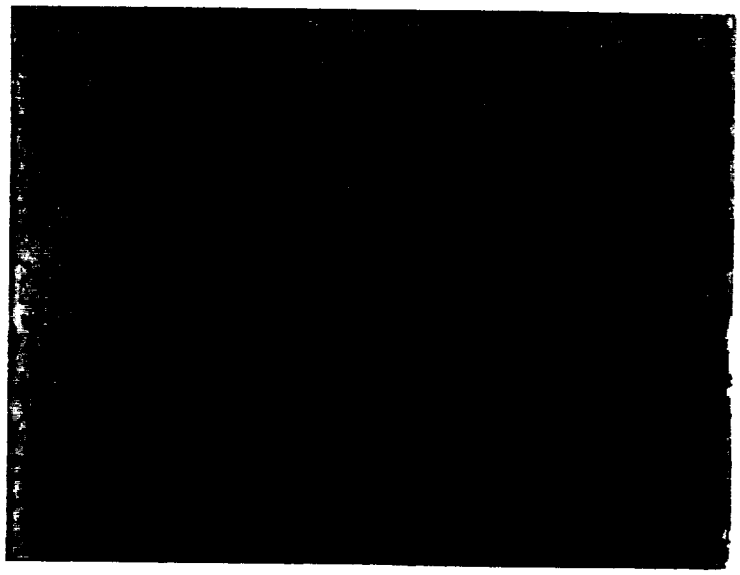

Inconel 718 Test #12; 500X

NASA-23 (C) Test #12; 200X

Figure 18. Optical Micrograohs of Inconel 718 and NASA-23 (C) After Test # 12.

D. Conclusions:

1. A hot hydrogen system was designed, constructed and employed successfully to study the effects of hydrogen at elevated temperatures on heat resisting alloys.
2. There was no weight change, no visible change on surface structure was detected also microstructure did not undergo any kind of transformation, thus indicating that the materials of interest do not have interaction with hydrogen under described conditions.

IV. APPENDIX: X-RAY DIFFRACTION SPECTRA FROM THE SAMPLES

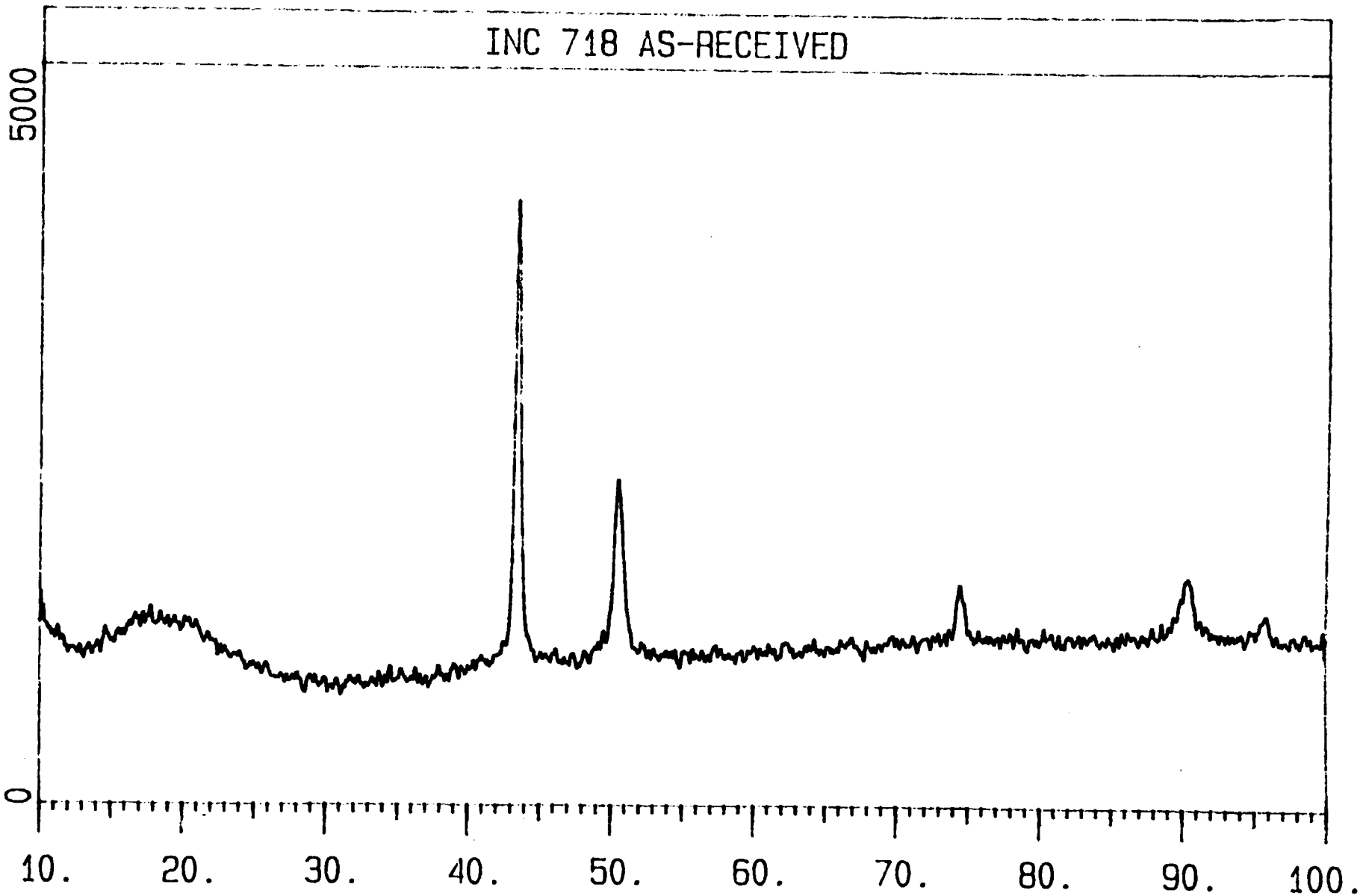
INC 718 AS-RECEIVED
5000
0
10.
20.
30.
40.
50.
60.
70.
80.
90.
100.

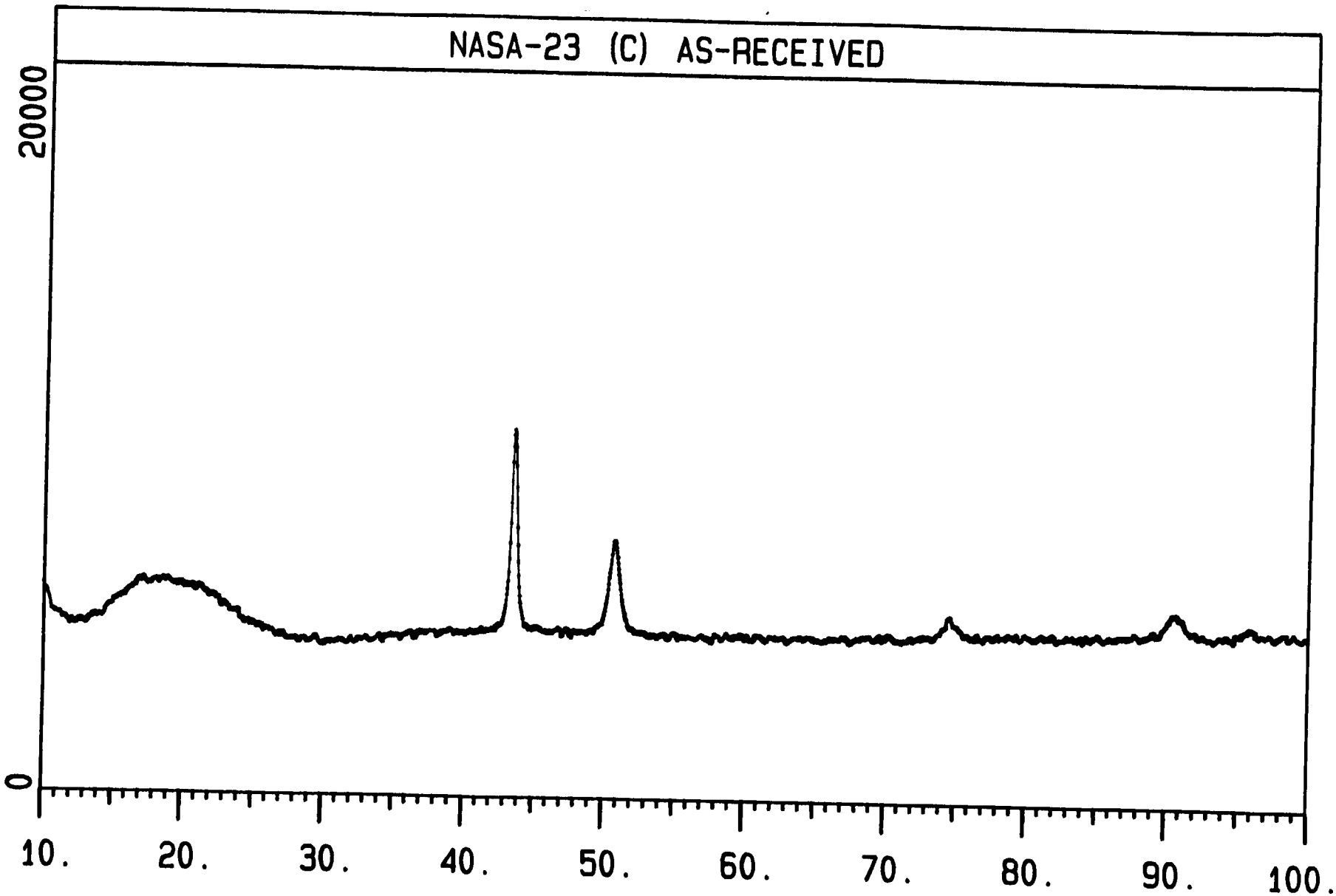
NASA-23 (C) AS-RECEIVED
20000
0
10.
20.
30.
40.
50.
60.
70.
80.
90.
100.

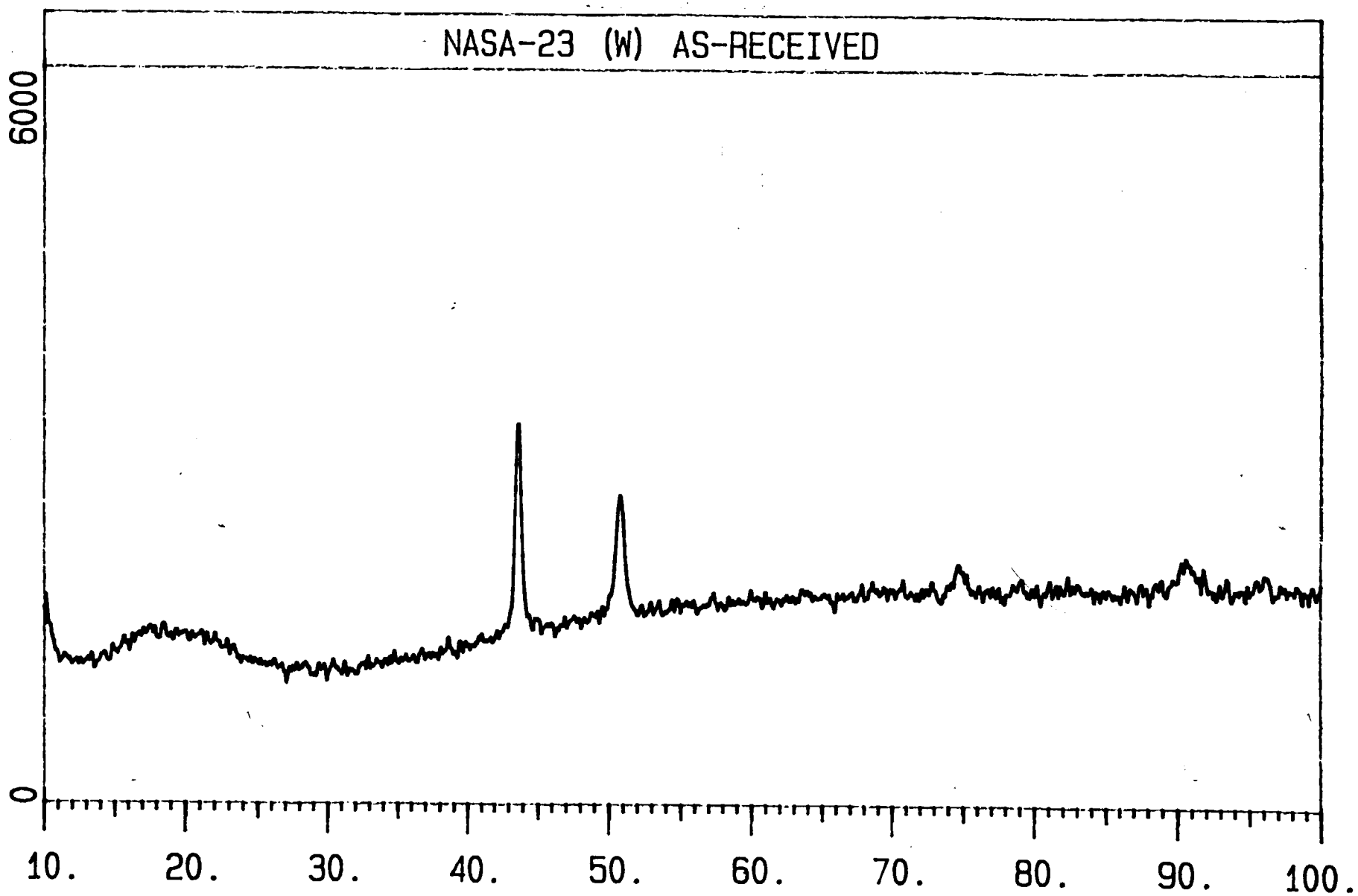
NASA-23 (W) AS-RECEIVED
6000
0
10.
20.
30.
40.
50.
60.
70.
80.
90.
100.

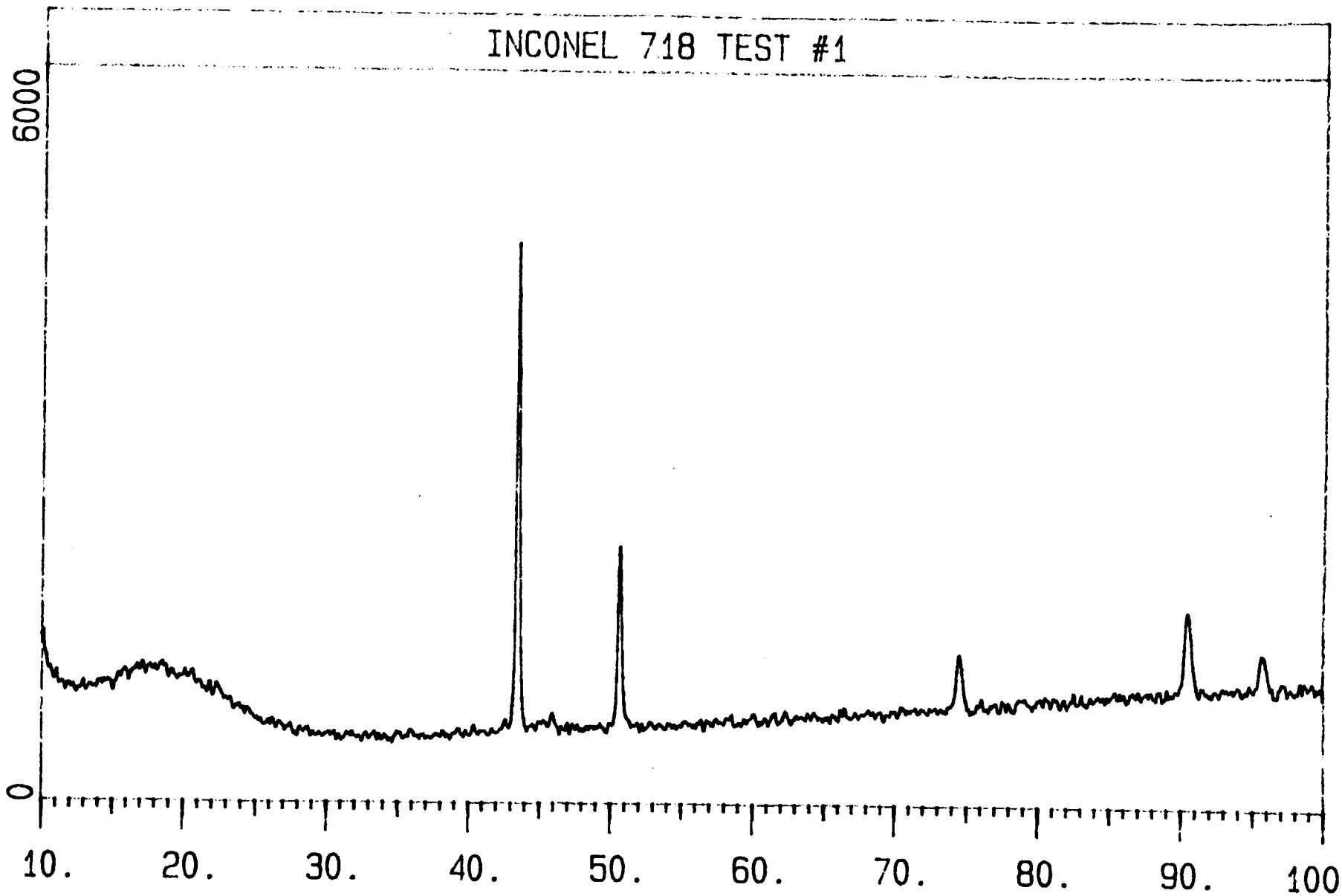
INCONEL 718 TEST #1
6000
0
10.
20.
30.
40.
50.
60.
70.
80.
90.
100.

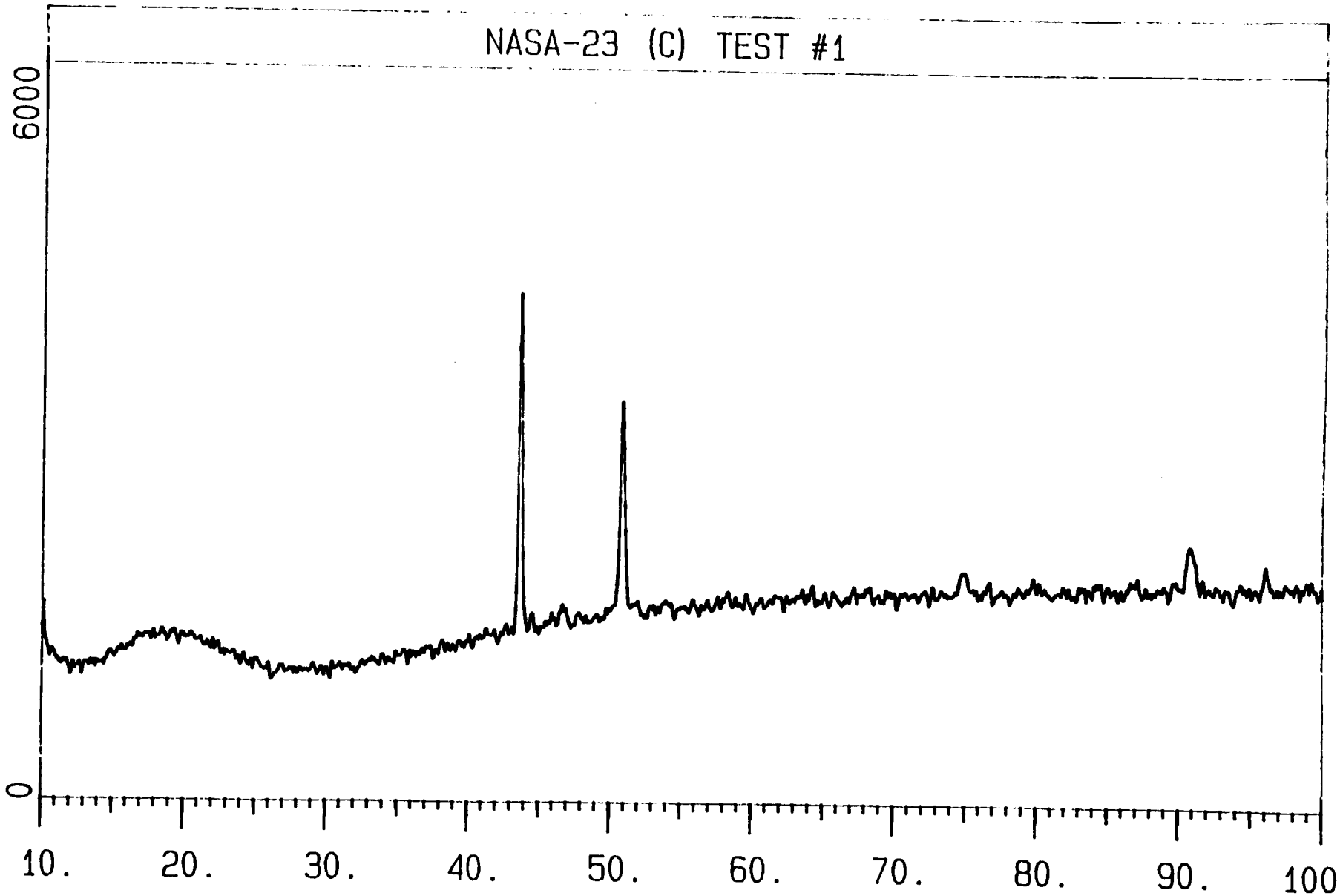
NASA-23 (C) TEST #1
6000
0
10.
20.
30.
40.
50.
60.
70.
80.
90.
100.

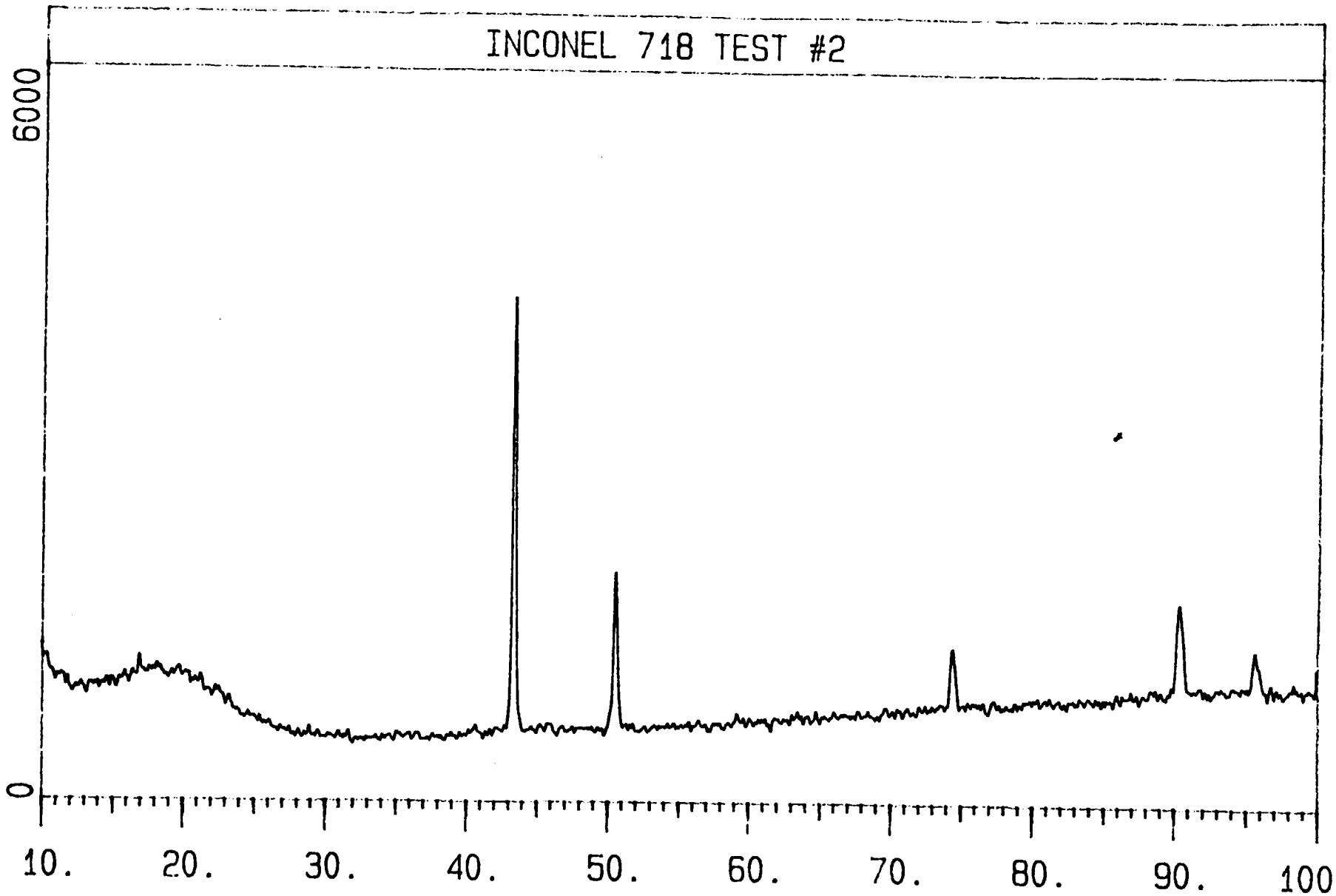
INCONEL 718 TEST #2
6000
0
10.
20.
30.
40.
50.
60.
70.
80.
90.
100.

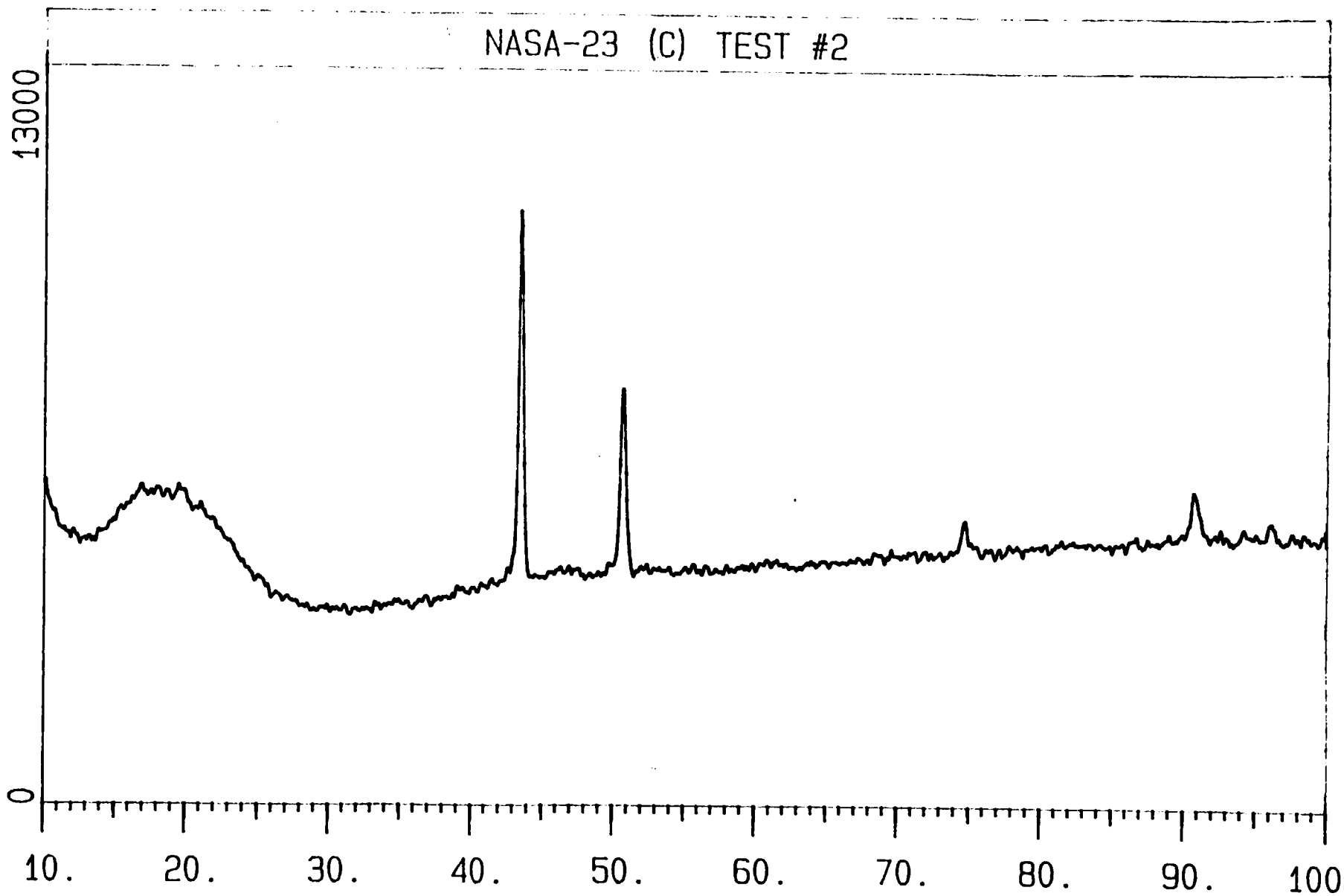
NASA-23 (C) TEST #2
13000
0
10.
20.
30.
40.
50.
60.
70.
80.
90.
100.

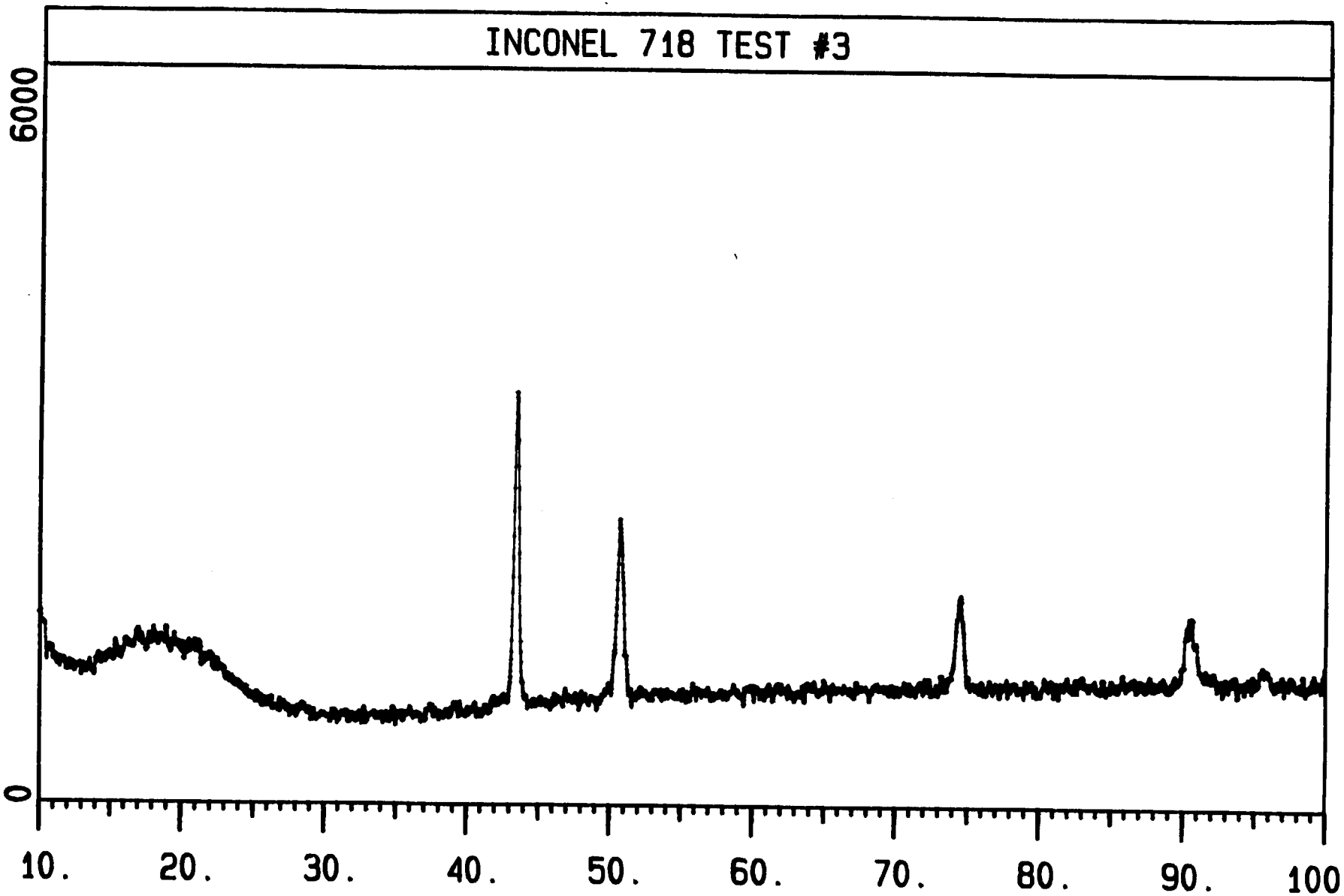
INCONEL 718 TEST #3
6000
0
10.
20.
30.
40.
50.
60.
70.
80.
90.
100.

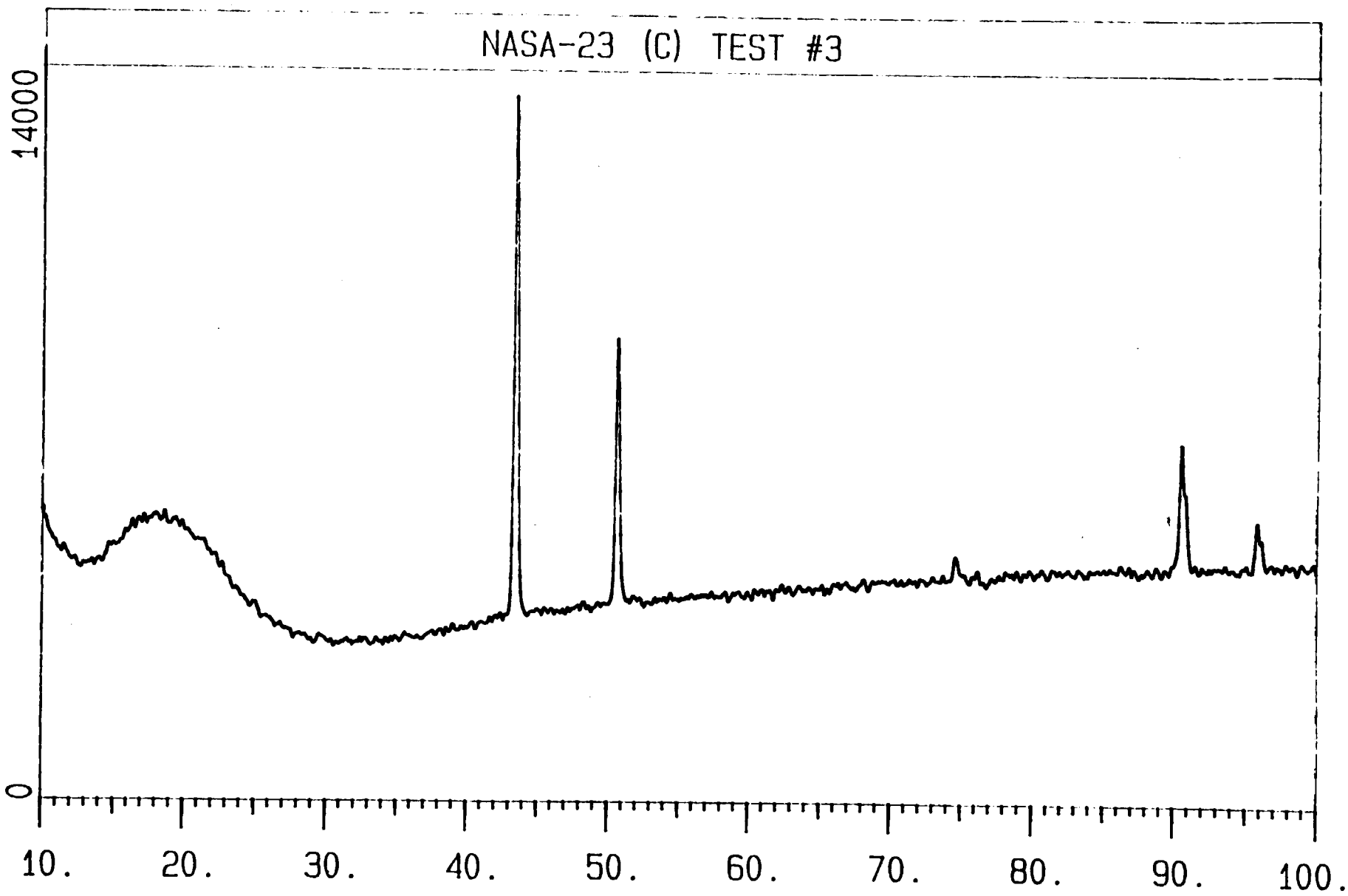
NASA-23 (C) TEST #3
14000
0
10.
20.
30.
40.
50.
60.
70.
80.
90.
100.

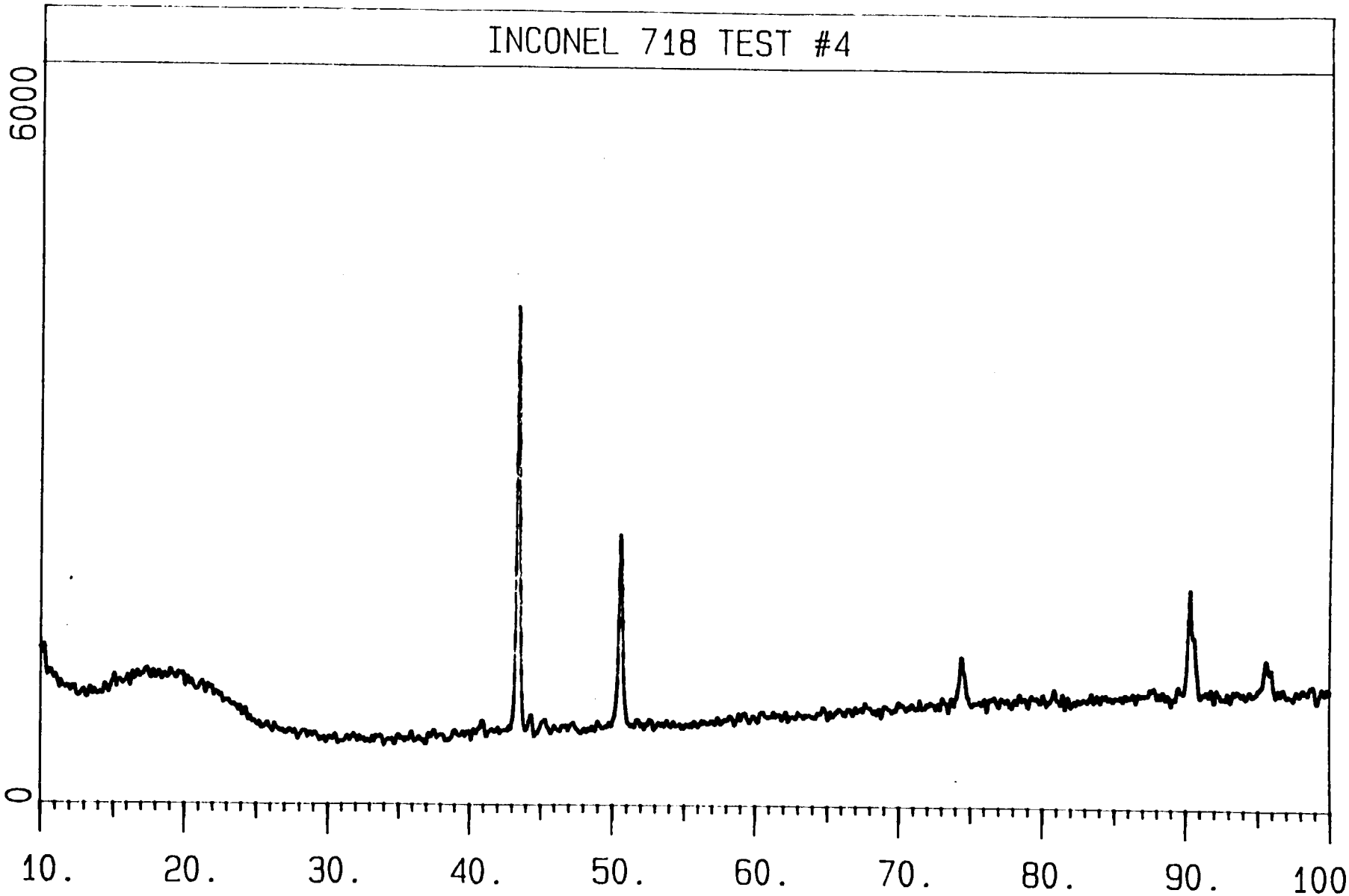
INCONEL 718 TEST #4
6000
0
10.
20.
30.
40.
50.
60.
70.
80.
90.
100.

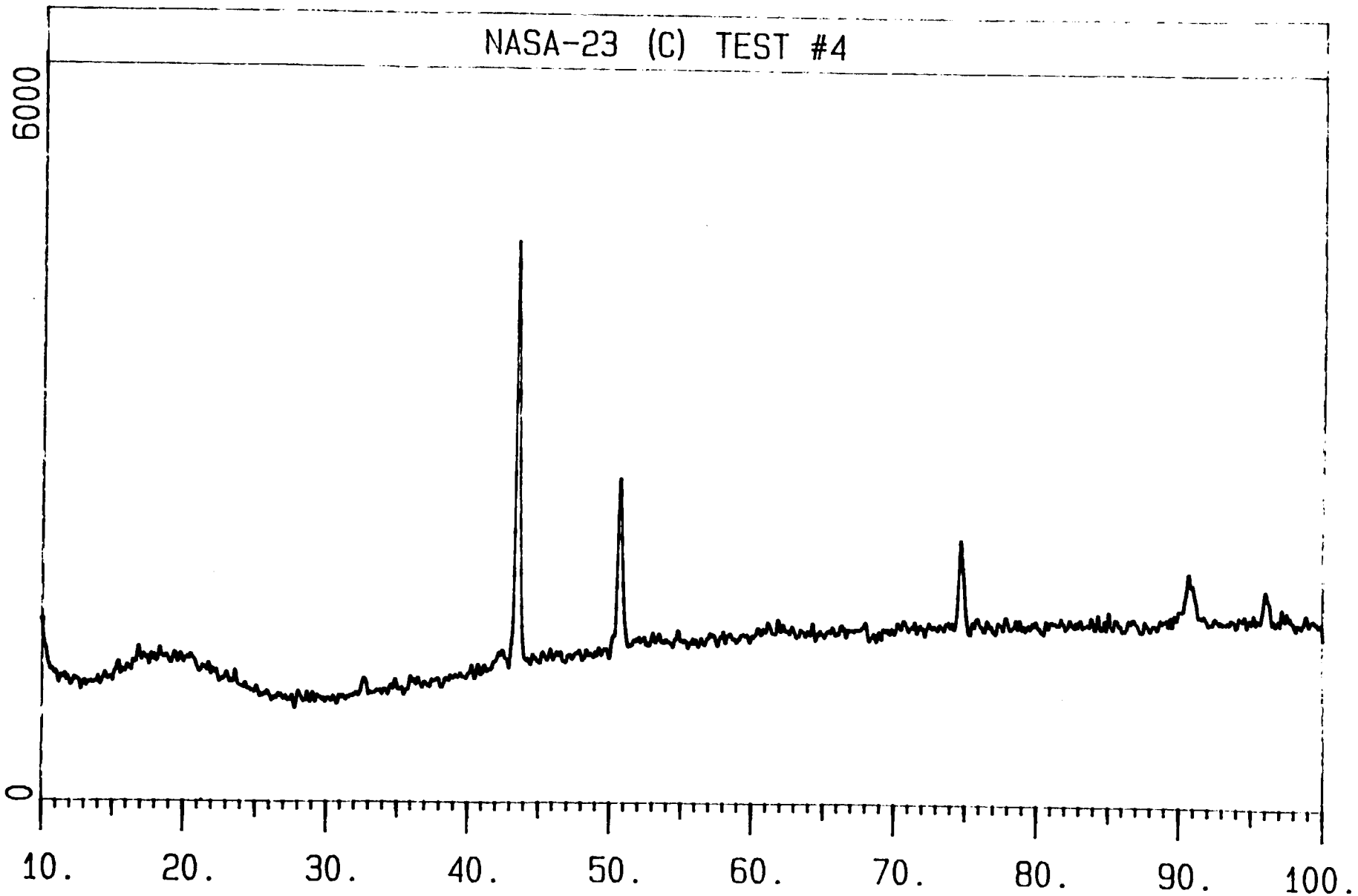
NASA-23 (C) TEST #4
6000
0
10.
20.
30.
40.
50.
60.
70.
80.
90.
100.

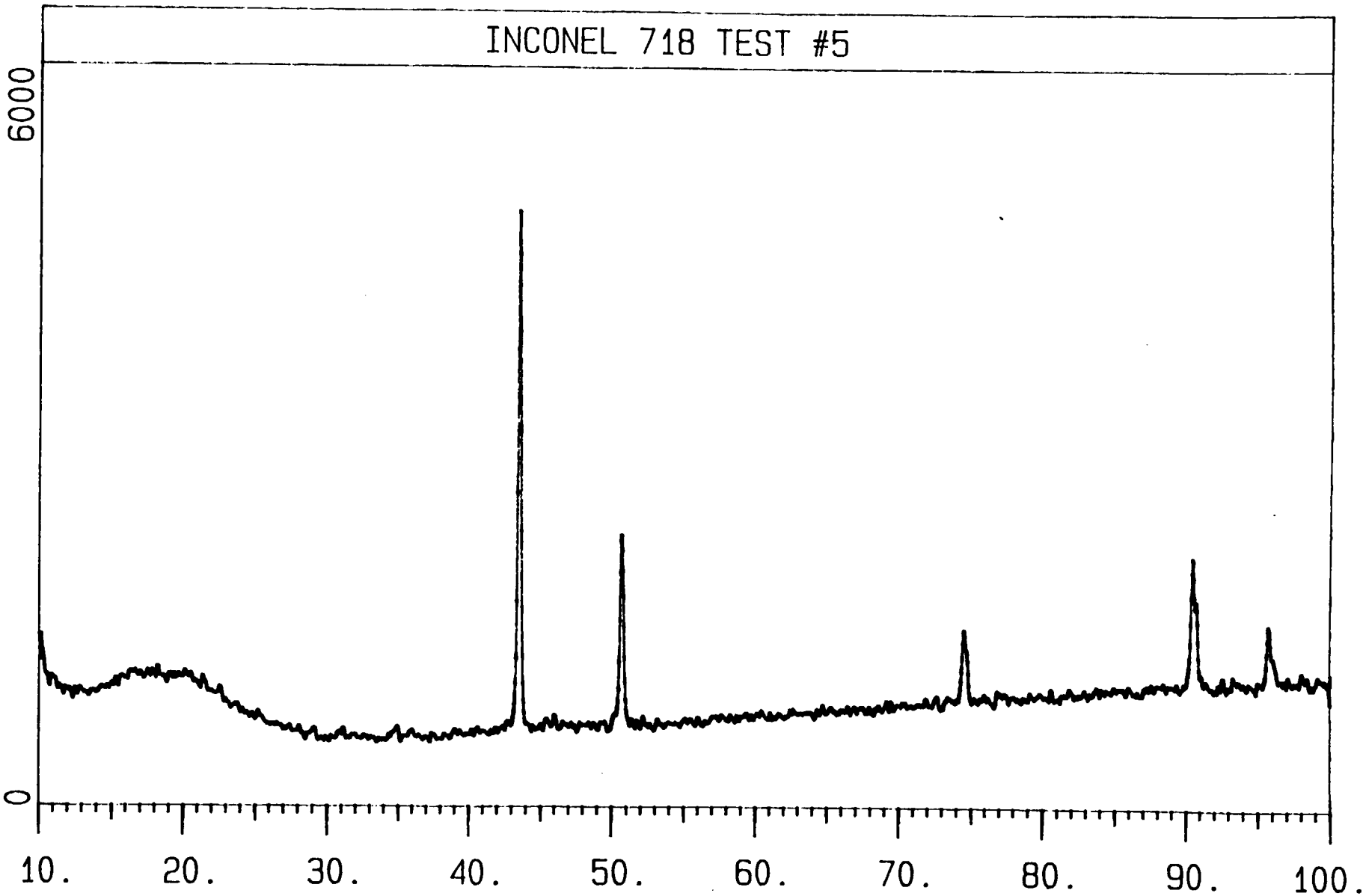
INCONEL 718 TEST #5
6000
0
10.
20.
30.
40.
50.
60.
70.
80.
90.
100.

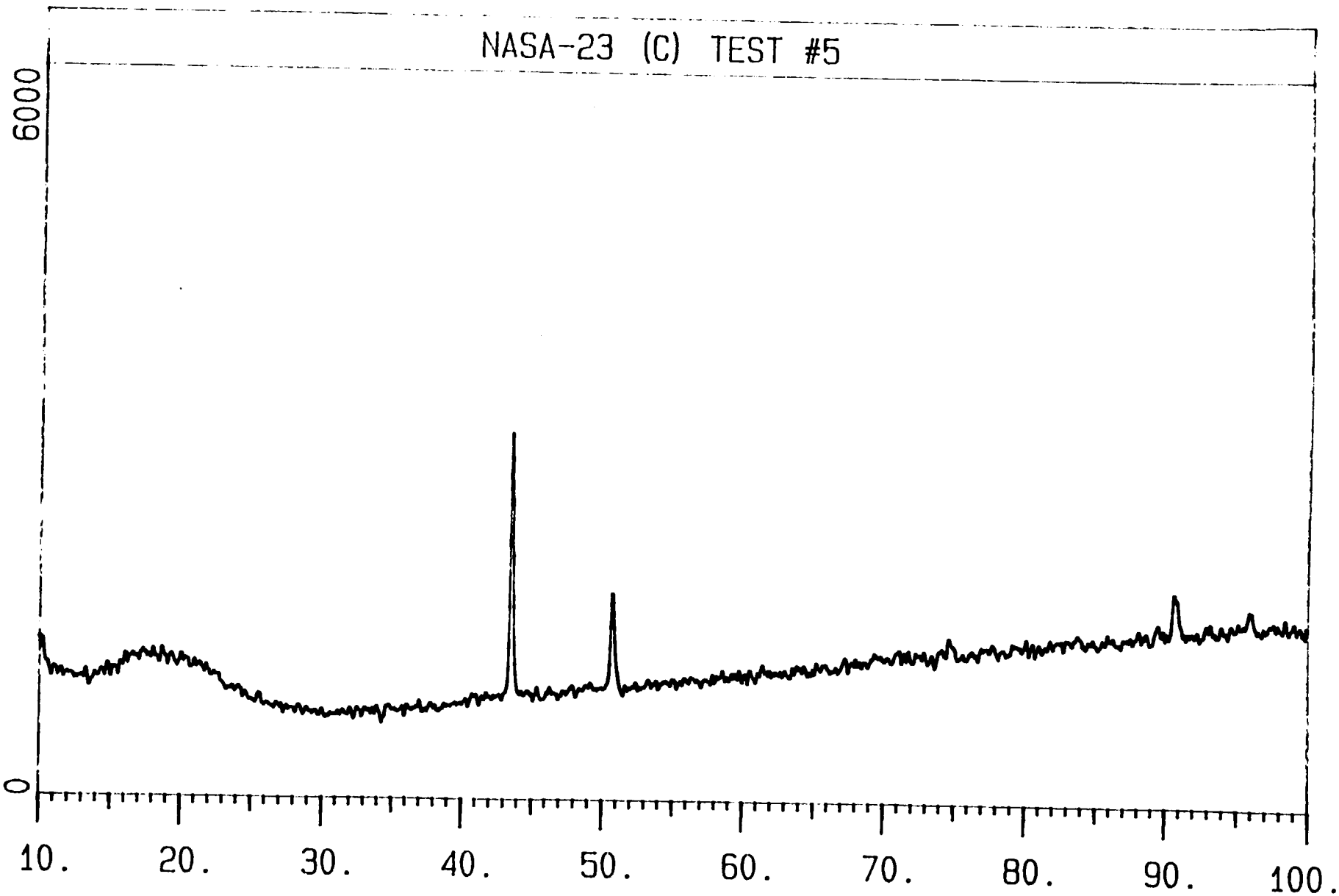
NASA-23 (C) TEST #5
6000
0
10.
20.
30.
40.
50.
60.
70.
80.
90.
100.

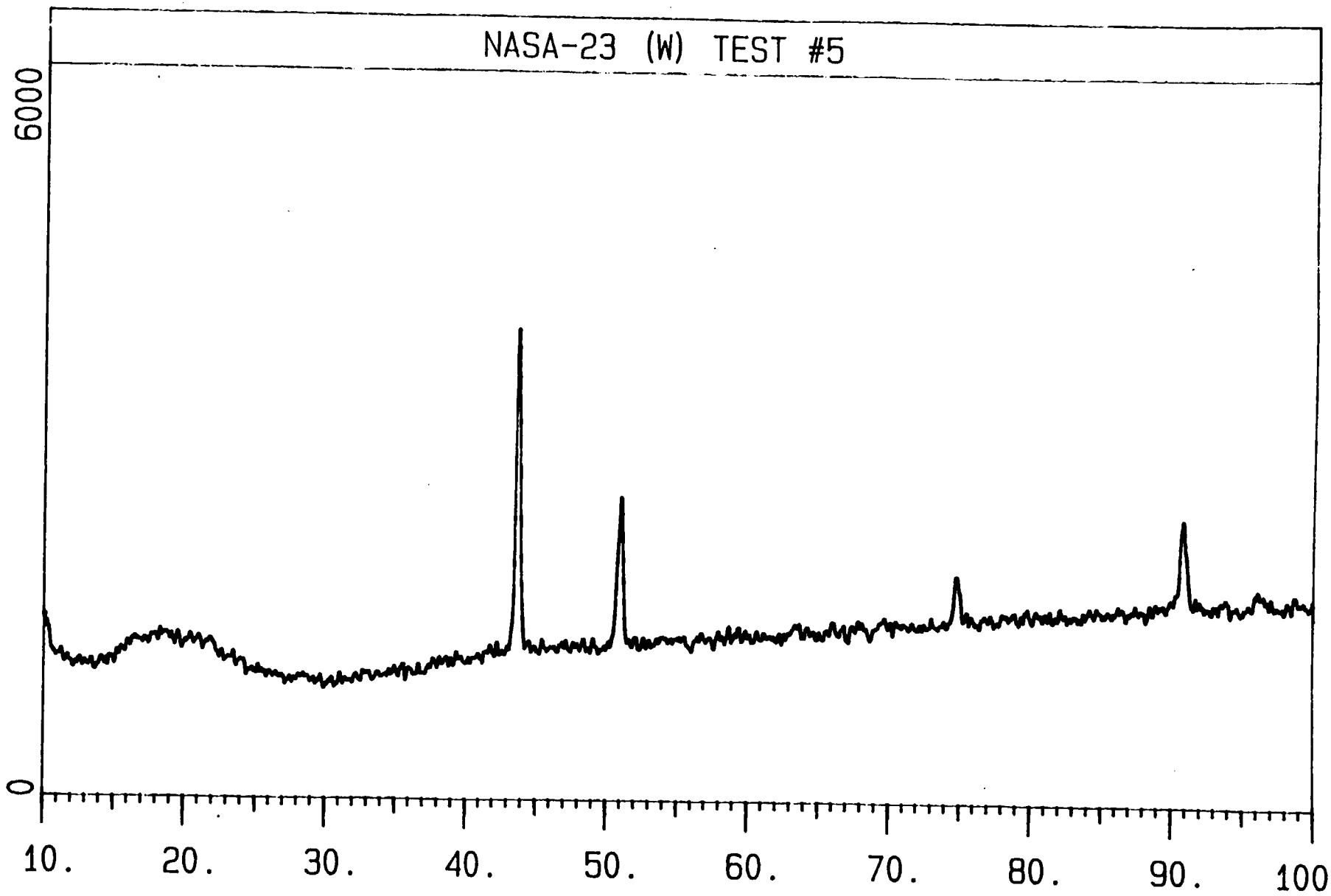
NASA-23 (W) TEST #5
6000
0
10.
20.
30.
40.
50.
60.
70.
80.
90.
100.

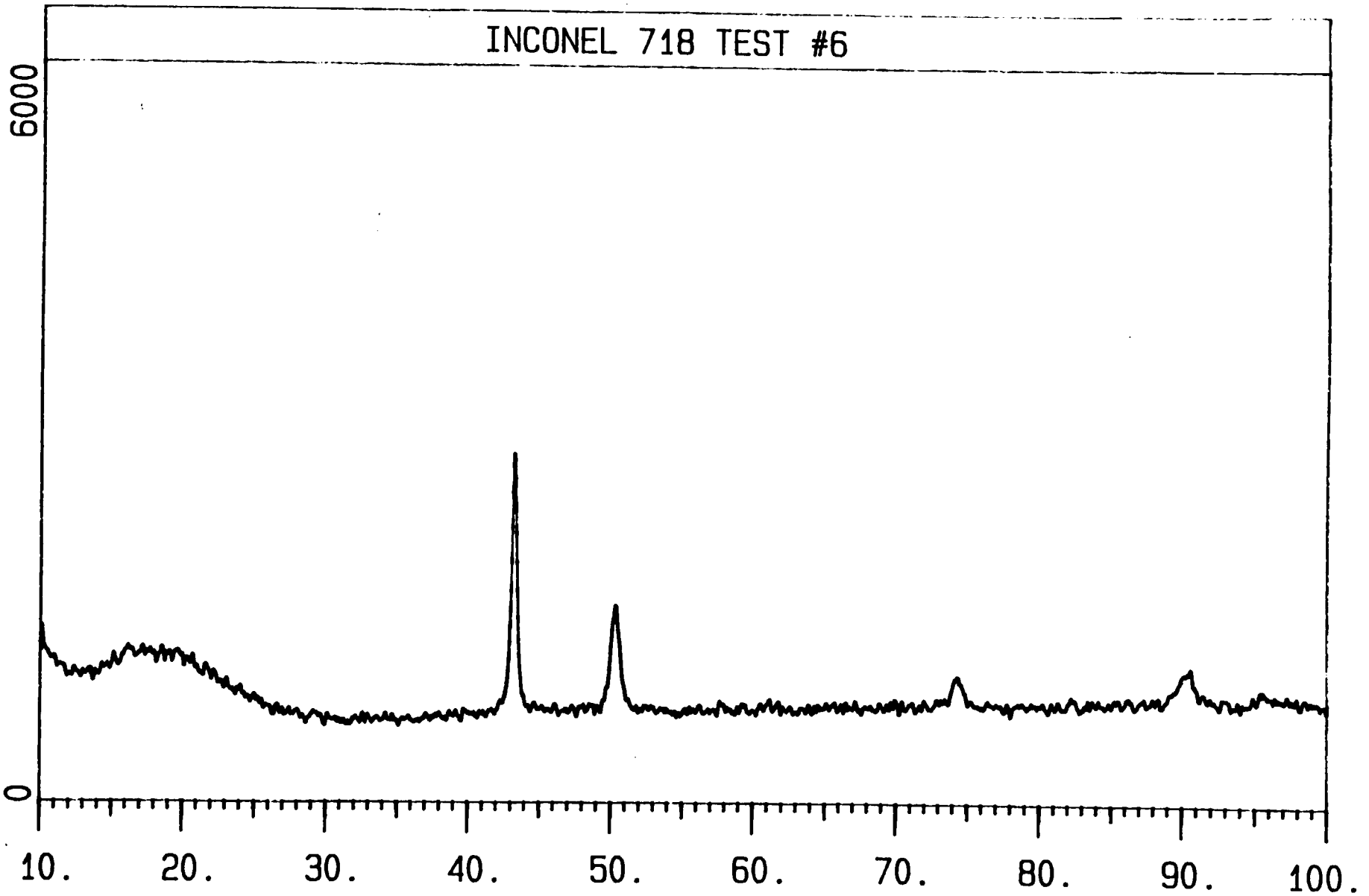
INCONEL 718 TEST #6
6000
0
10.
20.
30.
40.
50.
60.
70.
80.
90.
100.

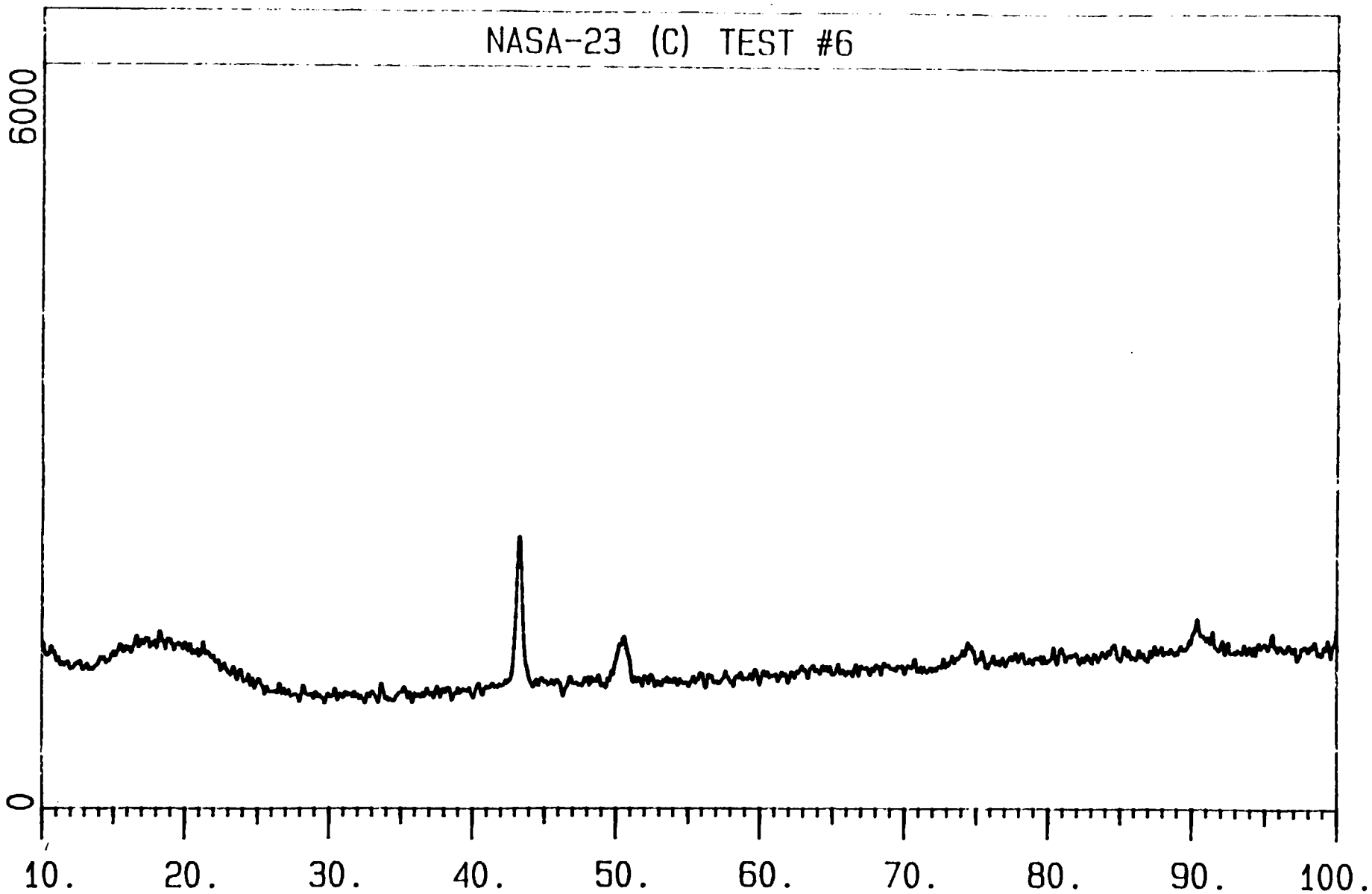
NASA-23 (C) TEST #6
6000
0
10.
20.
30.
40.
50.
60.
70.
80.
90.
100.

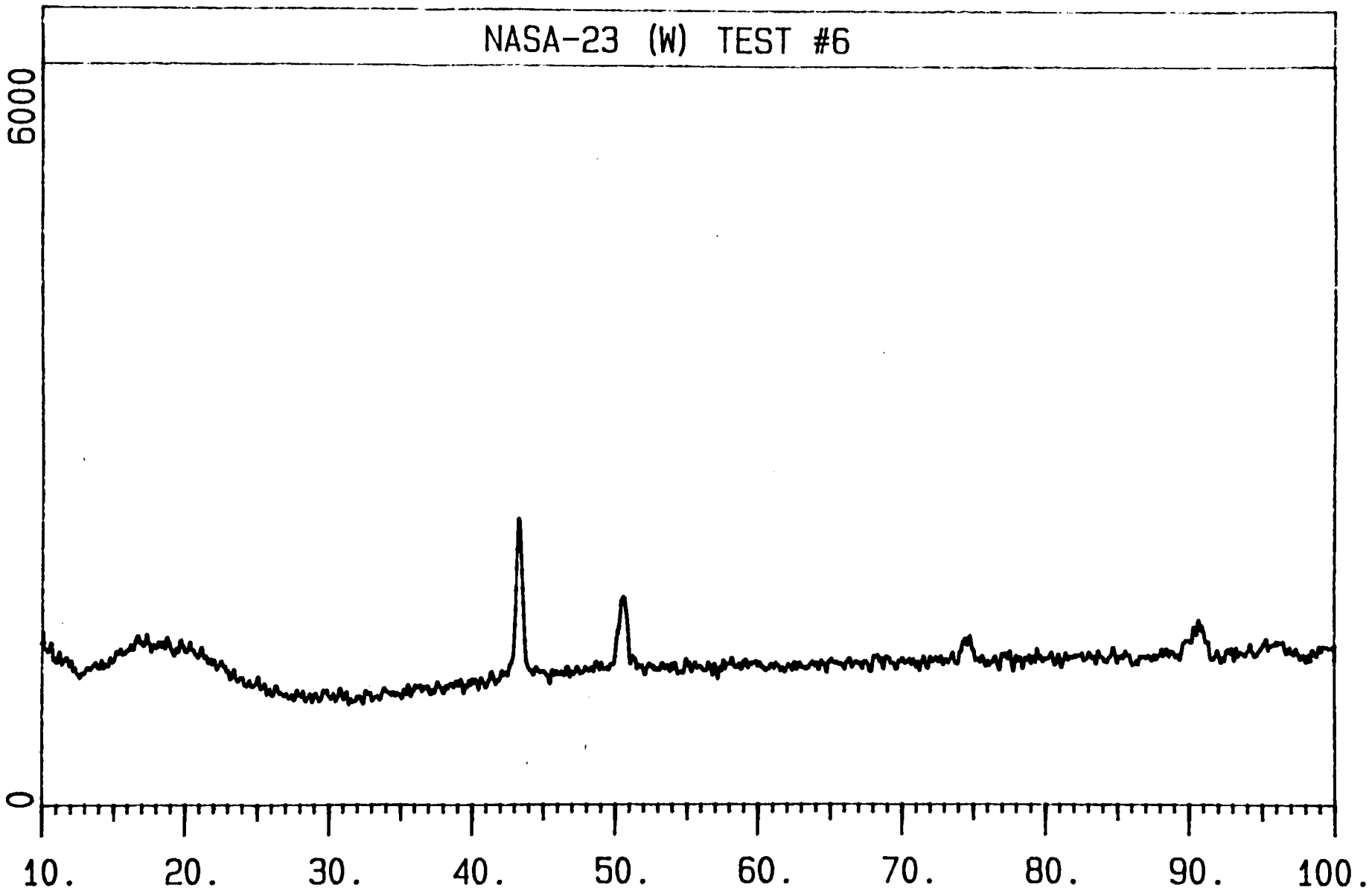
NASA-23 (W) TEST #6
6000
0
10.
20.
30.
40.
50.
60.
70.
80.
90.
100.

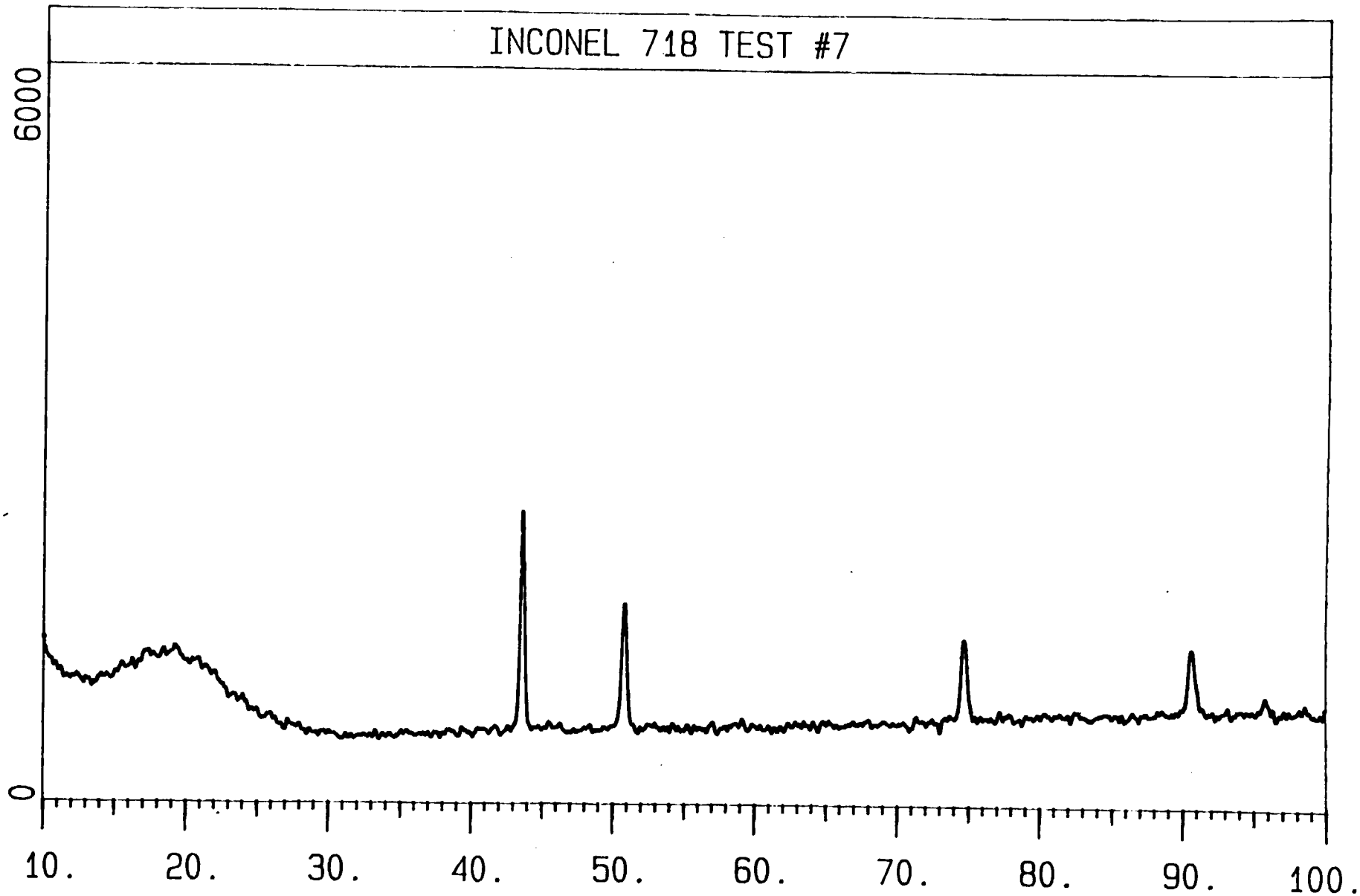
INCONEL 718 TEST #7
6000
0
10.
20.
30.
40.
50.
60.
70.
80.
90.
100.

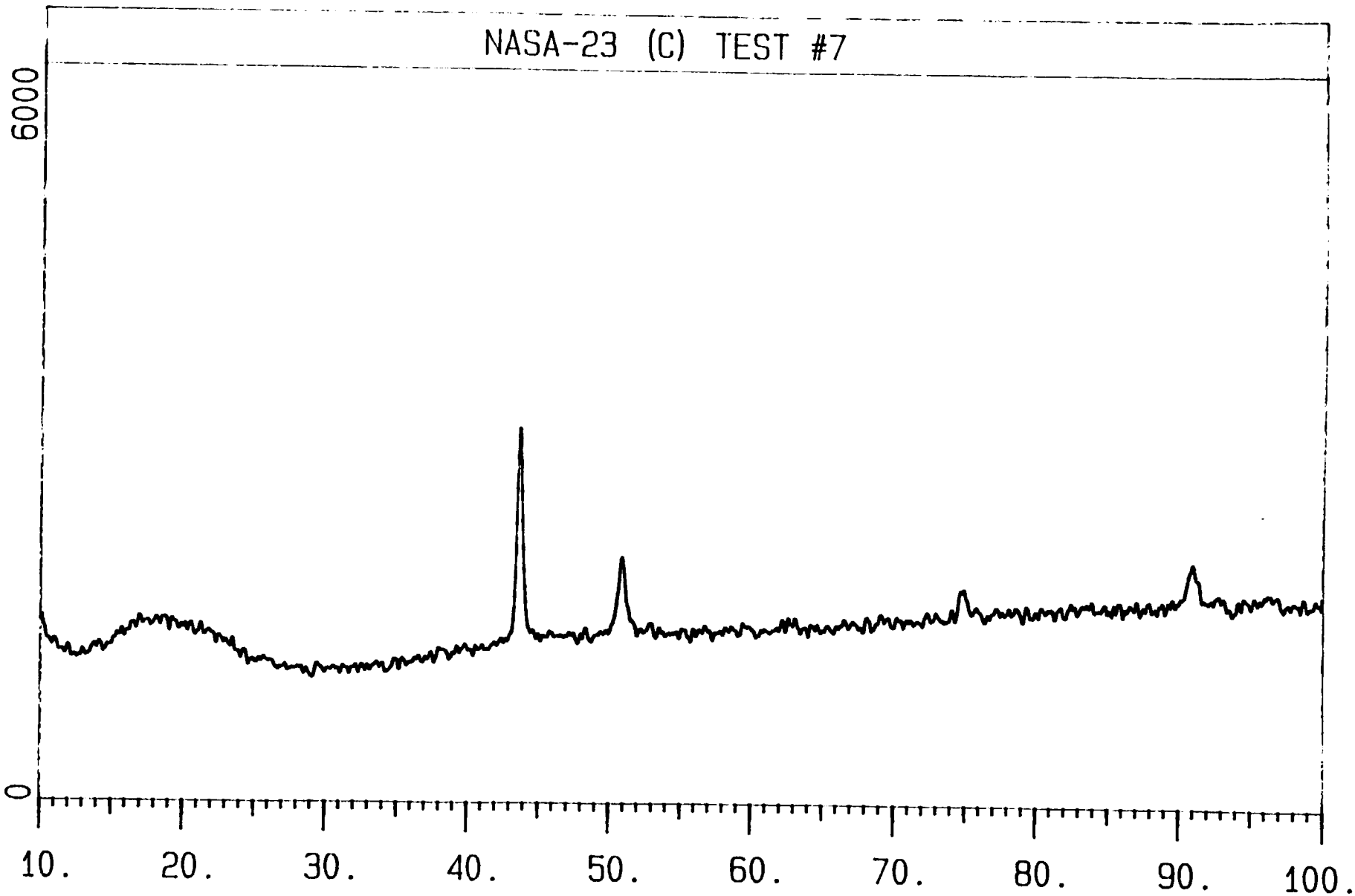
NASA-23 (C) TEST #7
6000
0
10.
20.
30.
40.
50.
60.
70.
80.
90.
100.

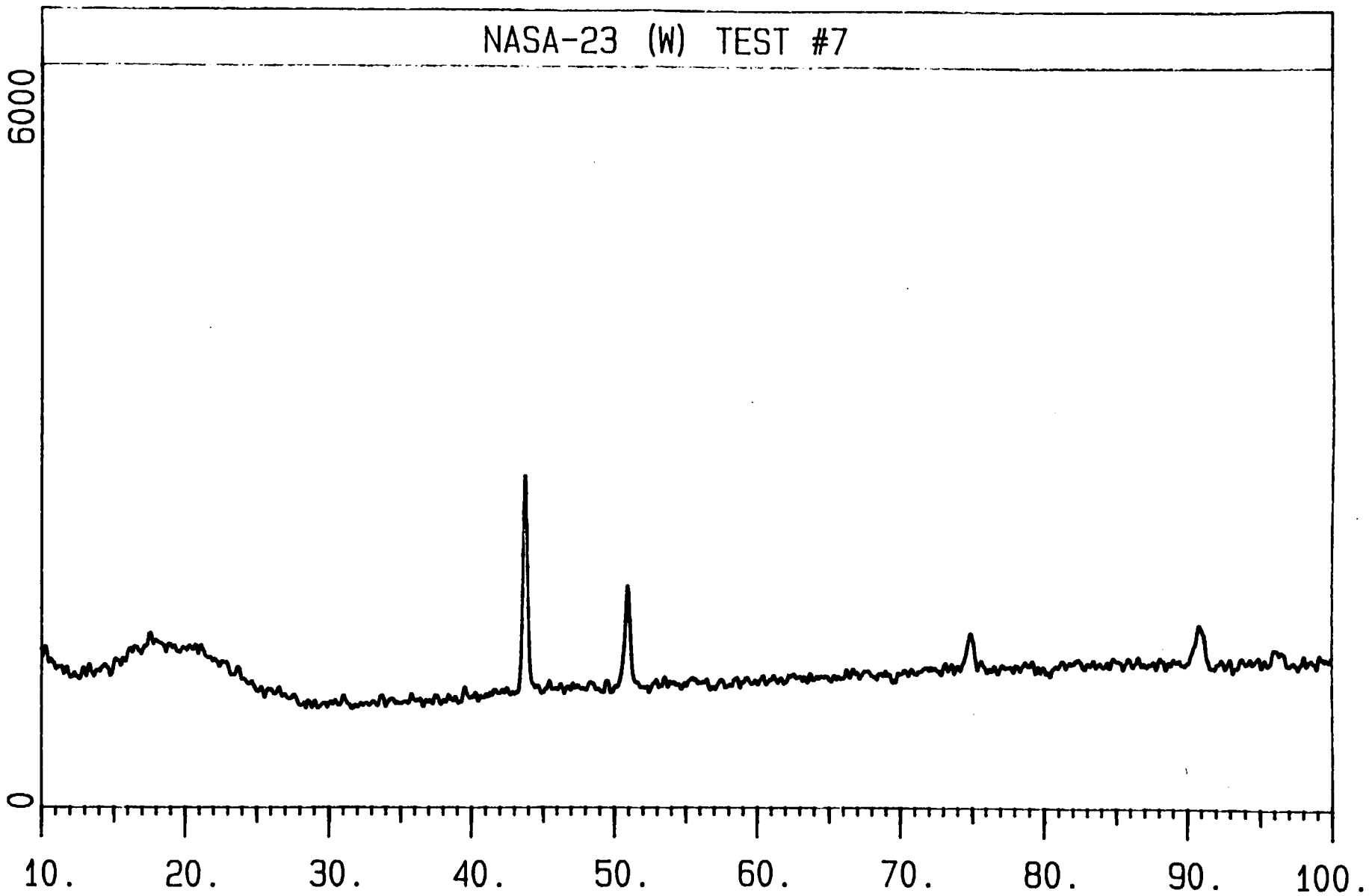
NASA-23 (W) TEST #7
6000
0
10.
20.
30.
40.
50.
60.
70.
80.
90.
100.

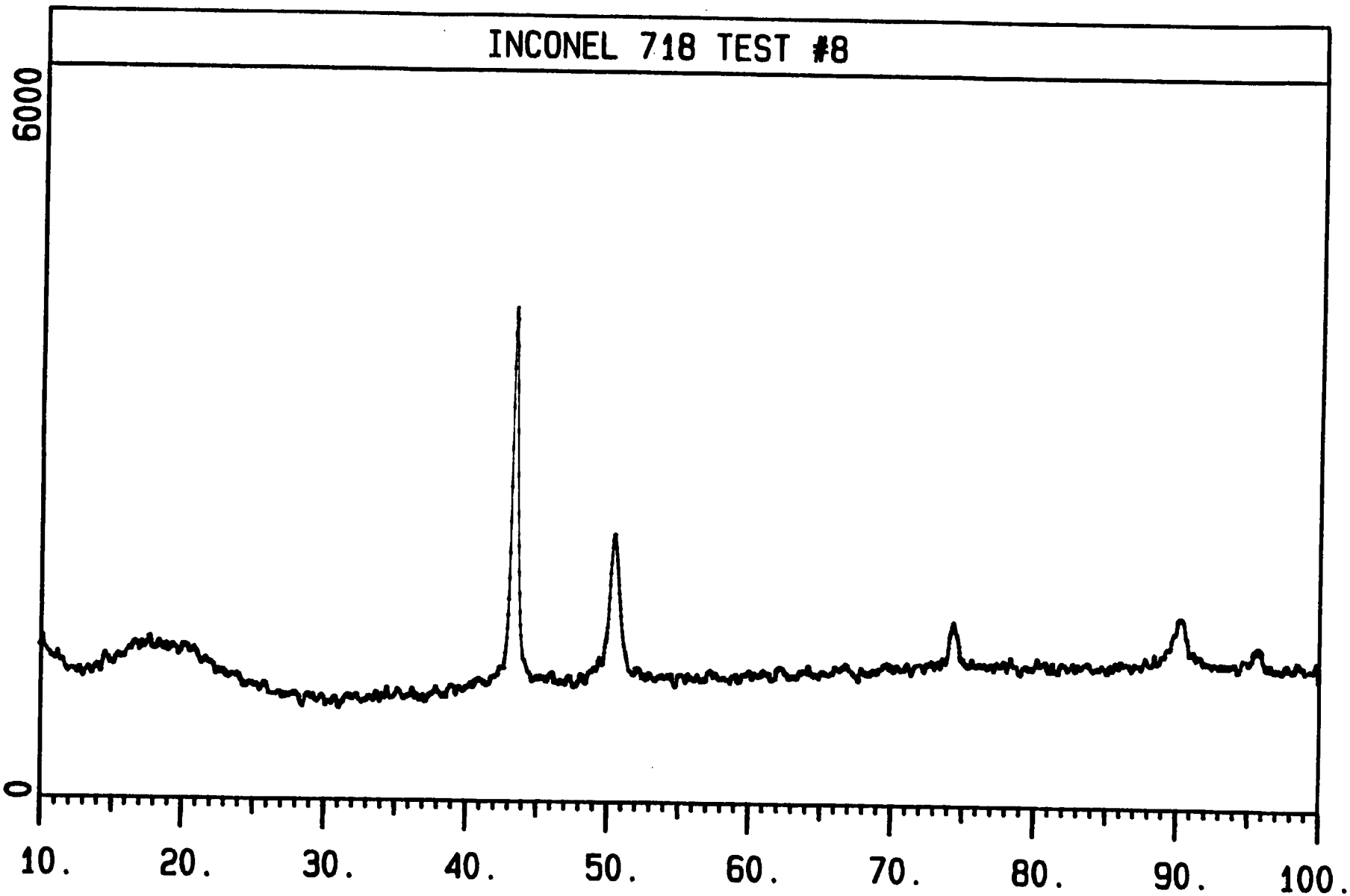
INCONEL 718 TEST #8
6000
0
10.
20.
30.
40.
50.
60.
70.
80.
90.
100.

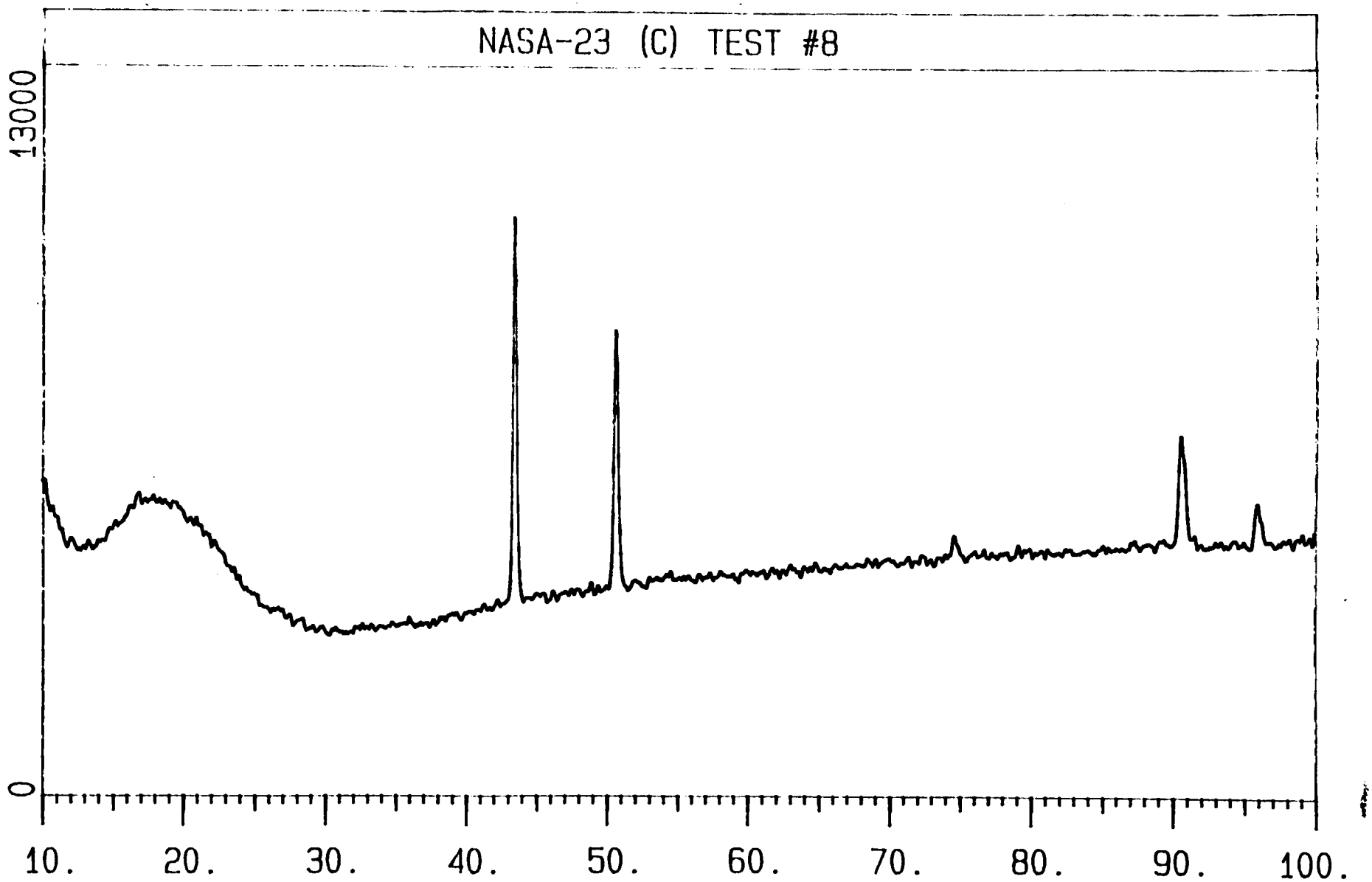
NASA-23 (C) TEST #8
13000
0
10.
20.
30.
40.
50.
60.
70.
80.
90.
100.

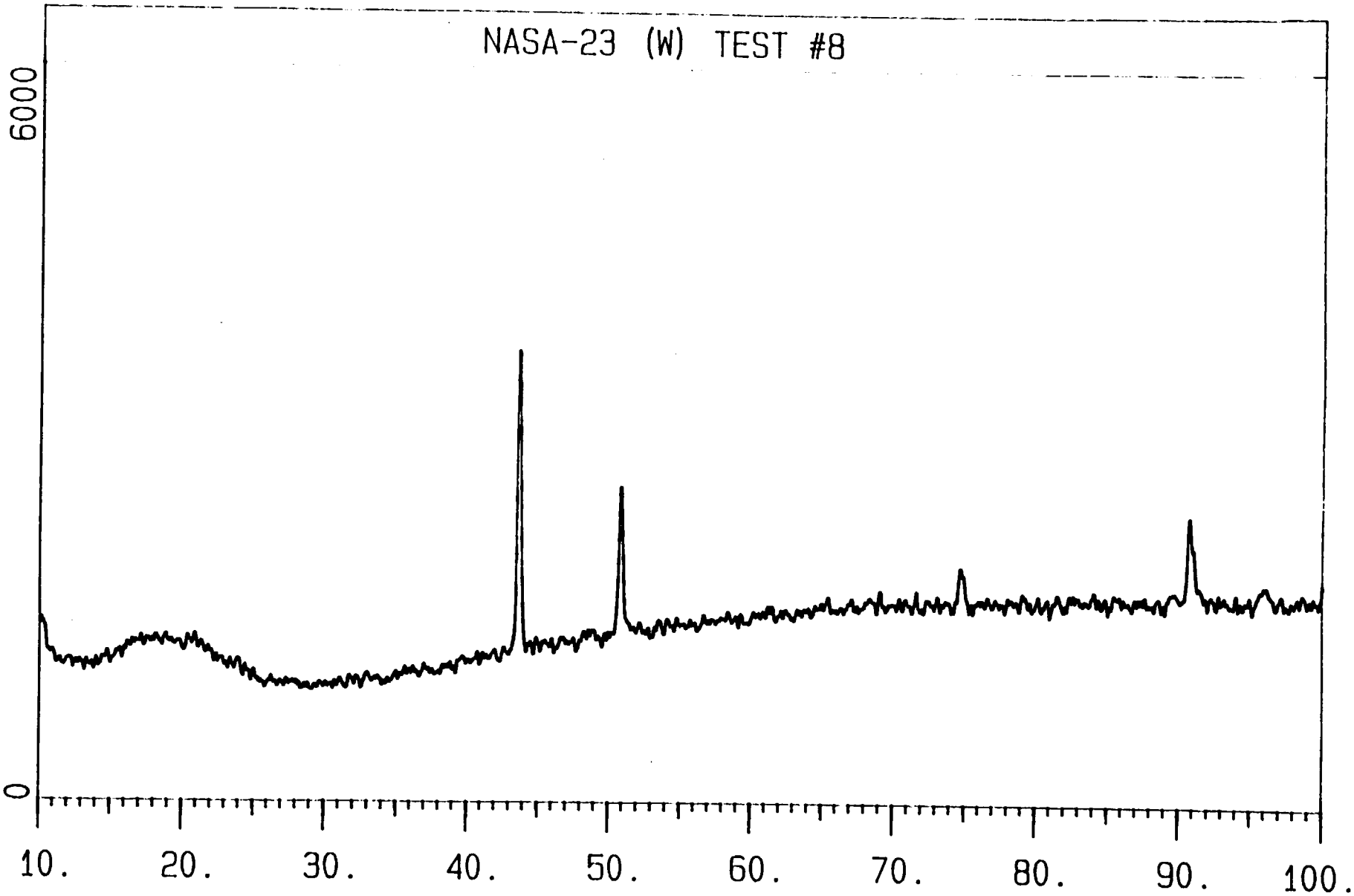
NASA-23 (W) TEST #8
6000
0
10.
20.
30.
40.
50.
60.
70.
80.
90.
100.

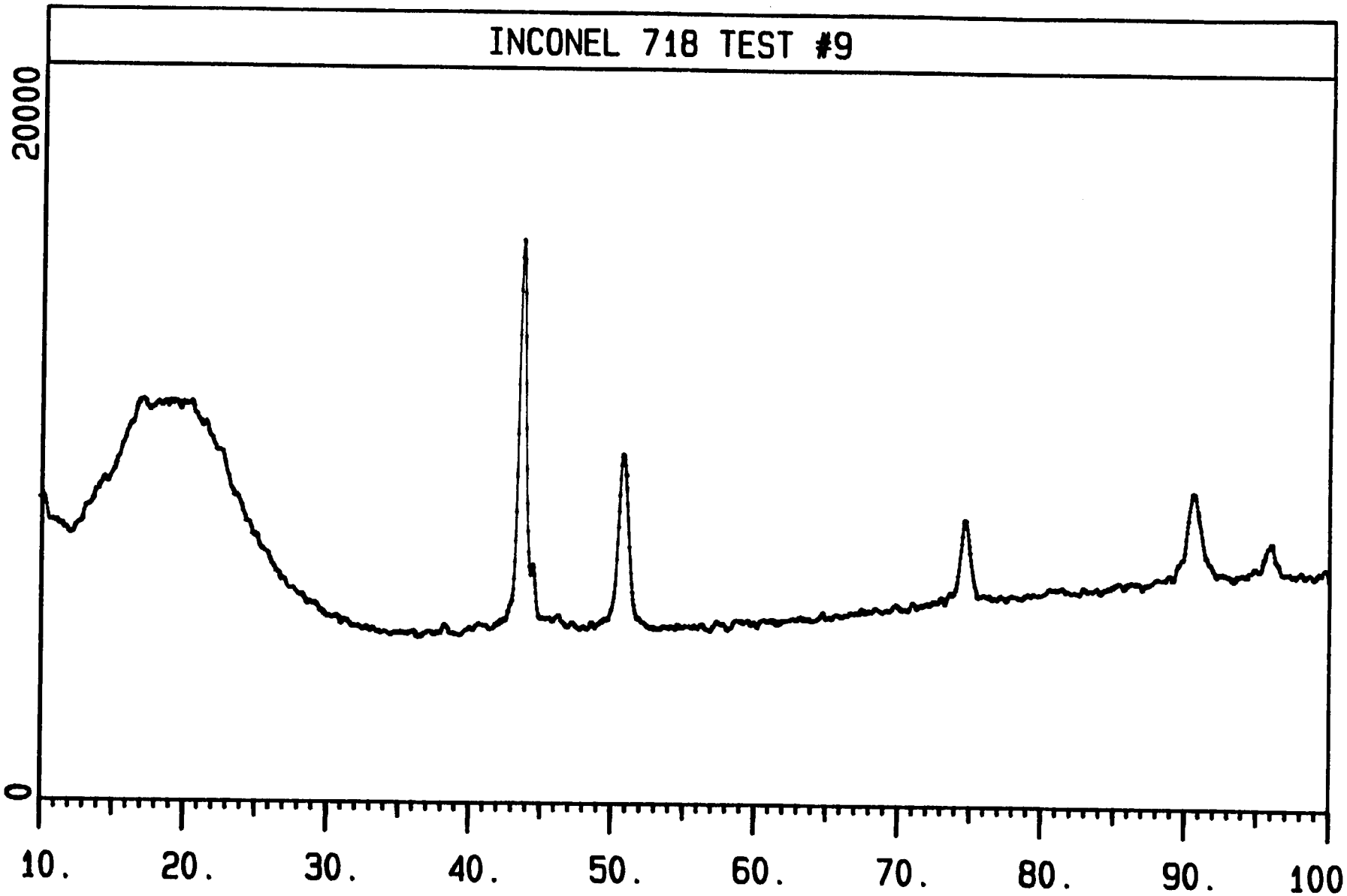
INCONEL 718 TEST #9
20000
0
10.
20.
30.
40.
50.
60.
70.
80.
90.
100.

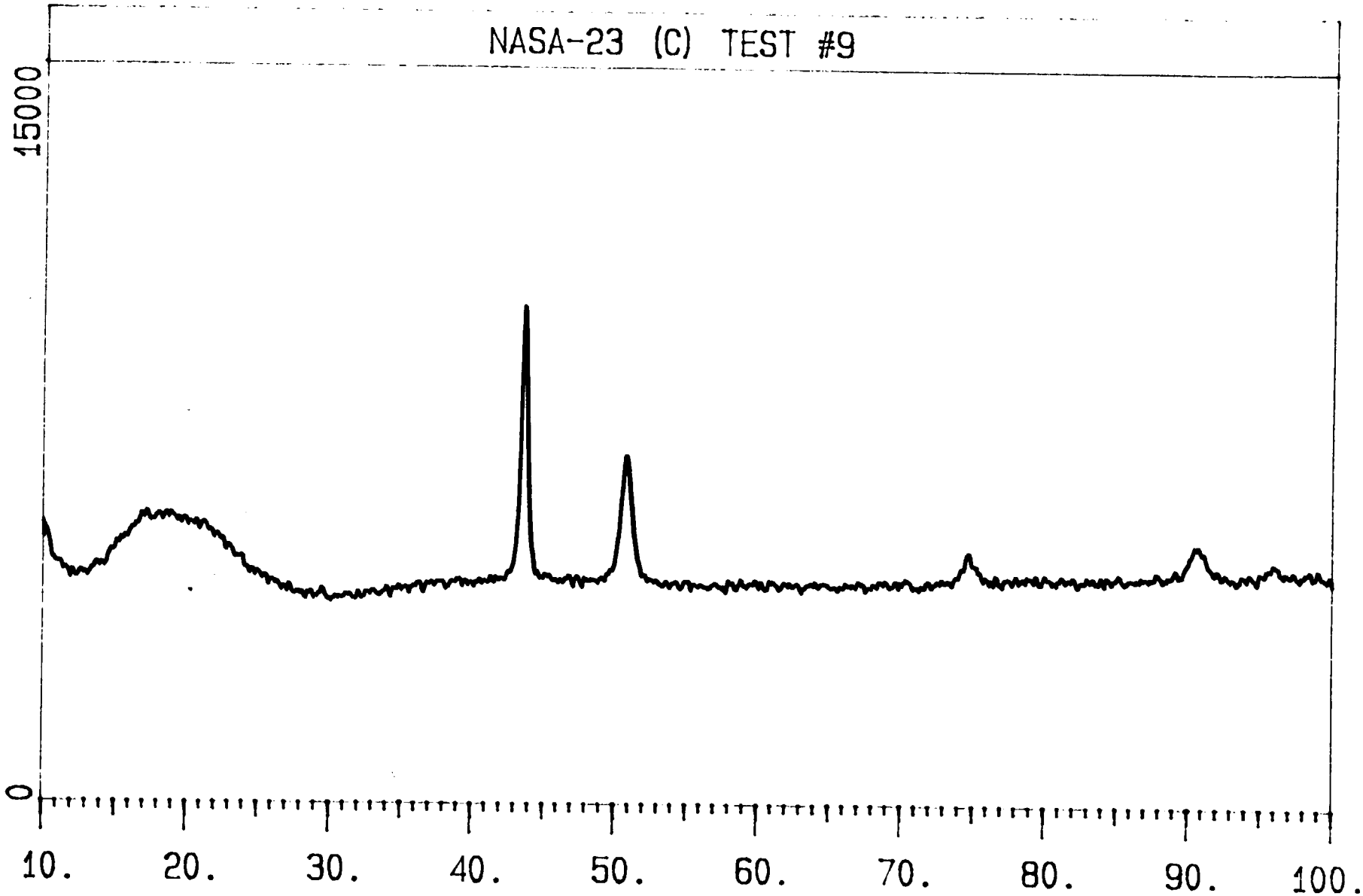
NASA-23 (C) TEST #9
15000
0
10.
20.
30.
40.
50.
60.
70.
80.
90.
100.

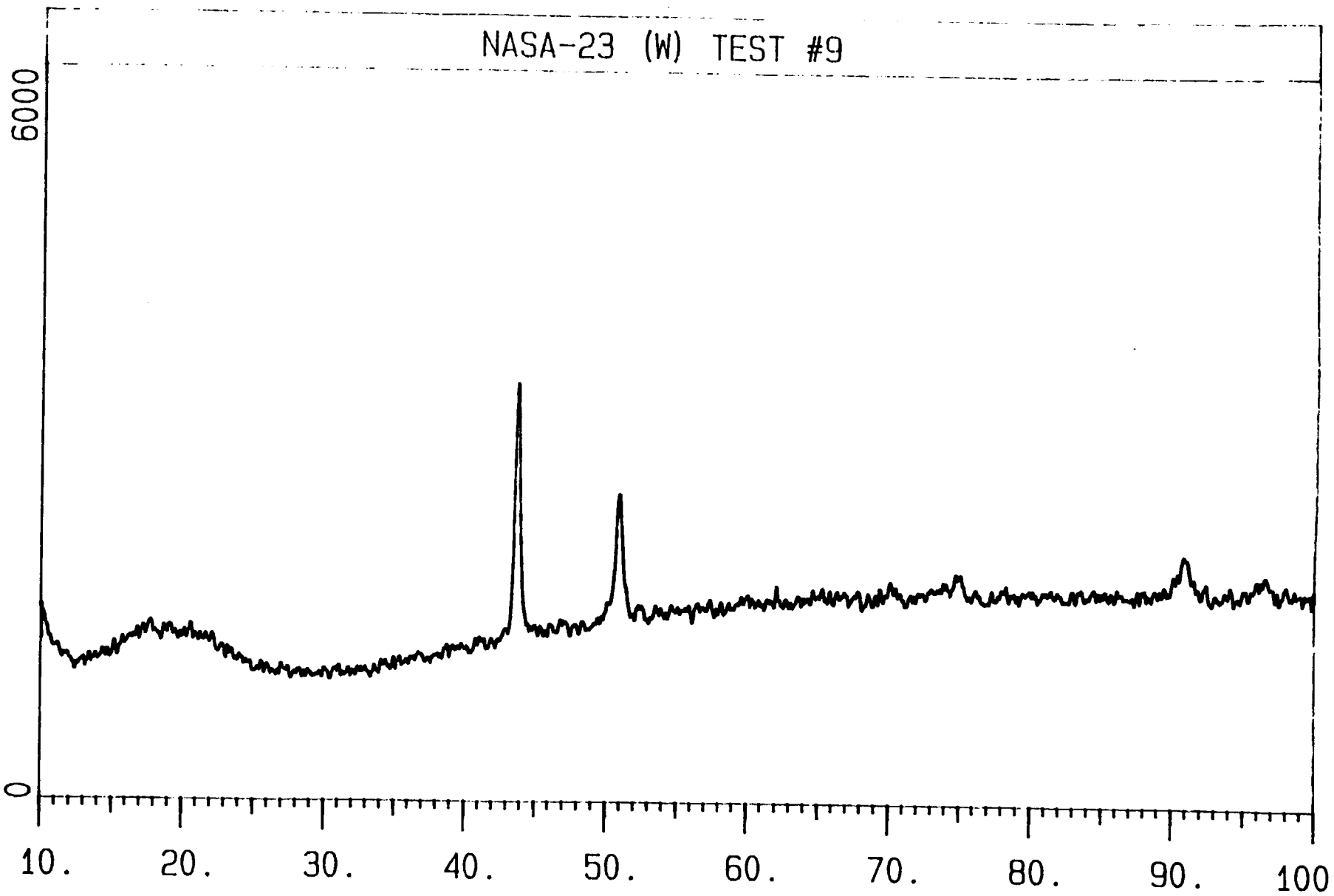
NASA-23 (W) TEST #9
6000
0
10.
20.
30.
40.
50.
60.
70.
80.
90.
100.

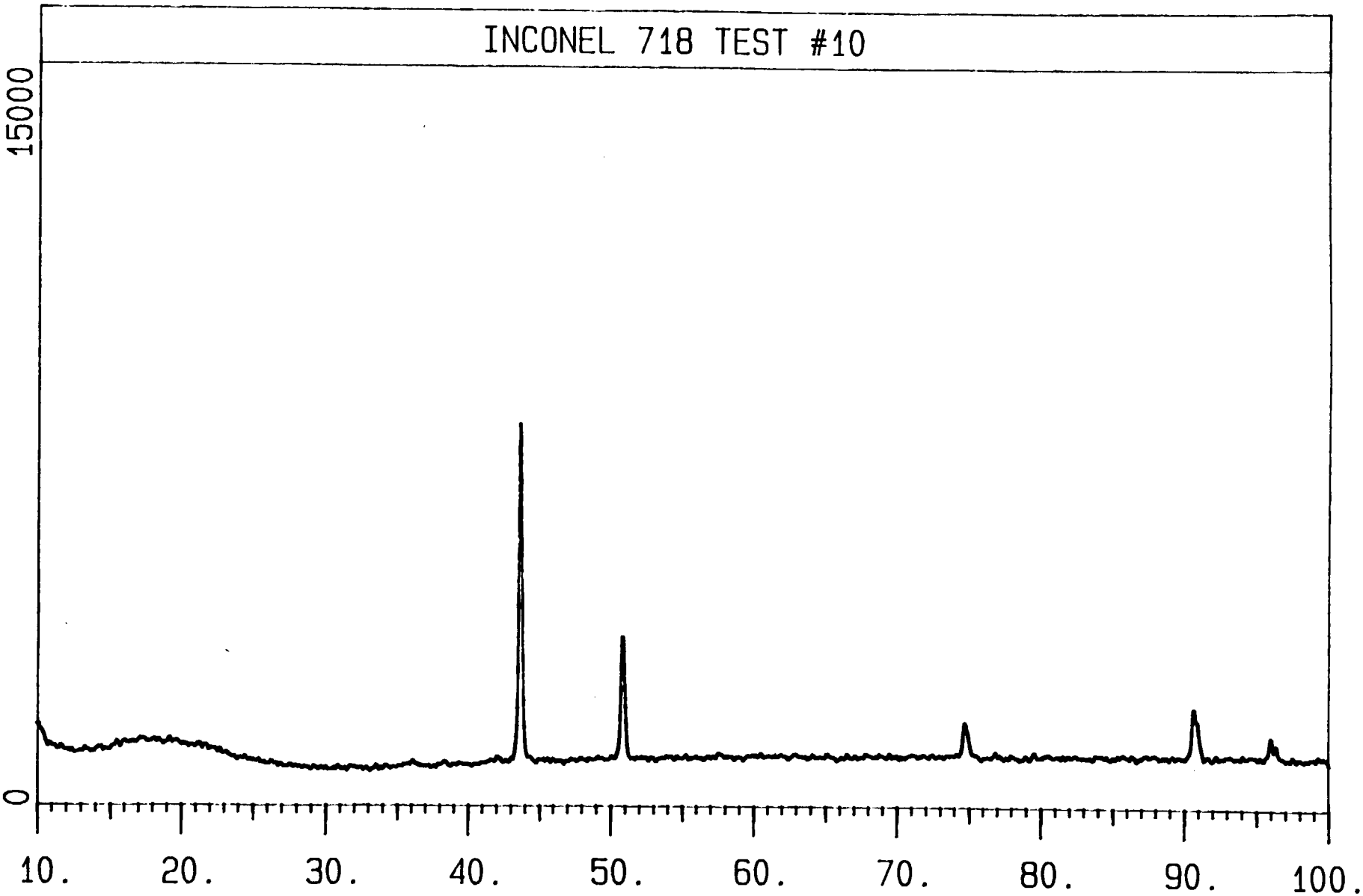
INCONEL 718 TEST #10
15000
0
10.
20.
30.
40.
50.
60.
70.
80.
90.
100.

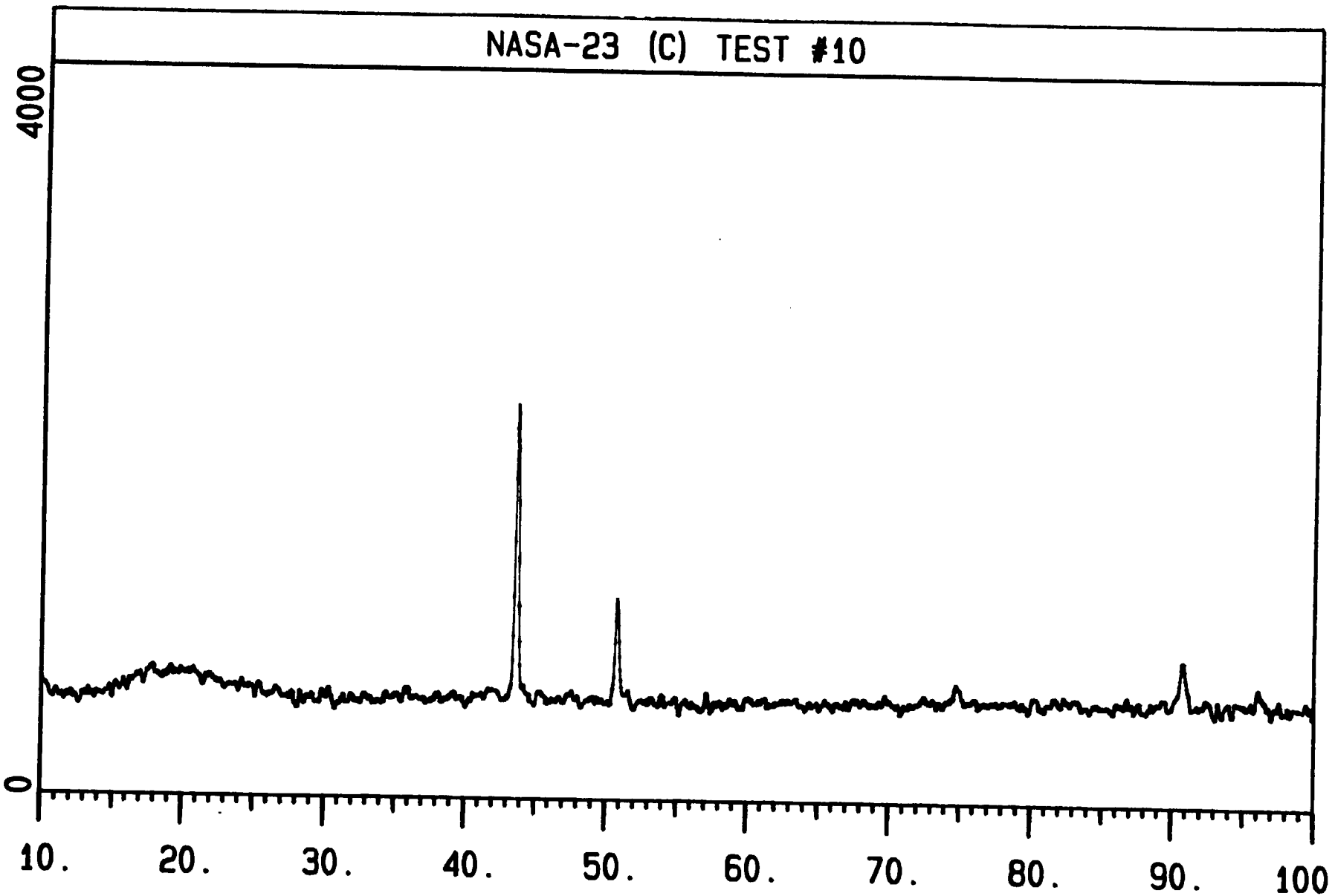
NASA-23 (C) TEST #10
4000
0
10.
20.
30.
40.
50.
60.
70.
80.
90.
100.

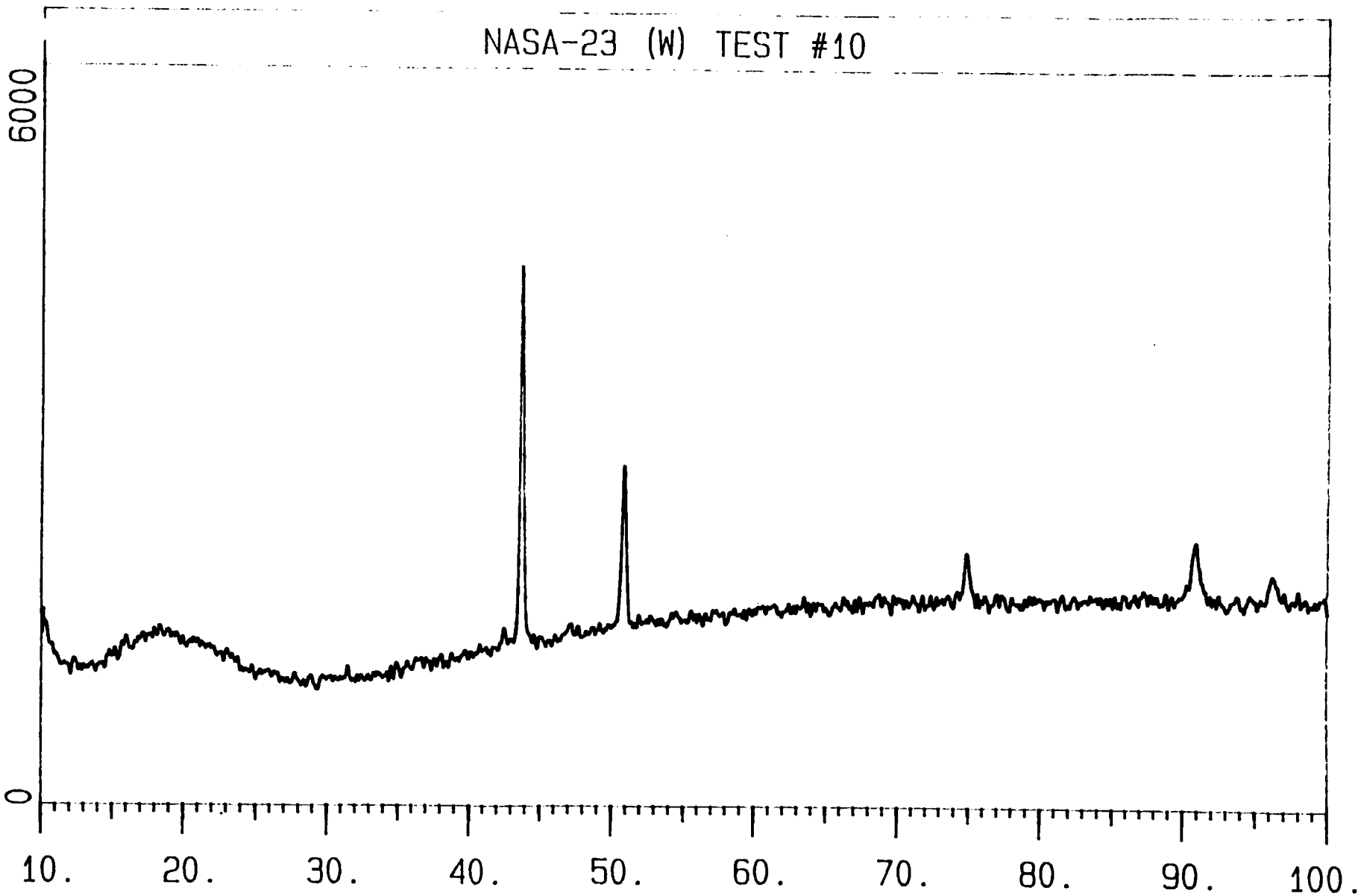
NASA-23 (W) TEST #10
6000
0
10.
20.
30.
40.
50.
60.
70.
80.
90.
100.

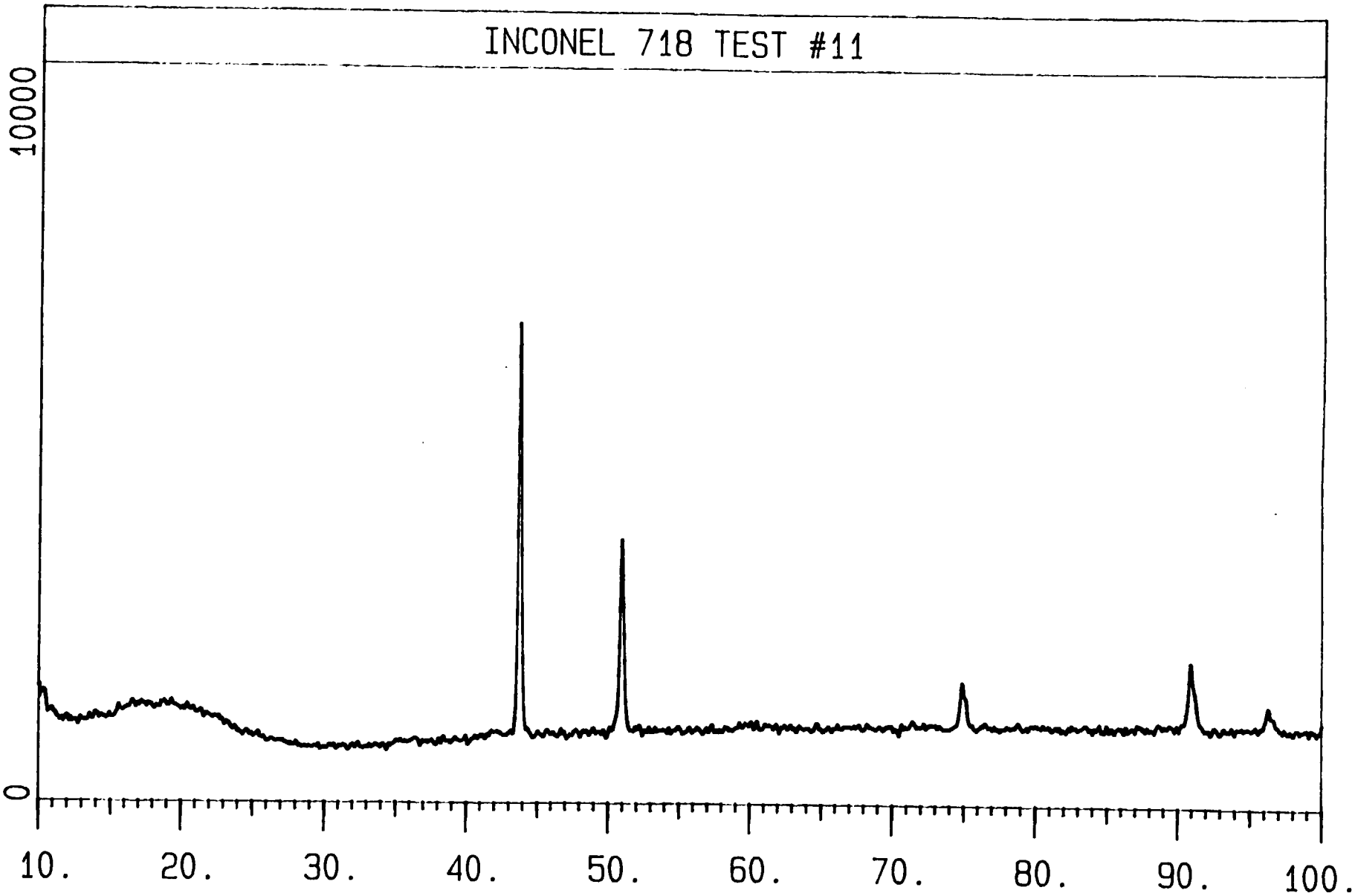
INCONEL 718 TEST #11
10000
0
10.
20.
30.
40.
50.
60.
70.
80.
90.
100.

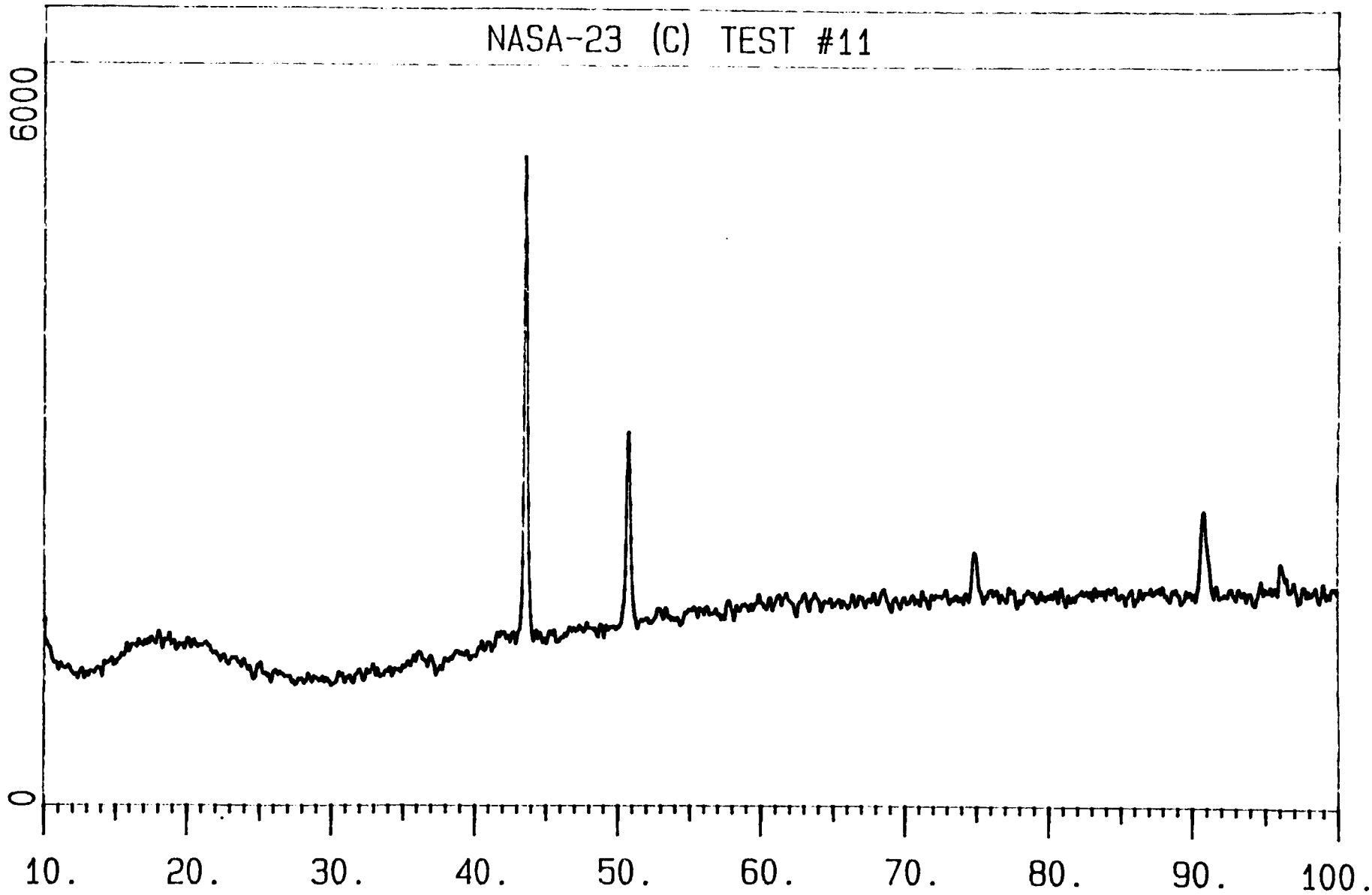
NASA-23 (C) TEST #11
6000
0
10.
20.
30.
40.
50.
60.
70.
80.
90.
100.

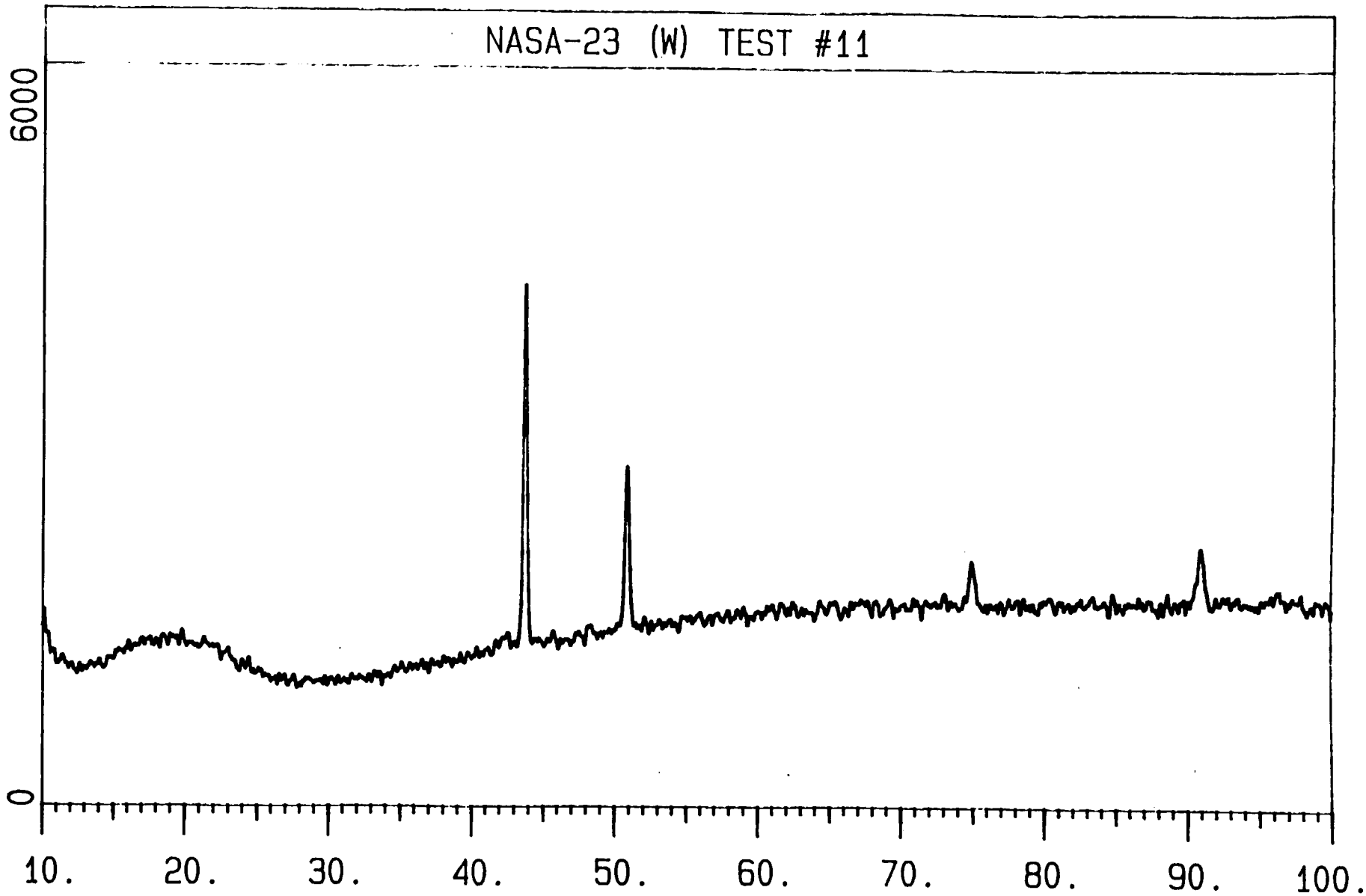
NASA-23 (W) TEST #11
6000
0
10.
20.
30.
40.
50.
60.
70.
80.
90.
100.

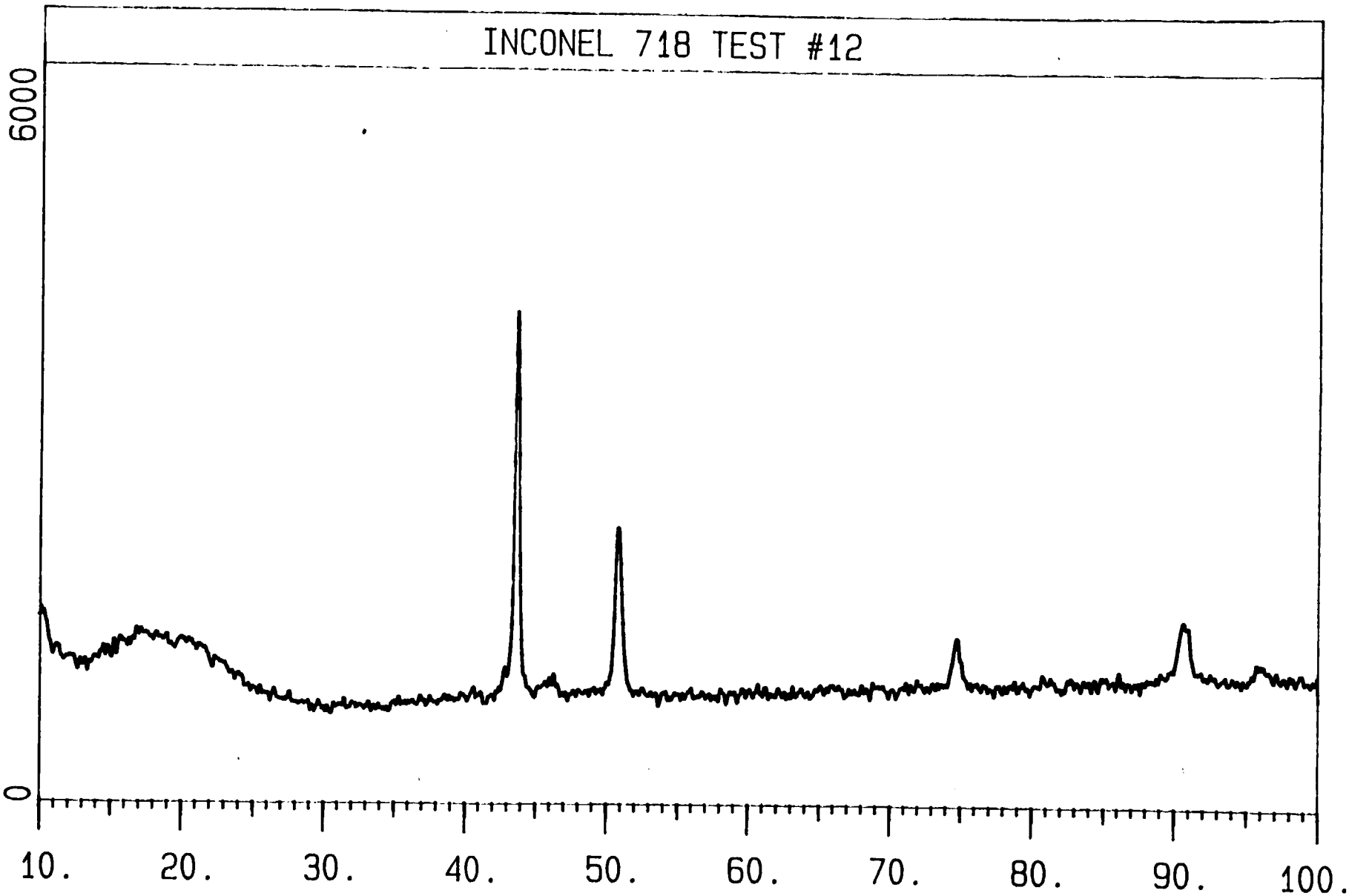
INCONEL 718 TEST #12
6000
0
10.
20.
30.
40.
50.
60.
70.
80.
90.
100.

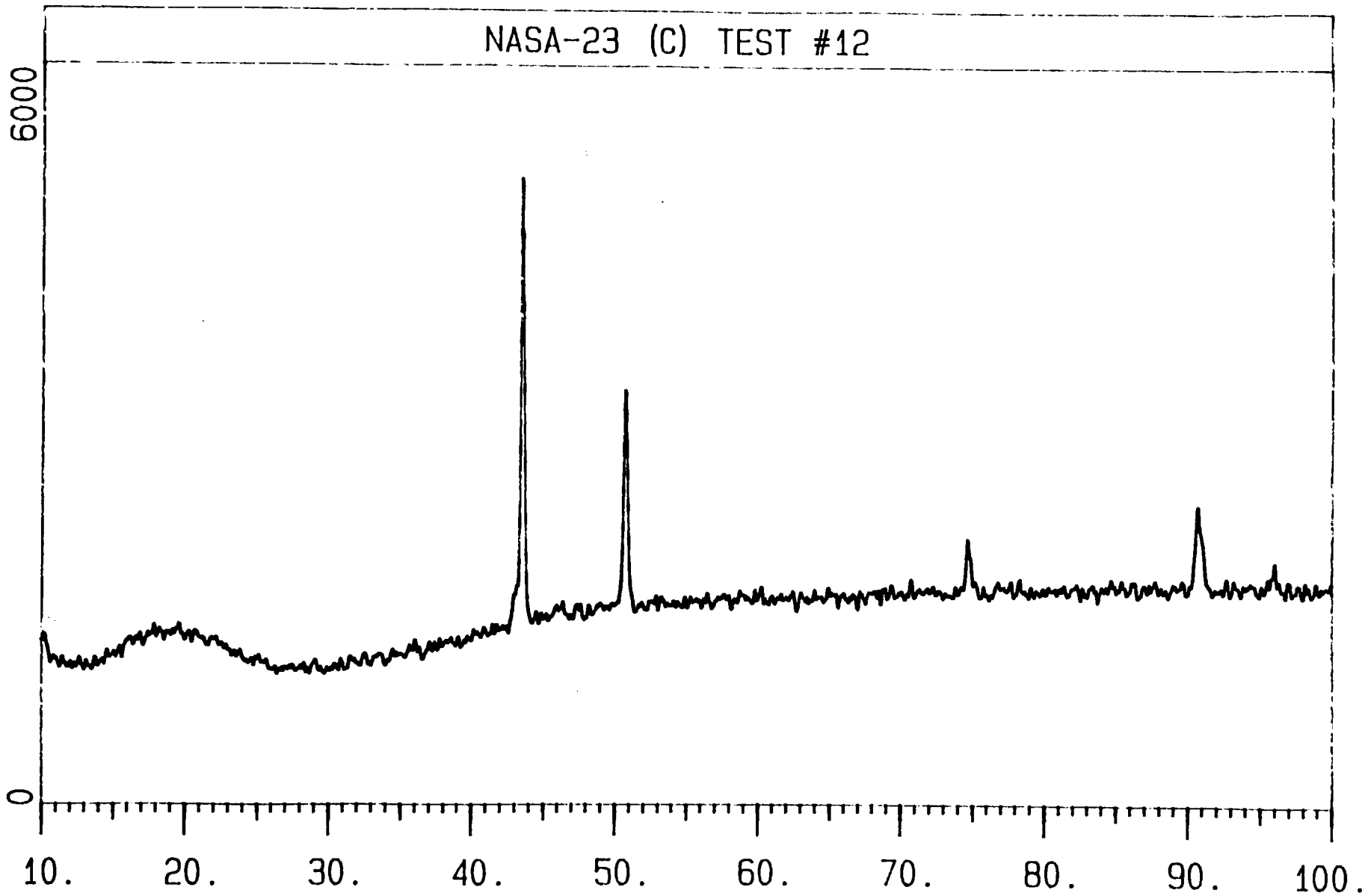
NASA-23 (C) TEST #12
6000
0
10.
20.
30.
40.
50.
60.
70.
80.
90.
100.

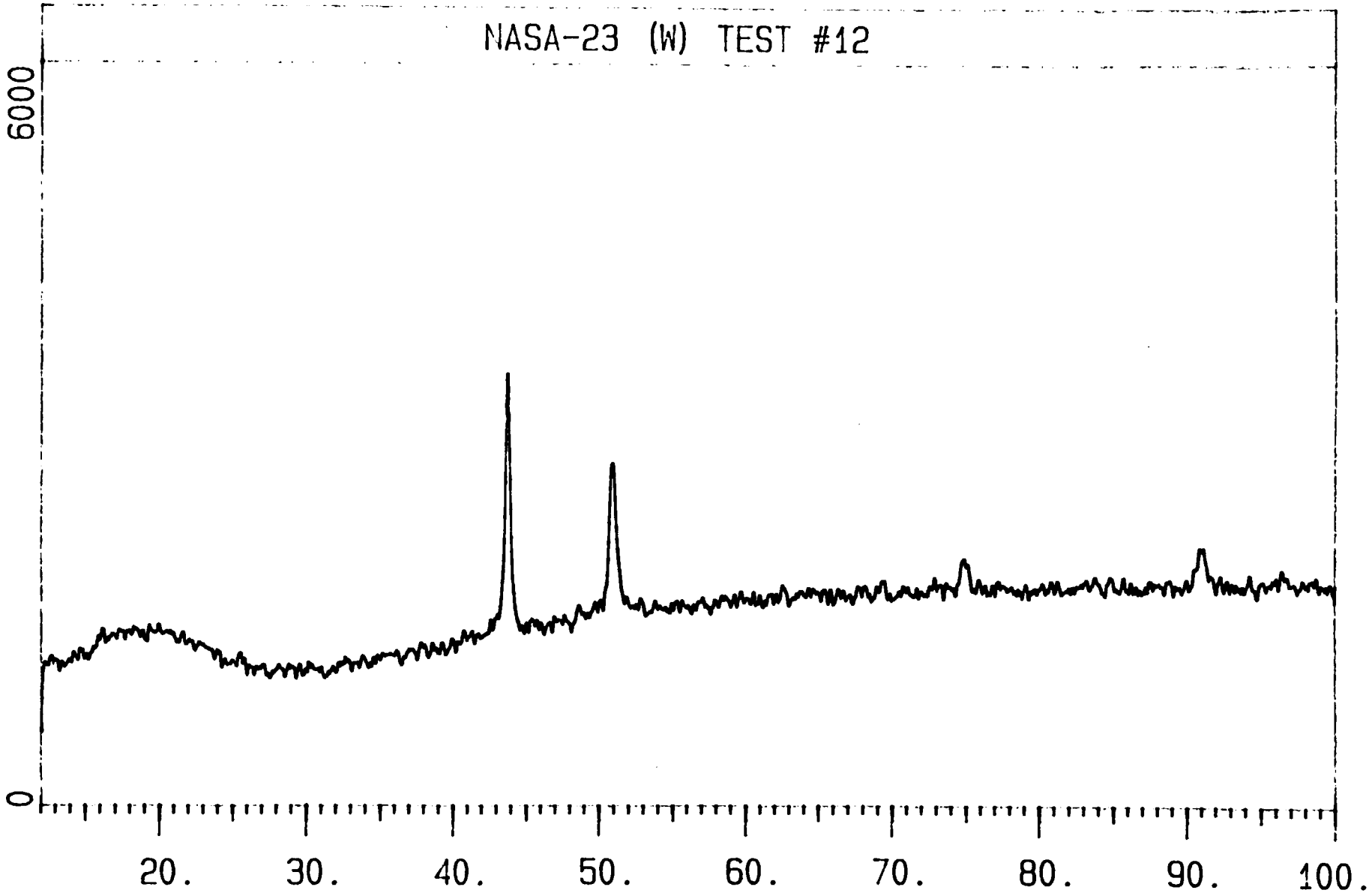
NASA-23 (W) TEST #12
6000
0
20.
30.
40.
50.
60.
70.
80.
90.
100.

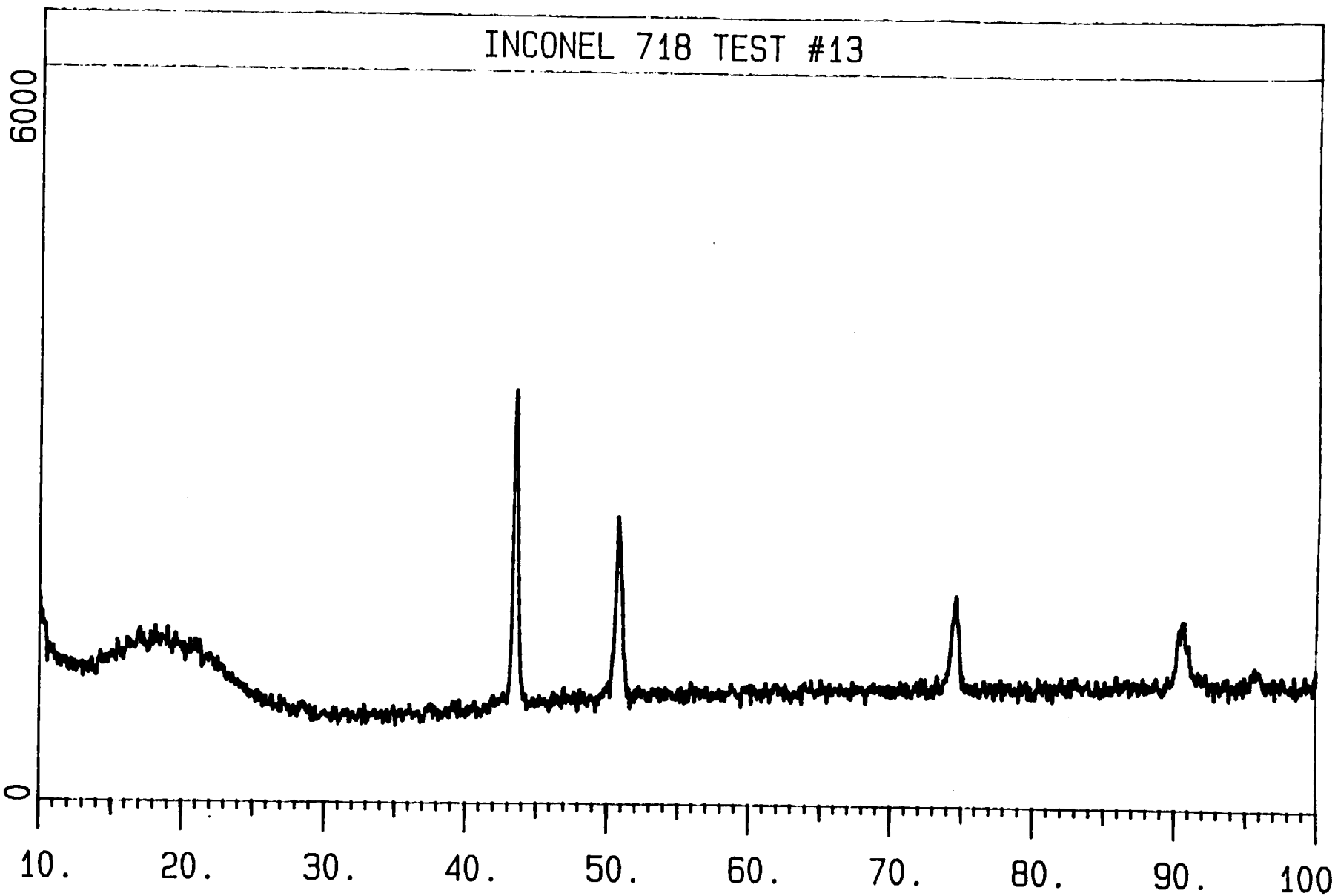
INCONEL 718 TEST #13
6000
0
10.
20.
30.
40.
50.
60.
70.
80.
90.
100.

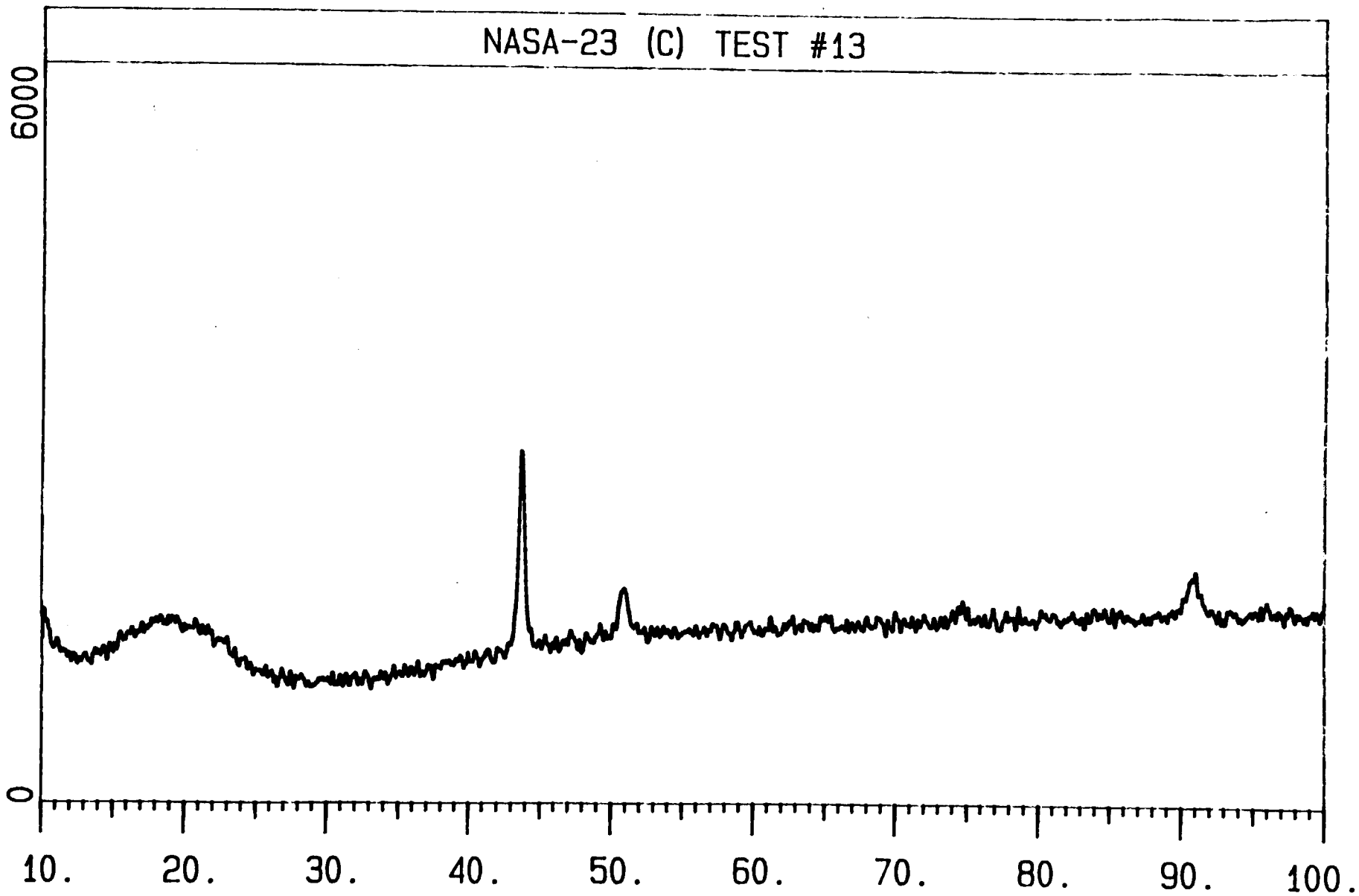
NASA-23 (C) TEST #13
6000
0
10.
20.
30.
40.
50.
60.
70.
80.
90.
100.

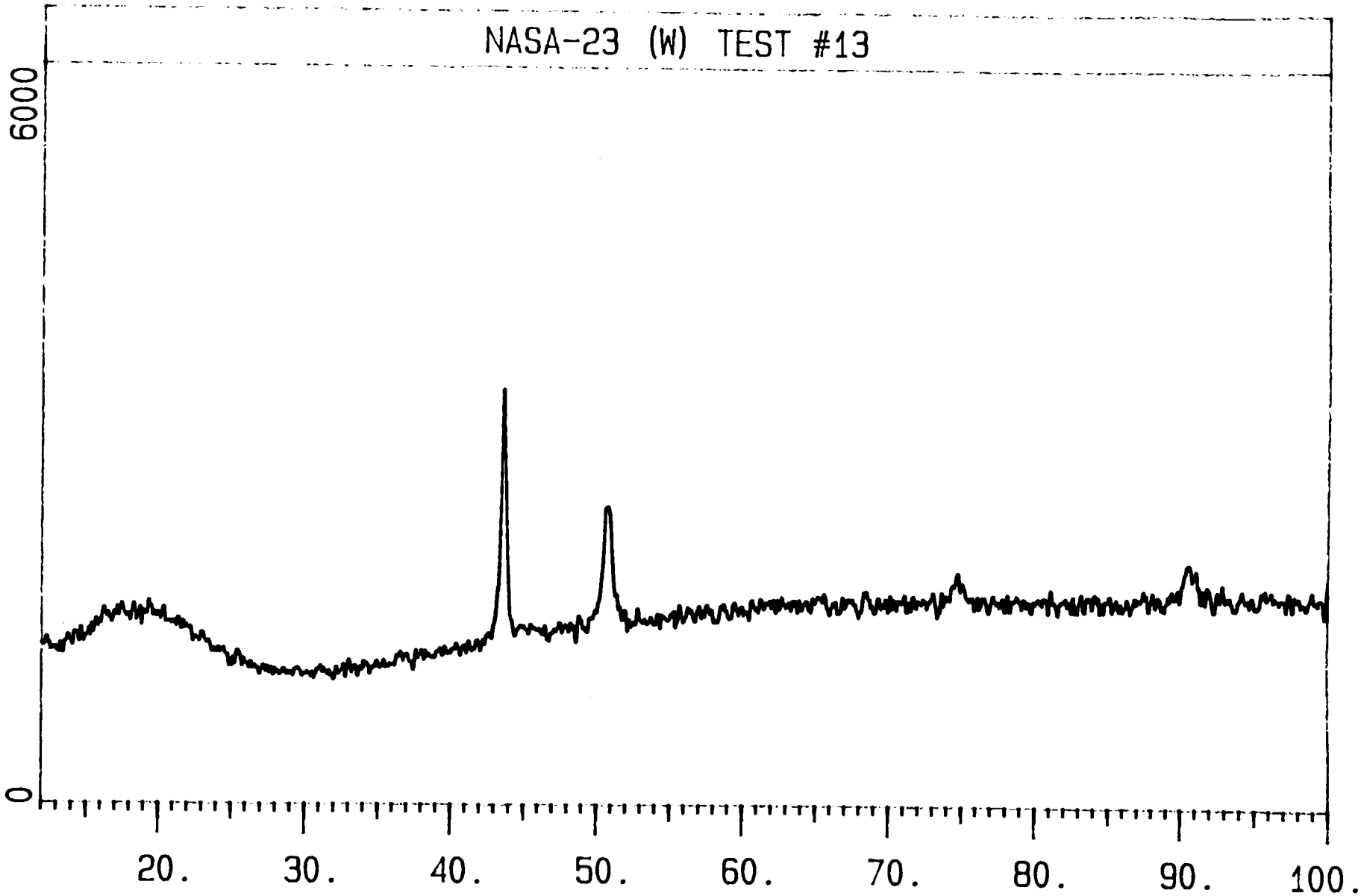
NASA-23 (W) TEST #13
6000
0
20.
30.
40.
50.
60.
70.
80.
90.
100.

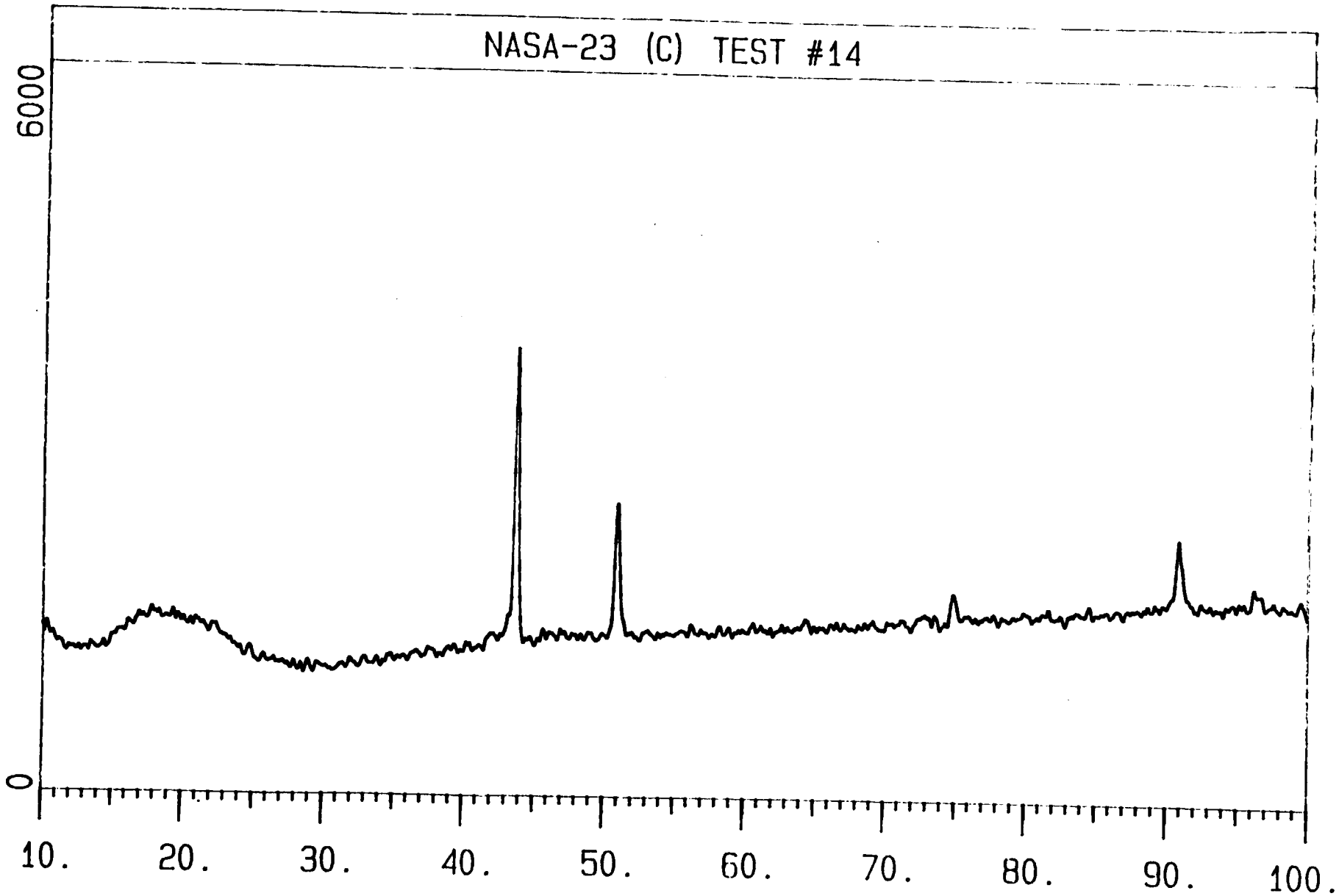
NASA-23 (C) TEST #14
6000
0
10.
20.
30.
40.
50.
60.
70.
80.
90.
100.

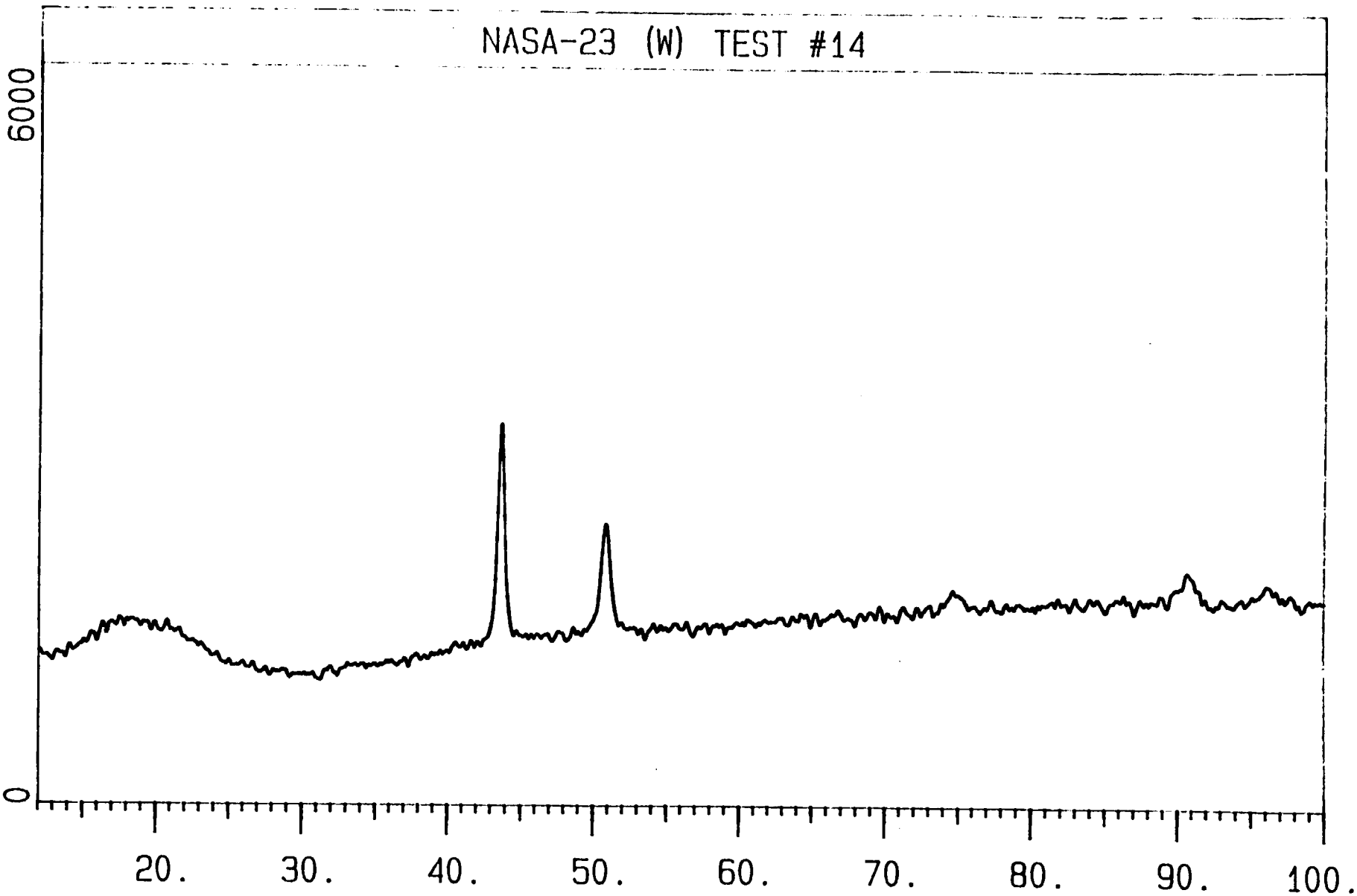
NASA-23 (W) TEST #14
6000
0
20.
30.
40.
50.
60.
70.
80.
90.
100.

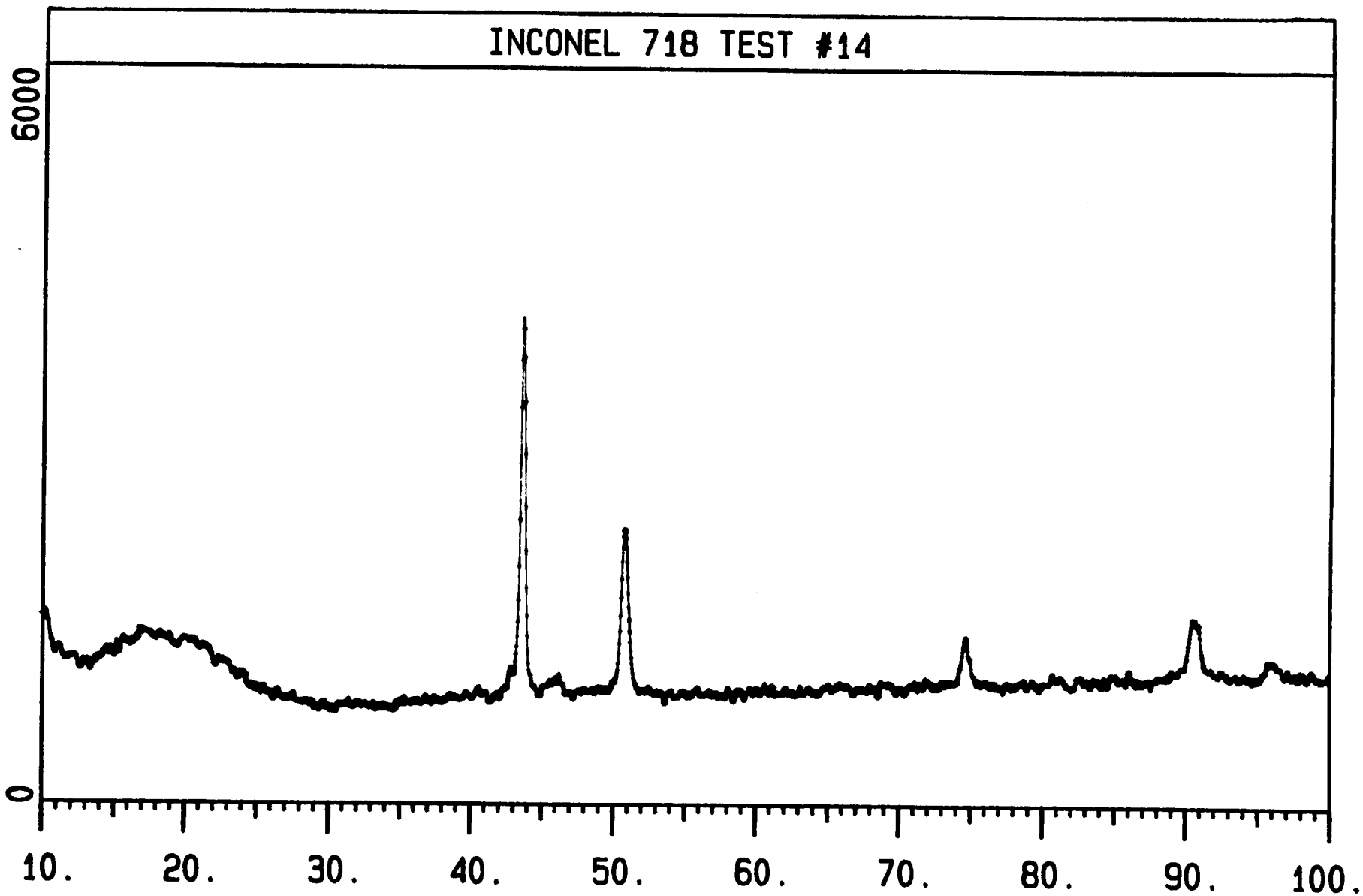
INCONEL 718 TEST #14
6000
0
10.
20.
30.
40.
50.
60.
70.
80.
90.
100.